UCSF

UC San Francisco Electronic Theses and Dissertations

Title

Identification of internal kinesin regions necessary for microtubule depolymerization

Permalink

https://escholarship.org/uc/item/5q4295qg

Author

Shipley, Krista M

Publication Date

2006

Peer reviewed|Thesis/dissertation

Identification of internal kinesin regions necessary for microtubule depolymerization

by

Krista M. Shipley

DISSERTATION

Submitted in partial satisfaction of the requirements for the degree of

DOCTOR OF PHILOSOPHY

in

Biophysics

in the

GRADUATE DIVISION

of the

UNIVERSITY OF CALIFORNIA, SAN FRANCISCO

Date   University Librarian

Degree Conferred:...

To Mom, Dad and Karie, for <u>always</u> being there

KMS

March 2006

and for being great neighbors since I switched groups, both on the 10th floor back at

Parnassus and now in the same 'hood at Mission Bay.

The S-414/416 neighborhood here has been a great place to mix with fellow structural

biologists and motor protein specialists, for good tips and stimulating chats in the

lunchroom. In addition to our lab, Robert Stroud's group has the hard-core

crystallographers, while Dave Agard's group does all sorts of cool stuff, from

enzymology to crystallography to electron microscopy, so there's a wide variety of

expertise to draw from. Roger Cooke's group, just one row over from me, have been

good for motor-protein discussions, and thanks to Roger, Nariman Naber, Christina

Karatzaferi and Tom Purcell I had a great time at two Biophysical Society conferences,

even without my PI and fellow labmates in attendance.

Several other professors here at UCSF have helped me through the stages of graduate

school. It was a wonderful experience working as a TA for Ken Dill, who of all the

professors here is one of the most dedicated to teaching. It was nice to meet once a year

with my academic advisor and fellow Jayhawk Dennis Deen, for a sympathetic ear during

some of the ups and downs of graduate school. And thanks to my challenging but nice

Oral Exam committee – Volker Doetsch, Tack Kuntz, Lily Jan and chair Robert

Fletterick – I cut through the nail-biting anxiety and learned how to plan and think my

way through a big scientific question.

In graduate school, everyone is a potential colleague and friend, so I've really appreciated

getting to know everyone in the Biophysics Program, as well as the other programs such

as Tetrad, Chemistry/Chemical Biology and BMI with which we mix on a regular basis. There's too many students to list, so I'd like to personally thank my classmates Alex Fay, who was a good housemate and friend during our rocky first years here; Helen Lai, who was a great teammate when we led middle-schoolers through biology labs for Science and Education Partnership; Horng Ou, currently braving the challenges of graduate school abroad in Frankfurt, Germany; Irina Grigorova, who put up with my feeble attempts to speak Russian; John Chodera, computer whiz, one-man-band and always up to something interesting; and Nick Endres, with whom I traded kinesin angst for tips.

Finally, I'd like to thank the ones who gave me the solid support I needed to finish graduate school. Julie Ransom, who keeps the Biophysics Program running as smooth as possible, was always available for advice or a good chat. A Predoctoral Fellowship from Howard Hughes Medical Institute (HHMI) kept me financially afloat for 5 years. And of course, my thesis committee members – Robert Fletterick, Roger Cooke and Ron Vale, the "3 R's" – have been an invaluable source of feedback, advice and support these past three years.

<u>Outside UCSF / Outside Science</u>

UCSF wasn't the first time I ever saw a research lab. James Calvet at KU Med Center was kind enough to let a high school student work in his lab for the summer, Ken and Sally Mason were my research and academic mentors during my undergraduate years at the University of Kansas, and I had a wonderful experience working as a technician for

science labs were a blast with Helen, Freddie, Ammon and Ray, and I highly recommend trying the program if you get the chance.

I've lived in the same house the entire 6.5 years, so I feel it's worth acknowledging Andrea Yee and her sons Alan and Alex Lee, who've been considerate landlords and just plain nice and interesting people. I'd also like to acknowledge the many merchants and residents who've made the Inner Sunset a friendly place to live, as well as the many different housemates, from all over the world, that I've gotten to know. It's certainly been wonderful to live in such a diverse and beautiful city as San Francisco.

Most precious of all are my old friends and family. I've known Courtney since middle school, and met Eva, Chris and Sarah in college, and it was a real thrill to attend weddings for three of them and even be a bridesmaid for one. My parents each have three siblings, meaning I have many cousins producing still more cousins, so instead of naming each of them I'd like to just thank them all for making the holidays fun and interesting. I wish everyone and their families all the best, and can't wait to see them again after I graduate.

I'd particularly like to thank my parents, Larry and Barbara Shipley, for supporting me all these years and letting me follow my interests and my dreams wherever they lead me. Most of all, I'd like to thank my twin sister Karie, who's literally been there all along as a confidant, sounding board and buddy, and I look forward to visiting with her in Denver during the interim before the next stage of my career.

Finally, I'd like to dedicate this work to my grandmother, who survived the Great

Depression, raising 4 daughters, her husband and a recent heart attack to reach the age of

97 and see her youngest grandchild receive her doctorate – her birthday's March 15, this

very day that I'm finishing writing and printing this for posterity. Her good humor and

quiet enjoyment of life have been an inspiration these years, and I hope to grow old as

she has.

Abstract

Identification of internal kinesin regions necessary

for microtubule depolymerization

Krista M. Shipley

Internal kinesins (KinI), which depolymerize microtubules instead of walking on them, are an interesting example of adapted evolution. Although they have extensions from the motor core at both the N- and C-termini (hence the name "Internal"), the motor core alone is sufficient for some depolymerization activity. Addition of the 50 amino-acid N-terminal "neck" to the motor core is enough to restore activity near that of the full-length protein, probably by helping the protein to localize to the microtubule ends.

In order to understand better what regions of these kinesins are necessary for microtubule depolymerization, and why, we first solved the x-ray crystallography structure of the Plasmodium falciparum KinI motor domain, and used a depolymerization spin-down assay, ATPase assay and electron microscopy to ascertain functional differences between the wild-type motor and alanine mutants of residues uniquely conserved in the KinI family. Our results showed that the motor Loop2 is specifically required for depolymerization, rather than ATPase activity or microtubule binding.

Next, I have been using molecular biology techniques to insert the human MCAK (KinI) N-terminal neck and Loop2 into walking kinesins KHC, NCD and Unc104, to

show that these regions are sufficient for depolymerization. I have successfully made

constructs of these motors with the N-terminal neck and C-terminal GFP (green

fluorescent protein), and obtained some soluble protein after expression and initial nickel

column purification, as confirmed by an anti-GFP Western blot. The next step will be to

insert Loop2 and use the spin-down assay from the prior study to assay for

depolymerization activity. It may also be necessary to assay for ability to localize to the

microtubule ends, using fluorescent microscopy to visualize the GFP-labeled protein on

stabilized microtubules.

Robert J. Fletterick, PhD

Advisor

TABLE OF CONTENTS

APPENDICES

REFERENCES

LIST OF TABLES

LIST OF FIGURES

Chapter 2: Testing sufficiency of KinI Loop2 and neck for microtubule end-targeting and depolymerization

Introduction to the Dissertation

One of the big questions in biology today, especially in this post-genomic era, is how to relate structure with function. It's easy to assume that proteins with similar sequence and structure will also have a similar function, but we can find many exceptions to this. For example, the TIM-barrel domain is a very common scaffold for enzymes catalyzing a wide variety of reactions. Even within the TIM-barrel Enolase Superfamily of enzymes, different enzymes that share the same fold and key catalytic residues are able to perform at least ten completely different chemical reactions. This seems to involve a slight variation on similar chemistry, such as common or similar intermediates (Gerlt and Babbitt, 2001).

The Kinesin-13 family is a good example of a motor protein where the usual properties are altered slightly to perform a very different function. They are also known as Internal Kinesins (KinI) because the catalytic motor core domain is located internally in the polypeptide chain, with both N- and C-terminal extensions, rather than being at one end or the other like other kinesins. They are unique not only in their architecture, but also in their function: instead of walking on microtubules (MT) in the plus- or minus-end direction like KinN's or KinC's, respectively, they bind at the ends of microtubules and depolymerize them. Certainly the large N- and C-terminal extensions contain parts important for regulating and transporting the protein for its new function, however the motor core by itself is sufficient to depolymerize microtubules, even ones that have been stabilized by taxol or GMP-CPP. Figure 1, a classic EM picture in the Kinesin-13 field,

1

shows the difference between GMP-CPP-stabilized MT's, which don't show curvature at the ends, with ones exposed to the KinI XKCM-1 in the presence of nonhydrolyzable analogue AMP-PNP. The tubulin needs to hydrolyze its GTP to break its longitudinal contacts with other tubulins, hence the tubulin protofilaments form long curls instead of breaking up into individual units as they normally would. This ability to hydrolyze stabilized MTs suggests that the act of microtubule binding, which fulfills more of an anchoring function in walking kinesins, can be adapted to exert force or stabilize the desired product (curved tubulin) more precisely, beyond the simple recognition needed for walking.
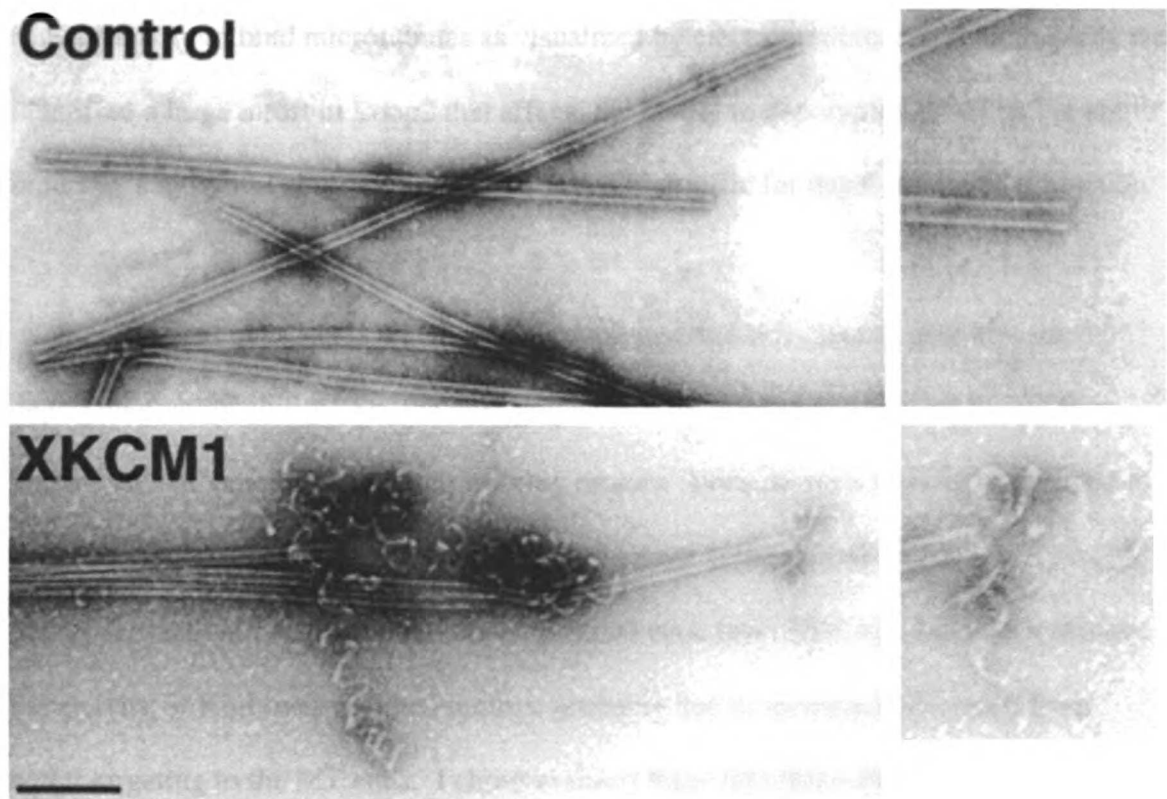
Figure 1: KinI-induced depolymerization. Here XKCM1 is inducing curvature in GMP-CPP-stabilized MT's, in the presence of AMP-PNP (both non-hydrolyzable nucleotide analogues). Reprinted from Desai et.al., 1999, with permission from Elsevier.

The first question then is what elements of the motor core, which is highly conserved across the entire kinesin superfamily, change the function to depolymerization? To study this question we crystallized the motor core from *Plasmodium falciparum* KinI, determined the 1.6 A structure of the protein and found some interesting differences from other kinesin structures. We also identified residues that are unique to the KinI family, i.e., conserved in KinI's but not found in other kinesins. We then mutated these residues to alanine, and assayed the affect on function in four ways: 1) their ability to depolymerize microtubules, 2) their ability to hydrolyze ATP in the presence of microtubules and 3) free tubulin, all three with simple assays, and 4) their ability to bind microtubules as visualized by electron microscopy. In this way we identified a large insert in Loop2 that affects the ability to depolymerize MT's, but not to bind MT's or hydrolyze ATP, indicating that it is specific for depolymerization function.

The next question is whether this Loop2 insert is sufficient to give kinesin depolymerization ability. So, the next project was to insert the conserved Loop2 from human MCAK (another KinI) into walking motors. Because such activity is expected to be weak, due to other parts of the binding surface not being optimized for depolymerization, I also included the N-terminal neck from hMCAK, because it increases the activity of KinI over neckless motors, probably due to increased efficiency from better targeting to the MT ends. I chose to insert these into three different well-studied walking kinesins (hsuKHC, dmNCD and ceUnc104), to improve the chances of at least one working as a protein that can be expressed, purified and assayed, and to have a large body of data for each to compare our results with. These constructs would then be

studied by two assays: 1) the depolymerization assay from the previous study, for obvious reasons, and 2) a fluorescence microscopy assay to determine whether or not the motors with KinI neck are localizing at the MT ends, instead of decorating the MT lattice as kinesins normally do.

The molecular biology ended up being rather difficult, but I have succeeded in making DNA constructs of all three motors with the hMCAK neck at the N-terminus and Green Fluorescent Protein (GFP) at the C-terminus, as well as controls without neck, without GFP, or using the hMCAK motor. The GFP was included for the localization assay but has also aided as a quick indicator of good protein expression. Expression and purification has also been non-trivial, but I have found that growing cells at 37C and expressing overnight at 15C gives good yield and some soluble protein. The induction IPTG concentration and purification conditions for optimal soluble protein yield still need to be found, and then the hMCAK Loop2 needs to be mutated in, but this is a good start on the project.

I also have some suggestions for other projects to help address the question of what it functionally important. For example, it appears that Loop2 is not completely accepted as being important for depolymerization – the three mutated residues could well be eliminating depolymerization by causing the protein to stick on the MT lattice and not act at the MT ends, in other words by mucking up the works rather than removing a critical component. The lack of a neck in the *Pf* construct also probably has some people skeptical about the results in the paper. To help address this question, I suggest deleting
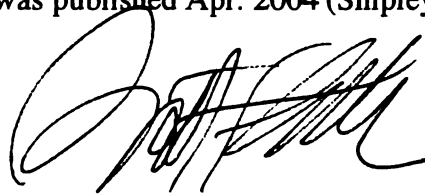
the entire Loop2 insert from full-length hMCAK and replacing it with the short Loop2

from KHC, rather than relying on the alanine-mutant results. A loss of depolymerization

activity, but not tubulin-stimulated ATPase activity or MT binding, would strongly affirm

the importance of Loop2 in function.

Chapter 1: Structure of internal motor kinesin from *Plasmodium falciparum* and mutational analysis of regions essential for microtubule depolymerization

When I joined the Fletterick lab, I picked up this project from Jennifer Turner, a former postdoc who left without publishing her results. I took on the task of finding her *Pf* KinI motor-core crystallography data and partially refined models, completing the refinement and preparing the structure for submission to the Protein Data Bank (PDB). I also worked with two collaborating labs to incorporate their *Pf* KinI results into the journal article I wrote (and include here as chapter 1). Mohammad Hekmat-Nejad and Roman Sackowitz of Cytokinetics performed microtubule-depolymerization and ATP hydrolysis assays, to compare the various alanine mutants Jennifer made with the wild-type motor construct. Carolyn Moores and Ronald Milligan of the Scripps Research Institute visualized *Pf* KinI motor and alanine mutants on microtubules, to qualitatively assess ability to bind and depolymerize them.

I prepared figures showing the prominent and unique features of the *Pf* KinI crystal structure, and location of the alanine mutants, then calculated the "% tubulin depolymerized" and ATPase rate for each protein assayed, and compiled this into a figuring comparing the mutants with wild-type. Carolyn Moores prepared Figure 7 (EM) for the paper, and also docked the *Pf* KinI X-ray crystallography structure into their 3-d EM data for *Pf* KinI decorating microtubules, shown in Figure 8. I sent her the *Pf* KinI coordinates used for the docking, gave feedback on the two figures she prepared for the paper, and prepared the last figure showing our model of KinI function, as well as a structure-based protein-sequence alignment of *Pf* KinI with other KinI's, huKHC and

ceNCD (Supplementary Figure). Robert Fletterick and Elena Sablin provided editoral

comments on the manuscript. The paper was first submitted to Cell, and then

successfully submitted to EMBO Journal, where it was published Apr. 2004 (Shipley

et.al., 2004).

Robert J. Fletterick, PhD

Advisor

Abstract

With their ability to depolymerize microtubules, Kin I kinesins are the rogue members of

the kinesin family. Here we present the 1.6Å crystal structure of a KinI motor core from

Plasmodium falciparum, which is sufficient for depolymerization *in vitro*. Unlike all

published kinesin structures to date, nucleotide is not present, and there are noticeable

differences in loop regions L6 & L10 (the plus-end tip), L2 and L8, and in switch II (L11

& helix4); otherwise the pKinI structure is very similar to previous kinesin structures.

KinI-conserved amino acids were mutated to alanine, and studied for their effects on

microtubule depolymerization and ATP hydrolysis. Notably, mutation of three residues

in L2 appears to affect primarily depolymerization, rather than general microtubule

binding or ATP hydrolysis. Results of this study confirm the suspected importance of

Loop2 for KinI function, and provide evidence that KinI is specialized to hydrolyze ATP

after initiating depolymerization.

Introduction

Each cell type in every eukaryotic organism contains multiple kinesin-superfamily members. To date, over 30 kinesins have been found in the human genome (Kinesin Homepage: http://www.proweb.org/kinesin/index.html). Though kinesin proteins differ widely in their cellular function, they all share the ability to modulate their interactions with microtubules (MT) through binding and hydrolysis of ATP by their conserved catalytic core, which constitutes the major part of the kinesin motor domain (Vale and Fletterick, 1997). Some kinesins translocate cargo towards the plus ends of microtubules; these kinesins have their motor domains at the N-terminus of their polypeptide chain, and are therefore classified into the KinN family (Vale and Fletterick, 1997; Vale et.al., 1985). Other kinesins move in the opposite direction; these have their motor domain at the opposite C-terminus, and are called KinC motors (Vale and Fletterick, 1997; McDonald et.al., 1990).

Kinesin subfamily KinI (termed so for the Internal location of the motor domain) performs a completely different function: it initiates MT depolymerization instead of acting as a motor (Desai et.al., 1999). MT depolymerization is involved in establishment and maintenance of the mitotic spindle and is vital for chromosome segregation during cell division (Inoué and Salmon, 1995; Rogers et.al., 2004). The MT depolymerizing activity is best understood for the KinI kinesins that localize to the kinetochore during mitosis; these are called XKCM1 in Xenopus (Desai et.al., 1999; Kline-Smith and Walczak, 2002) and MCAK in mammals (Wordeman and Mitchison, 1995; Hunter et.al., 2003). Kif2, another KinI kinesin type first found in murine brain (Aizawa et.al., 1992),

has also been shown to depolymerize MT *in vitro* (Desai et.al. 1999). A recent study suggests that Kif2 plays a non-mitotic role in development of the nervous system, by suppressing extension of superfluous branches at the cell edge of (post-mitotic) neurons (Homma et.al., 2003).

KinI perturbs the MT polymerization and depolymerization cycle, which is controlled by the GTPase cycle of the individual α/β-tubulin heterodimers in the polymer (as reviewed in Desai and Mitchison, 1997). GTP-bound tubulin dimers are straight, and polymerize to form straight MTs, while free GDP-bound tubulin dimers are curved. Thus, a tubulin dimer in a MT would prefer to adopt a curved shape after hydrolyzing its GTP to GDP, but is kept straight by side-by-side (lateral) interactions with adjoining protofilaments. There are fewer of these stabilizing interactions at the ends of the MT, where at least one of the dimers has a single lateral interaction. Consequently, GTP hydrolysis in these exposed end tubulin dimers will lead to curvature and peeling away of their respective protofilaments, and the start of depolymerization.

In vivo, growth and decay of MTs are vital for many cellular processes, so there are many proteins known that regulate the onset of depolymerization (Walczak, 2000). Some, such as op18/stathmin, are thought to initiate depolymerization by activating GTP-hydrolysis when they bind to the ends of MTs (Segerman et.al., 2000). KinI's likely employ a different mechanism, since they can depolymerize MTs stabilized by a non-hydrolyzable GTP analogue GMP-CPP (Desai et.al. 1999, Moores et.al. 2002, Hunter et.al. 2003).

In trying to understand KinI, many important details of their function have been elucidated. In particular, KinI's were shown not to walk along the MT, but rather target

directly to the MT ends (Desai et.al. 1999) or reach the ends by rapid one-dimensional diffusion (Hunter et.al. 2003). Like other kinesins, KinI are ATPases, but ATP hydrolysis is not necessary to disassemble MTs, because KinI bound to the non-hydrolysable ATP analogue AMP-PNP can induce MT protofilament peeling (Desai et.al., 1999; Moores et.al., 2002). ATP hydrolysis appears necessary for KinI to release from free tubulin dimer, in order to rebind the MT and depolymerize in catalytic fashion (Desai et.al., 1999). This is analogous to conventional human kinesin (KHC), in which the power-stroke, that propels the non-bound motor head forward, is induced by ATP-binding, and ATP hydrolysis weakens the association with the MT (Rice et.al., 1999). It also appears that hydrolysis occurs before release of the KinI-tubulin complex from the MT, because (full-length) MCAK has higher ATPase activity in the presence of MTs than free tubulin (Hunter et.al. 2003), and because AMPPNP-bound KinI forms rings from non-stabilized MTs (Moores et.al., 2002).

Although KinI's appear to function as dimers *in vivo*, KinI monomers were shown to be sufficient to depolymerize MT (Maney et.al. 2001, Niederstrasser et.al. 2002, Moores et.al. 2002). XKCM1 dimers are also able to depolymerize antiparallel, zinc-stabilized tubulin macrotubes. The latter finding suggests that XKCM1 does not bind at the protofilament interface to tear it apart, but rather acts on a single protofilament (Niederstrasser et.al. 2002). Limited proteolysis experiments showed that removal of the tubulin C-terminus reduced gliding kinesin processivity (Thorn et.al., 2000; Okada and Hirokawa, 2000; Wang and Sheetz, 2000). Similar experiments showed that the C-terminal tubulin region, while dispensable for binding of KinI to MT, is necessary for MT depolymerization by KinI (Moores et.al. 2002, Niederstrasser et.al. 2002).

Plasmodium falciparum KinI can depolymerize MT *in vitro* as a monomer, using just the catalytic core domain with no N-terminal neck attached (Moores et.al. 2002). However, the presence of the neck markedly increases the rate of depolymerization in the mammalian homologue MCAK (Maney et.al. 2001). The role of the KinI neck is still under scrutiny, but it is generally thought that it might improve efficiency of MT depolymerization by targeting the protein to MT ends. Alternatively, the presence of the neck could decrease the off-rate from MTs, which would contribute to higher KinI activity found at physiological conditions (Ovechkina et.al. 2002).

Since the crystal structure of any kinesin motor in complex with tubulin is not yet available, our understanding of how kinesins interact with MTs is restricted to lower-resolution techniques, such as proteolytic mapping (Alonso et.al., 1998), mutagenesis experiments (Woehlke et.al., 1997), and fitting atomic coordinates of kinesins motor domains into electron density maps derived from EM experiments (Mandelkow and Hoenger, 1999; Kikkawa et.al., 2001). As for KinI, the only prior information on how it specifically interacts with the microtubule has been made by inference from fitting crystallographic models of other kinesin motors into EM maps of KinI bound to microtubules (Moores et.al., 2002; Moores et.al., 2003).

The most intriguing question to date about the Internal Kinesins is how the catalytic core alone, being almost identical in its primary structure to other kinesin core domains, can perform a function so different from the usual gliding motion. To understand better how KinI works, we determined the crystal structure of *Plasmodium falciparum* KinI catalytic core to 1.6Å resolution. Furthermore, we mutated family-

conserved residues to study how their loss affected protein activity. These combined

studies identified structural elements of KinI that are important for MT depolymerization.

Results

Crystal Structure of the KinI catalytic core

While several KinI have been characterized, for our structural studies we used the

readily-crystallizable catalytic core domain of the *Plasmodium falciparum* MCAK

homologue (pKinI), which is sufficient to perform MT depolymerization *in vitro* (Moores

et.al., 2002). The pKinI catalytic core was expressed, purified and crystallized, and its

structure determined by molecular replacement, as described in Experimental Methods.

The current crystallographic model is refined to 1.6Å with R/R_{free} values of 0.2023 and

0.2304 (Table 1), and consists of 318 amino acid residues (12 of the total 330 residues are

disordered). The structure of pKinI (Figure 1-1) revealed a protein domain similar to

previously determined kinesin catalytic cores (Figure 1-2). Kinesin core structures are

generally "arrowhead" shaped, consisting of a central β-sheet region surrounded by α-

helicies, and have always been found complexed with adenosine nucleotide (Kull and

Endow, 2002). The pKinI structure differs most from previous kinesin models in that

there is no nucleotide present in the ATP binding site. Furthermore, in contrast to most

kinesin structures, the switch II loop L11 of pKinI is ordered and forms a short two-turn

helix. Microtubule-binding loop L8 does not form a long strand-pair pointing towards the

MT-binding face, which is seen in most gliding kinesins. Instead, L8 appears to point in the opposite direction, although it is too disordered to resolve its structure completely.

Some features of the pKinI structure are not strictly unique, but found in only a few kinesin structures. For example, the "pointed tip" of the kinesin "arrowhead" (loops L6 and L10), is noticeably bent in the pKinI structure. In the recently-solved Eg5 structure (Turner et.al., 2001), this region is also bent, but in the opposite direction. MT-contacting L2 is noticeably longer in pKinI, although the same region in NCD and Eg5 approach it in length. The long, MT-contacting switch II helix α4 is visible and structured for its entire length, a feature previously seen in the Kif1a-ADP structure (Kikkawa et.al, 2001).

Nucleotide-binding pocket of pKinI

Prior to pKinI, all kinesins have been crystallized with an adenosine nucleotide bound, despite numerous attempts at crystallizing a nucleotide-free motor (Muller et.al., 1999). Strikingly, the ATP-binding pocket of pKinI does not have a bound nucleotide (Figure 1). Although there is no continuous electron density consistent with the presence of the bound nucleotide, the nucleotide-binding site is not empty. Figure 1-3a shows the electron density (in green) found in the nucleotide-binding site of pKinI. For reference, ADP from the superposed Kif1A model is included (1I5S, Kikkawa et.al., 2001). At the exact position of the β-phosphate found in other structures, crystalline pKinI contains a single sulfate ion, which is likely derived from the crystallization buffer (see Methods). To confirm the absence of bound nucleotide, we performed one round of refinement after replacing the sulfate ion with ADP. As illustrated in Figure 1-3b, the presence of ADP is

not consistent with the experimental data, since its inclusion results in a strong negative density peak (colored red).

Since this is the first example of nucleotide-free kinesin, we analyzed how this state would be reflected in the structure of the nucleotide pocket. In general, the structure in the vicinity of the nucleotide-binding pocket more closely resembles ADP-bound kinesins, with the switch II helix in the "down" position (Figure 1-4a). All conserved amino acid residues that normally contact bound ADP (P-loop and switch II loop) have similar side-chain positions in both ADP-free pKinI and ADP-bound kinesins. The only difference is that, in pKinI, switch II loop residue D236 does not form a highly-conserved hydrogen bond with P-loop T99 (see Figure 1-4c for location of these residues). The absence of this hydrogen-bond is explained by the switch II loop backbone being displaced about 1Å away from the nucleotide binding pocket towards the MT-binding surface, compared to the ADP-bound kinesin structures. Switch I shows a similar 1Å shift (Figure 1-4b), and these two shifts combined could indicate a slight opening of the binding pocket in the absence of nucleotide.

The structures of the switches, and the networks of switch I – switch II hydrogen-bonds, vary greatly among ADP-bound kinesin structures (Kull and Endow, 2002), so it is difficult to draw conclusions from any differences in these regions between pKinI and other kinesin structures. The most notable difference in this region is the two-turn helix in switch II L11, which is stabilized by two hydrogen bonds (Figure 1-4c): a unique bond between kinesin-required switch I residue R211 and KinI-conserved switch II loop residue D245, and a rare bond between switch I residue S210 and switch II loop residue R242. R242 is usually displaced away from the binding pocket, but it points toward

switch I in Kif1a-ADP so this feature is not unique to pKinI. As a result of these two hydrogen bonds, the pKinI structure lacks the switch I R211 – switch II E241 hydrogen bond that had been seen in some kinesin structures.

Besides the slight shift in the switch I and switch II loop backbone, which may indicate a slight opening of the pocket, and the unique R211-D245 hydrogen bond that helps to stabilize switch II, no significant binding-pocket difference is seen between the nucleotide-free pKinI structure and ADP-bound kinesin structures. These observed differences are small compared to the conformational changes found between Kif1a-ADP and Kif1a-AMP-PNP (Kikkawa et.al., 2001).

Mutational studies on pKinI

Since the KinI family performs such a distinct function, we were interested in identifying the residues specifically conserved within the KinI family. Multiple sequence alignment (Supplementary Figure 1-10) showed that such residues are located in microtubule-binding regions of the protein. Three individual KinI-specific residues and two sets of residues were mutated to alanines and assayed for their effects on MT depolymerization and ATP hydrolysis (Figure 1-5).

Two of the chosen conserved residues, Arg 242 and Asp 245, are located in the switch II loop L11. In the pKinI structure these residues stabilize L11, which is disordered in most kinesin crystal structures, to form a short helix that precedes the switch II helix α4 (Figure 1-4c). Interestingly, the stabilizing hydrogen-bonds that these residues form are with switch I residues (Ser 210 and Arg 211) that are conserved in all kinesins and crucial to their function (Supplementary Figure 1-10).

The other KinI-specific conserved residues that were mutated, KVD (Lys40-Val41-Asp42), KEC (Lys268-Glu269-Cys270) and Arg272, were expected to affect MT or tubulin binding by pKinI. KEC and Arg272 are located in the region proven to be the major MT-binding site for kinesin motors, at the C-terminus of the long switch II helix adjacent to the L12/α5 region (Woehlke et.al., 1997). KVD is a set of pKinI-conserved amino acids in the family-specific insertion in loop L2, which might also contact the MT based on EM experiments in pKinI (Moores et.al., 2003) and proteolysis experiments in NCD (Alonso et.al, 1998).

To analyze how the chosen family-specific residues may confer MT depolymerization activity on a kinesin motor, we assessed the ability of the purified mutant proteins to depolymerize MT. Results of these studies (Figure 1-6, blue bars) showed that most of the selected residues affect the depolymerization activity of the protein, with KEC and KVD mutants showing no significant depolymerization, and R272A and R242A mutants displaying activities significantly lower than that found for wild-type pKinI. One notable exception is the D245A mutant, which depolymerized MT as well as wild-type pKinI.

To further study the interaction of the mutants with microtubules, we employed EM methods (Figure 1-7). In the presence of the non-hydrolyzable ATP analogue AMPPNP, wild-type pKinI forms characteristic motor-tubulin ring structures (circles in Figure 1-7), which reveal the tubulin deformation mechanism of KinI-catalyzed microtubule depolymerization (Moores et al., 2002). Only one of the pKinI mutants, D245A, formed these ring structures, consistent with its ability to depolymerize microtubules with an activity similar to that of wild-type pKinI (Figure 1-6). We

examined the microtubule binding activities of the pKinI mutants both by visual inspection (arrows in Figure 7) and optical diffraction (not shown). The pKinI mutants displayed a range of microtubule decoration by these criteria - from KEC, which showed essentially no decoration, to KVD, which showed very clear decoration (Figure 1-7). These results reflect a general trend in the degree to which the alanine substitutions affect the motor's ability to interact with its microtubule substrate. The KVD mutant was particularly striking in this respect since it was able to bind the microtubule lattice (Figure 1-7) but showed no depolymerization activity (Figure 1-6).

To determine which steps in the pKinI catalytic cycle are affected by the introduced mutations, we also analyzed the ATPase activities of the mutants (Figure 1-6), in the presence of either microtubules (red bars) or free tubulin dimers (yellow bars). Our results showed that MT and tubulin subunits at concentrations of 100 μg/mL (0.91 μM) equally stimulated ATP hydrolysis by wild-type pKinI. Similar results were obtained in other studies (Moores et.al. 2003, Hunter et.al. 2003), confirming that KinI ATPase activity can be stimulated by GDP-bound tubulin dimer. This finding contrasts with the ATPase activities of other kinesin motors, which are highly stimulated by MT but not by tubulin.

In our study, R242A mutant showed only half the ATPase activity of wild-type pKinI, with addition of either MT or tubulin. D245A mutant had ATPase activity similar to wild-type for both MT and tubulin. KEC mutant had almost no activity in the presence of MT, but ~27% activity in the presence of tubulin compared to wild-type pKinI. R272A mutant had only about a third of wild-type activity in the presence of both MT and tubulin. Finally, KVD had very little activity with MT but retained most of its

activity with tubulin. The latter mutant contrasts with the other tested mutants, which showed similar decreases in activity under both conditions.

The pKinI-MT complex

We put these observations concerning the structure and activity of pKinI into the context of its MT interaction by docking our crystal structure into the electron density of a pKinI-ADP-MT map determined using cryo-electron microscopy and helical image analysis (Figure 1-8; Moores et al., 2003). This modeling experiment showed the location of mechanistically significant parts of the motor with respect to the MT surface. We also docked the tubulin heterodimer structure (Löwe et al., 2001) into the MT portion of the map to create a pseudo-atomic model of the motor-MT interaction. As with other kinesins, and described previously (Moores et al., 2003), pKinI makes its main contacts with the MT surface by interacting with the C-terminal helices H11 and H12 of α- and β-tubulin (in yellow).

The switch II cluster of pKinI (shown in red), which includes the mutated residues R242, R245 in loop 11 and R272 and KEC in α4, abuts the intra-dimer interface of the $\alpha\beta$-tubulin heterodimer and thus plays a key role in the pKinI-MT interaction. In particular, this explains the reduced binding and ATPase activity of the R242A, R272A and KEC mutants. The absence of effect of the R245A mutation in this key area suggests that this conserved residue is likely to have a role in the context of full-length pKinI. KinI-specific residues may also help to couple ATP binding with movement of the α4 helix between the tubulin subunits of the dimer, bringing about the characteristic KinI ATP-induced deformation of the dimer and subsequent MT depolymerization.

Loop L2, the location of the KVD mutation, is depicted in cyan and lies close to the MT surface. It also lies close to the conformational change which pKinI undergoes when it releases ADP on binding to the MT (black density; Moores et al., 2003). Since this loop contains a number of KinI-specific residues, it is an ideal structural candidate for participating in KinI-specific functions associated with MT-lattice regulation of pKinI activity (Moores et al., 2003) and MT-end stimulated depolymerization. The fit shown has L2 hanging partially outside the pKinI EM density, strongly supporting the idea that L2 undergoes a conformational rearrangement relative to the crystal structure when initially bound to its MT substrate. The behavior of the KVD mutant also points to the role of L2 in the pKinI bending step of depolymerization, so it is likely to undergo further conformational changes as depolymerization proceeds.

Loops L8 and L12 (in orange) are proposed to be the other major point of contact between kinesins and MTs (Woehlke et al., 1997; Alonso et al. 1998). The MT surface is not accessible to L8, due to both its unusual conformation and the length of α4 in our pKinI structure, which perhaps reflects a preference for binding instead to the curved tubulin dimer. However L12, along with L2, is sufficient to form anchor points on the MT surface at either end of the motor, between which the ATP-sensitive switch II components can act directly on the motor substrate.

Discussion

Structure: differences from other kinesins

A unique feature of the pKinI structure is the conformation of switch II. The long switch II helix (α4) is stabilized to be 3 turns longer than in the NCD structure (Figure 1-2), and the switch II loop (L11) is stabilized by family-specific residues to form a short helix (Figure 1-4c). This stabilization of the switch II region by family-specific residues may be important for pKinI's unique depolymerization activity. However, a long switch II helix and ordered switch II loop have been seen in a few other kinesin structures, such as Kif1a-ADP (Kikkawa et.al., 2001), so it is difficult to interpret this structural feature in terms of KinI function.

Other specific structural features of pKinI may also relate to its function as a depolymerizing enzyme. The "arrowhead" tip (L6 and L10) is the site where the neck linker docks on the catalytic core in other kinesins (Sablin et.al., 1998). The fact that the pKinI tip is bent away from the MT-binding site (Figure 1-2) suggests that its neck may dock onto the catalytic core in a novel way, possibly accommodating a better fit of the motor to the curved surface of the tubulin protofilament. The opposite pole of the motor is distinguished by the long loop L2 which contains family-specific insertions (Figure 1-2, 1-5), and our docking experiment demonstrates that this region is involved in specific interactions with the MT. The structure of L8, another MT-binding loop, might also be related to pKinI function. The unique configuration of this loop could reduce normal kinesin-MT interactions and allow a better fit to curved tubulin.

<u>Structure: lack of nucleotide</u>

A surprising feature of the pKinI structure is the absence of the nucleotide in the binding pocket. The first structure of myosin S1 also had sulfate in place of nucleotide (Rayment et.al., 1993), and additional myosin structures have been obtained in this state as well as other nucleotide states (Houdusse et.al, 2000; Coureux et.al, 2003), but this is the first such kinesin structure found. Moreover, though many crystallization conditions were tried with numerous ATP/ADP analogues, we have not yet been able to grow pKinI crystals with nucleotide bound.

Kinetic data suggest that ADP release in the absence of MT is much faster for pKinI than for all other kinesins analyzed, (M. Hekmat-Nejad, manuscript in preparation), which might explain the absence of bound nucleotide in the pKinI pocket. However, although some binding-pocket residues differ between KinI and other kinesins (Supplementary Figure 1-10), there is not a difference striking enough to explain how local environment could lead to pKinI's lower affinity for ADP. In addition, it is possible that our crystallization conditions, a combination of high sulfate (1.6M) and low pH, might have also helped to shift the protein toward the nucleotide-free state, by providing the sulfate ion that occupies the binding pocket. However, a nucleotide-free structure was not obtained for human conventional kinesin at a similar sulfate concentration (Sindelar et.al., 2002). The nucleotide-free pKinI structure is probably a reflection of both high sulfate conditions and possible lower affinity for ADP, and we do not expect that this state would predominate under more *in vivo* conditions.

Our analysis of the key elements in the nucleotide binding pocket (Figure 1-4) suggests that the pKinI crystal structure has essentially an ADP-like conformation. It is

difficult to draw further conclusions from this fact, because the nucleotide state and structural state are often unrelated for crystal structures of both kinesins and myosins; some ADP-bound structures display an ATP-like state, apparently because the barrier between the ADP-like and ATP-like states is low in the absence of their respective polymer substrate (MT or actin) (Kikkawa et.al., 2001). A structure of KinI in a more radically-altered, ATP-like state is desirable in order to understand better the conformational changes that occur during the KinI nucleotide cycle.

pKinI ATPase activity: tubulin vs. MT

Plasmodium KinI ATPase activity increases in the presence of tubulin dimer as well as MT. These results are consistent with the recent finding that MCAK ATPase activity is enhanced in the presence of free tubulin dimers (Hunter et.al., 2003). However in contrast to the results with full-length MCAK, which showed relatively low ATPase activity in the presence of tubulin compared to MTs, the ATPase activity of pKinI catalytic core was comparable in the presence of 100 µg/mL (0.91 µM) of MT and tubulin. The most likely explanation for this difference in relative activities is that the non-core portions of full-length KinI, which are not present in our construct, might help the motor to distinguish polymer ends from free tubulin dimers, increasing the enzyme's efficiency. Supporting this, pKinI ATPase activity is actually inhibited at higher concentrations of MT (Moores et.al., 2003); similar results are seen for the mutants with significant MT-stimulated ATPase (R272A, R242A, D245A – data not shown).

pKinI mutants: strategy

pKinI has a number of characteristic properties which include microtubule depolymerization, ATPase stimulation by both polymerized and unpolymerized tubulin, binding to the microtubule lattice and the ability to form tubulin-motor ring complexes in the presence of the non-hydrolyzable ATP analogue AMPPNP. All these properties likely reflect aspects of a general KinI depolymerizing mechanism. The crystal structure of pKinI provided us with the opportunity to visualize the location of KinI-specific residues. We mutated a number of these residues and tested for the above activities and were able to develop a consistent view of the role these residues might play in the KinI mechanism.

pKinI mutants: microtubule-depolymerizing loop 2 (KVD)

In the KinI family, L2 has an insert of highly conserved family-specific residues (K40-V41-D42) (Supplementary Figure 1-10), so this region was expected to be especially important for the family's unique function. The KVD mutant, with the three L2 residues mutated to alanine, showed only a small reduction in ATPase activity in the presence of free tubulin dimer (Figure 1-6), indicating that the protein's ATP binding and hydrolysis apparatus was relatively unaffected, along with its ability to bind tubulin in order to stimulate hydrolysis. EM results also showed that this mutant could bind MT well. However, it showed very little if any depolymerization activity, paralleling its low ATPase activity in the presence of microtubules. Because the very low depolymerization rate for KVD is not due to changes in the ATP hydrolysis machinery itself, or an inability to bind microtubules or tubulin, this family-specific insertion in L2 is the first region identified as specific for initiating MT depolymerization.

A pseudo-atomic model of the pKinI-MT complex (Figure 1-8) demonstrated that L2 is located close to the MT surface, as has been shown for this region in other kinesin family members (Kikkawa et al., 2001; Sosa et al., 1997). However, the mobility of this region suggested by the docking, and the proximity of L2 to a site of significant conformational change during the motor's ATPase cycle, support a specific role for L2 in pKinI regulation and depolymerization.

pKinI mutants: microtubule-binding switch II helix (KEC and R272)

Four KinI-conserved residues were mutated in the central kinesin-MT binding site (α4). Mutating KEC to alanine led to essentially no depolymerization or ATP hydrolysis in the presence of MT, and substantial decrease in ATPase activity in the presence of free tubulin (Figure 1-6). EM images show that KEC barely decorates the MT (Figure 1-7). The latter results strongly suggest that the low depolymerization activity seen for this mutant is due to its lowered ability to bind MT. The alanine mutant of R272, the residue that emanates from α4 one helical turn below KEC (Figure 1-5), shows similar assay results (Figure 1-6), supporting a similar role of this residue in MT binding, while our docking experiment clearly demonstrates the proximity of these residues to the MT surface. The lesser effect of the R272A mutation on MT-binding and ATP hydrolysis is likely due to only one residue being mutated, instead of three in the KEC mutant. Similar ATPase activities of these mutants in the presence of free tubulin, as compared to R242A, suggest that both mutants partially retain their ability to bind tubulin in its curved form.

pKinI mutants: nucleotide-contacting switch II loop (R242 and D245)

In pKinI, the switch II loop, which links the bound nucleotide to the conformation of the microtubule-binding site (Song and Endow, 1998), contains two family-conserved residues, R242 and D245. R242A mutant showed about half the wild-type activity for depolymerization and for ATP hydrolysis in the presence of both MT and tubulin (Figure 1-6), and EM results also showed that the ability of this mutant to depolymerize is partially impaired (Figure 1-7). However, although R242 is absolutely conserved in the KinI family, basic amino acids at this position are not unique to KinI (Supplementary Figure 1-10). This suggests that, unlike KVD, R242 is not specifically important for depolymerization. This idea is supported by the general reduction in ATP hydrolysis activity for R242A, which points toward the mutant having its primary effect on hydrolysis, and affecting depolymerization only as a result of this. R242A mutant can still bind to MT (Figure 1-7), and the residue is close to the binding pocket and hydrogen bonds with an important switch I residue (Figure 1-4c), suggesting that R242 plays a more direct role in ATP hydrolysis, and possibly MT binding as well but to a smaller degree (Figure 1-8).

For the D245A mutant, depolymerization and ATPase activities, in the presence of either MT or tubulin, are not reduced by the alanine substitution. It is possible that D245, which is conserved only in the KinI family, plays its role in the activity of full-length dimeric KinI. Most other kinesins have a basic residue at this site, suggesting that negatively-charged D245 might help to reduce non-productive binding of KinI to the MT surface. In addition to this residue, the other parts of the full-length KinI protein, especially the ~60 a.a. neck domain, might be important for targeting the motor to the

ends of the MT, so that non-productive binding does not occur and depolymerization efficiency is maximized.

pKinI ATP-hydrolysis requires binding to curved tubulin dimer

Studying ATPase activity in the presence of either MT or tubulin dimers allowed us to further compare the pKinI mutants. They fall into two types: those that decrease KinI ATPase activity to the same degree under both conditions (R242A, R272A), and those that decrease the activity more in the presence of MT (KEC, KVD) (Figure 1-6). KVD is especially striking for the discrepancy in its relative activity between the two conditions. Combined results of these studies show a general pattern: relative depolymerization activity of each test mutant is very similar to its relative MT-stimulated ATPase activity. In particular, KVD mutant has intact ATP hydrolysis machinery, as seen in the tubulin assay, but can neither depolymerize microtubules nor hydrolyze ATP when bound to them (Figure 1-6).

Earlier studies showed that KinI bound to non-hydrolyzable AMP-PNP induces curvature in stabilized microtubules (Desai et.al., 1999; Moores et.al., 2002), supporting the idea that MT curvature occurs before ATP hydrolysis and not at the same time. This, along with our results, suggests that the motor domain only hydrolyzes ATP when bound to curved tubulin, either as free GDP-bound dimers, or at the ends of microtubules where curvature has been induced to start depolymerization. This suggests a model for the enzyme's mechanism: KinI binds to the straight tubulin protofilament, but cannot hydrolyze ATP until it has forced the tubulin dimer to which it is attached to become curved, i.e. until it has initiated depolymerization. Only then can it hydrolyze ATP and

release itself from the tubulin surface. Thus, the only difference between ATPase activity in the presence of MT and of free tubulin dimer is that the MT must be depolymerized first.

Model for KinI core-domain function

Based on combined results of our structural and mutational studies, we present here revisions to the KinI mechanism (Figure 1-9). We propose that when KinI has reached the MT end and lost its ADP nucleotide, the switch II cluster makes the major contact with tubulin at the interdimer interface, while the family-specific L2 residues and the N-terminal "neck" domain (along with L12 and possibly L8), which are located at opposite ends of the catalytic core (Figure 1-9), provide anchor points around the switch II cluster.

ATP binding induces a conformational change that results in L2, the neck, and L12 (and maybe also L8) tugging and bending the tubulin protofilament underneath. In the resulting "curved" tubulin conformation, contacts between the KinI and the tubulin dimer are maximized, perhaps by enabling L8 to contact tubulin. This stabilizes the activation state, triggering hydrolysis of the ATP. After ATP hydrolysis the KinI binding to the tubulin dimer is weakened, leaving KinI free in solution to bind another MT protofilament and further catalyze depolymerization.

Methods

Crystallization and model determination: Cloning, expression and purification of the

motor domain of MCAK from *Plasmodium falciparum* is described in Moores et al.,

2002 (Supplemental Data). Protein fractions of >95% purity were pooled and

concentrated to 10-20 mg/ml. Crystals were grown in sitting drops by mixing equal

volume of protein solution with well solution containing 1.4-1.8M ammonium sulfate,

100 mM sodium acetate, pH 5.0 and 200 mM sodium nitrate. Crystals typically appeared

in 1-2 days and were harvested after growth of 1-2 weeks at 4C. Crystals (typically

100x50x50 μm) were transferred to well solution containing 30% glycerol and then

frozen in liquid nitrogen. Diffraction data were collected at beamline 9-1 at SSRL and

8.3.1 at ALS. At least 10 different data sets were collected in an effort to obtain crystals

with nucleotide bound to the protein. All attempts were unsuccessful, as judged by the

electron density maps obtained by molecular replacement methods. The structure

presented here reflects data collected at ALS beamline 8.3.1. The data were processed

with DENZO and SCALEPACK (Otwinowski and Minor, 1997) and the structure solved

by molecular replacement methods using CNS programs (Brunger et.al, 1998) and the

KAR3 structure (Yun et.al., 2001; PDB code 1F9T) as a search model. The model was

built using QUANTA (Accelrys) and refined using CNS programs, with three final

rounds of refinement using Refmac 5.1.24 (Collaborative Computational Project No. 4,

1994) and validation using PROCHECK (Laskowski et.al., 1993). Figures were prepared

using Bobscript v2.4 (Esnouf, 1997). The model presented here contains 318 amino

acids, 306 waters and one sulfate. It has working R=0.202 and R_{free}=0.230. Residues

157-167 are disordered. It has been submitted to the PDB and is accessible with reference code 1RY6.

Preparation of pKinI mutants: Point mutations were introduced using the QuikChange kit (Stratagene). Proteins were purified as described by Moores et al., 2002 (Supplemental Data).

ATPase Assay: The ATPase activity of pKinI was measured using the NADH-coupled system of Huang and Hackney (Huang and Hackney, 1994). Initial rates of microtubule- or tubulin-stimulated ATP hydrolysis by pKinI were measured at several different pKinI concentrations ranging from 5 to 40 μg/ml (0.12 to 0.98 μM) at room temperature in BrB25 buffer consisting of 25 mM Pipes [pH6.8], 2 mM $MgCl_2$, 1 mM EGTA, 1 mM DTT and with 1.5 mM ATP, 100 μg/ml microtubules or 100 μg/ml tubulin subunits (0.91 μM for tubulin dimer subunits, both free and in polymer). Results are shown for 10 μg/ml (0.25 μM) pKinI.

Microtubule depolymerization assay: All concentrations are final in the reaction mixture. Microtubules were polymerized from purified, prespun porcine tubulin at 37°C for 30 minutes in the presence of 1.2 mM GTP, 1 mM DTT, and 10% DMSO followed by another 5-minute incubation at 37 °C with 20 μM taxol. Polymerized microtubules were spun over 1 ml of sucrose cushion consisting of 40% sucrose in BrB25 buffer with 20 μM taxol in 1-ml aliquots at 25 °C. Microtubule pellets were washed and resuspended in BrB25 buffer with 20 μM taxol. 20 μg/ml *Plasmodium* KinI (0.49 μM) was incubated

with 200 µg/ml (1.8 µM) of purified microtubules in the presence of 3 mM ATP or 5 mM

ADP and 10 units/ml of apyrase (in this case pKinI was preincubated with ADP and

apyrase for 15 minutes prior to the addition of the microtubules) or with no nucleotide

added for 15 min at room temperature. Microtubule polymers were separated from

tubulin subunits by ultracentrifugation of 150 µl of the reaction mixture at 55,000 RPM

in a TLA-100 rotor at 25°C for 15 minutes. Aliquots of the samples prior to

ultracentrifugation, the supernatant and pellet fractions were analyzed by SDS-PAGE.

Tubulin bands on coomassie-stained gels were quantified using the Fluorchem digital

imaging system (Alpha Innotech Corporation).

The molecular weights used for calculating the molar concentrations of pKinI and tubulin

dimers are 40711 and 110,000 respectively. "% tubulin depolymerized" shown in Figure

1-6 was calculated by determining the percentage of free tubulin (tubulin in S / (tubulin

in S + tubulin in P)) for the reactions incubated with pKinI and ATP, and subtracting

from this the percentage of free tubulin from the reactions with no pKinI. This yielded

the percentage of tubulin that was depolymerized actively, rather than through MT

dynamic instability.

Electron microscopy of pKinI mutants and microtubules: pKinI mutants incubated

with AMPPNP (ICN) and taxol-stabilized microtubules were prepared as described in

Moores et al. (2002). The concentration of polymerized tubulin in the assay was 5µM and

of each of the constructs was: wild type pKinI 11µM, D245A 17µM, R242A 24µM, KEC

6µM, R272A 10µM and KVD 7µM.

Table 1-1: Data Collection and Refinement Statistics

Crystallization	
Space group	$P3_221$
Unit Cell Dimensions	
a (Å)	105.59
c (Å)	84.77
Molecules per asymmetric unit	1
Resolution (Å)	1.6
Number of unique reflections	66077
Completeness (%)	91.5 (84.5)
R_{symm} (%)	4.8 (36.9)
$< I/\sigma(I) >$	15.52 (1.75)

Refinement (24.9 - 1.60 Å)	
R	0.2023
R_{free}	0.2304
Rms deviation from ideality	
Bond length (Å)	0.022
Bond angle (°)	1.871
Average B factor (Å^2)	27.0

Number in parenthesis is for the last resolution shell (1.62–1.69 Å)

$R_{symm} = \Sigma_h |I_h - I| / \Sigma_h I$, where (I) is the mean intensity of reflection h

R_{free} is for 5% of total reflections not included in the refinement
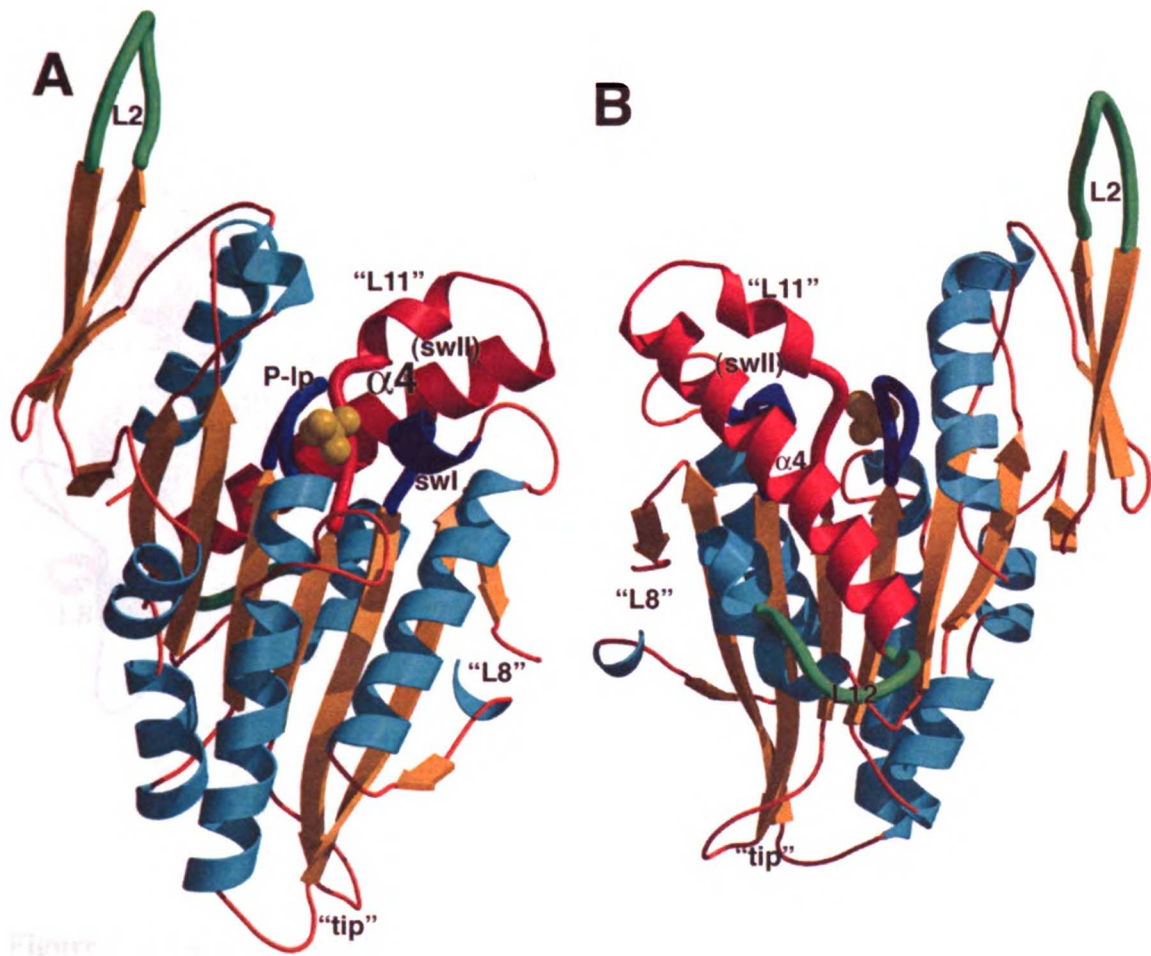
Figure 1-1. 1.6 Å X-ray crystal structure of pKinI. Important areas for kinesin function are highlighted: part of the MT-binding surface (L2, L12) in green; blue nucleotide binding pocket (P-loop, switch I); and red switch II (L11-α4), which contacts both the MT and the nucleotide. The sulfate found at the β-phosphate position is represented as yellow balls.

Figure 1-2. Comparison of pKinI with the most structurally-similar gliding motor, NCD. Common elements are shown in gray, differing pKinI parts in red and differing NCD parts in blue. The sulfate ion that marks the β-phosphate of ADP is shown in yellow. The largest differences are the length of L2, the positioning of the "tip" (L6 and L10), the direction of L8, and the unusual stability of the switch II region (L11-α4).

33
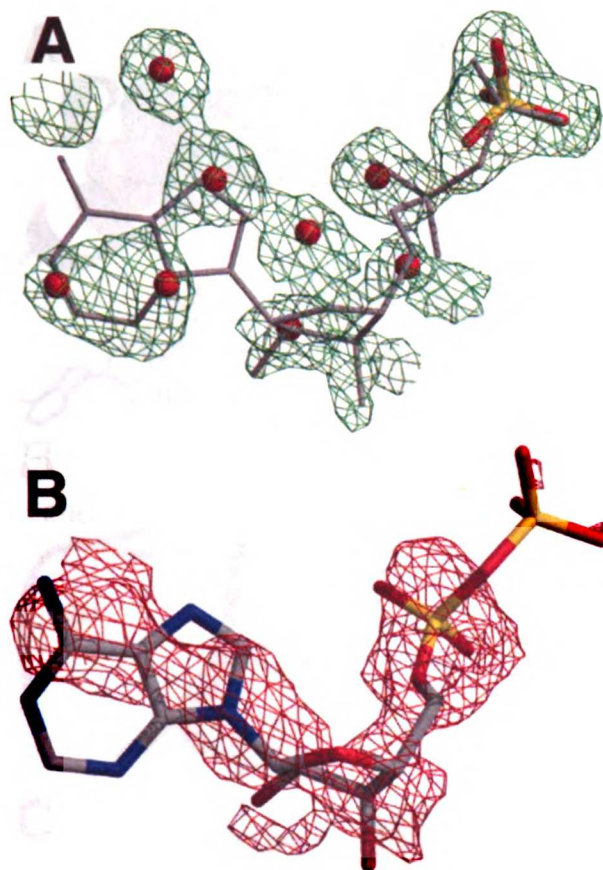
Figure 1-3. Electron density in pKinI nucleotide-binding pocket shows solvent. A) Green 3Fo-2Fc map (level = 1σ) shows where both the data and model predict density (sulfate and waters – ADP in gray for reference, from Kif1a-ADP model). B) With inclusion of ADP in the pKinI model, and one round of refinement, red Fo-Fc map (level = -2.5σ) indicates where the model predicts density that the data do not support.
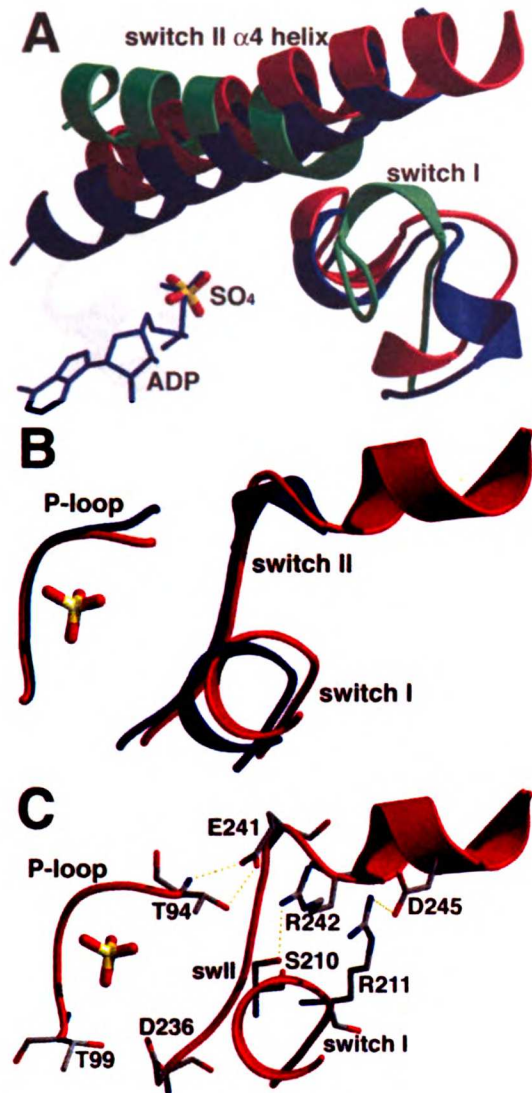
Figure 1-4. Switches I and II and the binding pocket region of nucleotide-free pKinI.
A) Comparison of switch regions between pKinI (red), Kif1a+ADP (blue) and Kif1a+AMP-PNP (green). Stick models are shown for ADP (blue) and the sulfate from the pKinI model that sits at the β-phosphate position. B) Shift of the switch I and switch II loops of pKinI (red), compared to Kif1a-ADP (blue). This may represent an opening of the binding pocket in the absence of nucleotide, but it is very small. C) pKinI binding-pocket hydrogen bonds, as discussed in the text, between KinI-conserved switch II residues R242 / D245 and absolutely-conserved switch I residues S210 / R211.

Figure 1-5. Location of pKinI amino acid substitutions. Red spheres mark the 3 residues and 2 residue triplets (K40/V41/D42 and K268/E269/C270) that were mutated to alanine and assayed for their effects on ATP hydrolysis and MT depolymerization.
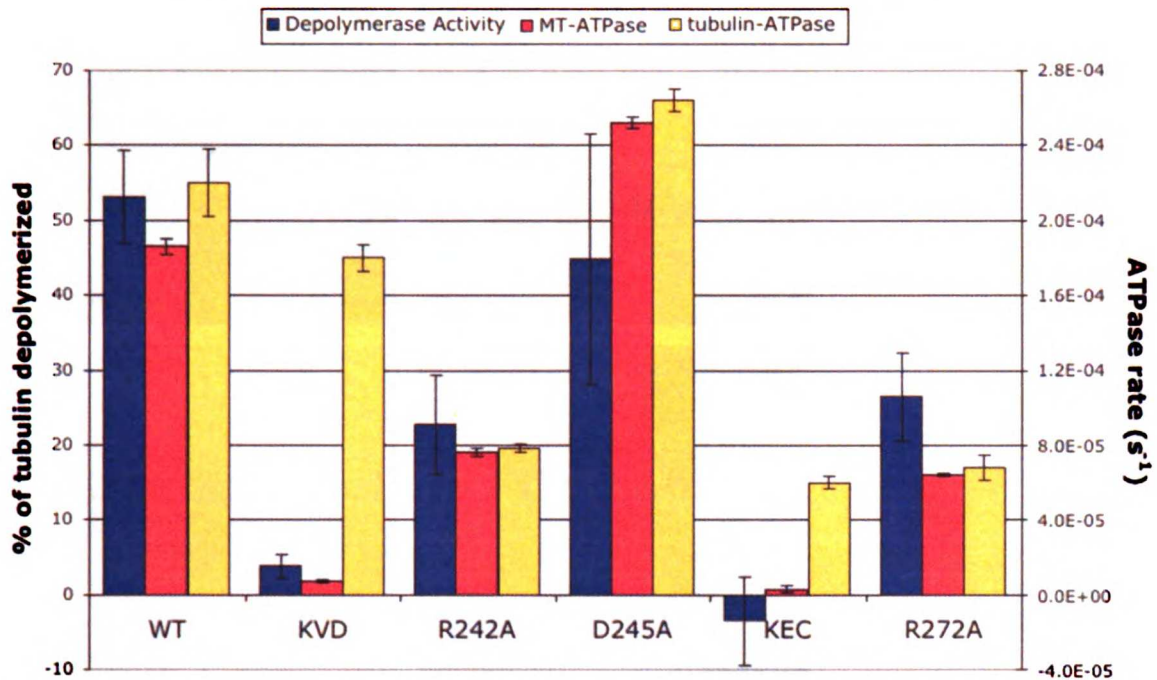
Figure 1-6. ATPase and depolymerase activities of wild-type pKinI and the alanine mutants. Depolymerization activity is shown by the blue bars. ATPase activity in the presence of MT is shown in red, while ATPase activity in the presence of free tubulin dimer is shown in yellow. Error bars represent one standard deviation. Note the large difference between MT-ATPase and tubulin-ATPase activities seen for KVD, and to a lesser degree for KEC. Note also that decreases in depolymerization activity roughly correlate with decreases in MT-ATPase activity.
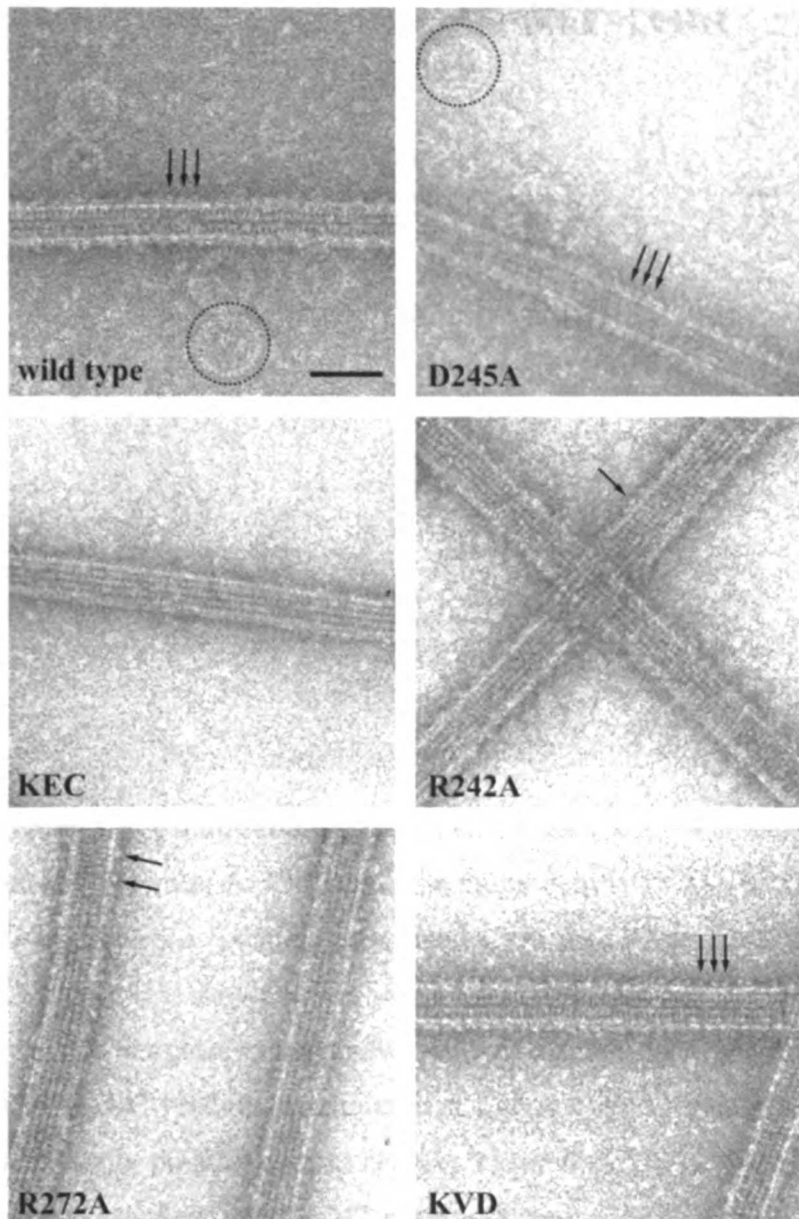
Figure 1-7. Mutations in the pKinI motor core affect its ability to bind and depolymerize microtubules in the presence of the non-hydrolyzable ATP analogue AMPPNP. Each pKinI construct was incubated with AMPPNP and taxol-stabilized microtubules, the mixture was centrifuged and the pellet fraction was resuspended and examined by negative stain microscopy. Characteristic motor-tubulin ring complexes which form under these conditions are shown in the dotted circles and examples of motors bound along the microtubule lattice are indicated with arrows. Tubulin oligomers are also observed in the background. Scale bar = 400Å.

MT +end
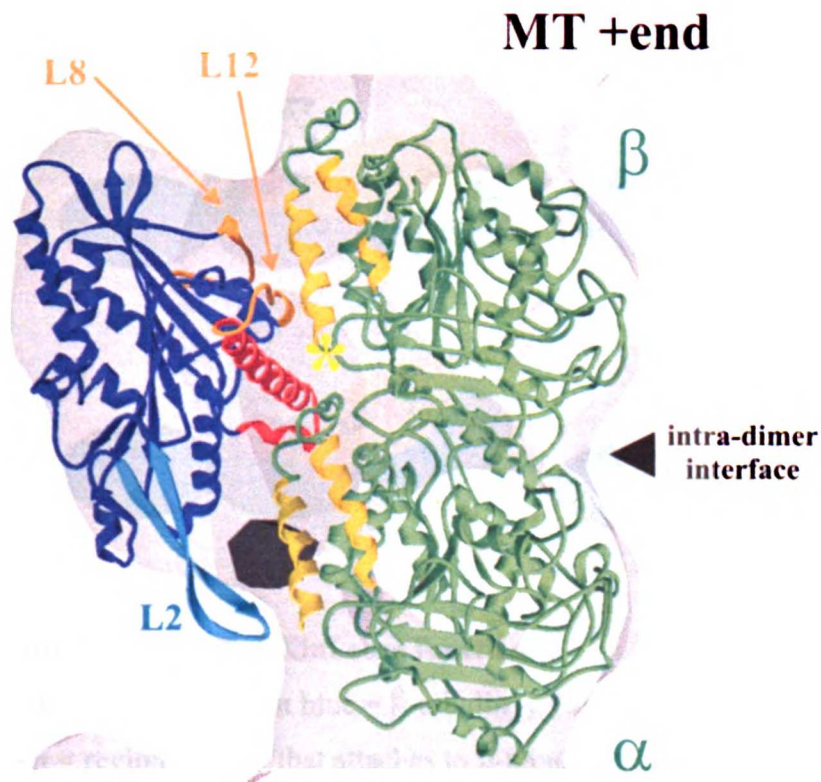
Figure 1-8. Pseudo-atomic model of the pKinI- MT complex. The crystal structure of pKinI (blue) was docked within the motor density of the pKinI-ADP-MT map (grey). The switch II cluster (including the mutated residues R242, R245 in loop 11 and R272 and KEC on α4) is shown in red, while loop L2 (location of KVD mutation) is depicted in cyan. L2 lies close to the conformational change which pKinI undergoes when it releases ADP on MT binding (black density). Loops 8 and 12 (orange) are proposed to be the other major point of contact between kinesins and MTs. The structure of GTP-tubulin (green) was fit within the MT portion of the map; H11 and H12 helices of α- and β-tubulin are shown in yellow and the position of the disordered β-tubulin C-terminus, essential for pKinI depolymerization, is marked with a yellow asterisk (to the right of the long red switch II helix). The figure was prepared by manually docking the coordinates of pKinI and the αβ-tubulin heterodimer (1JFF, Löwe et.al., 2001) into the pKinI-ADP-MT map using AVS (Advanced Visual Systems).
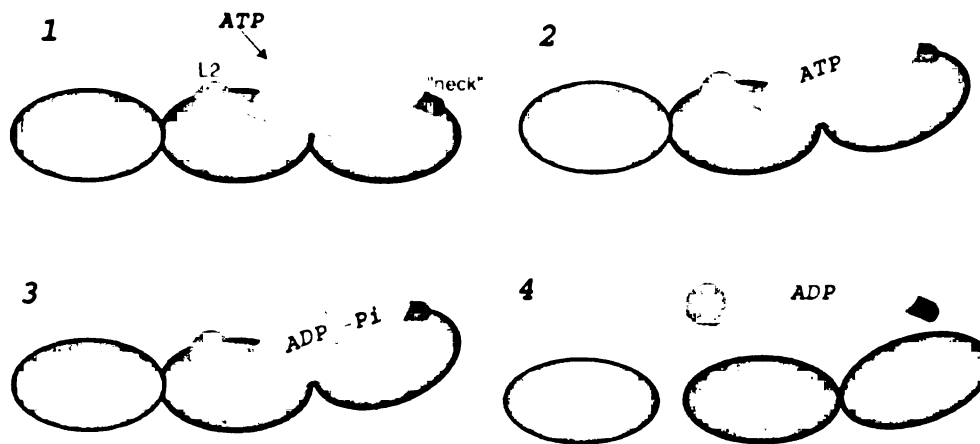
Figure 1-9. Model of KinI core function.

purple = α-tubulin, light blue = β-tubulin, yellow = KinI catalytic core, red = loop 2, green = region of KinI that attaches to β-tubulin (possibly N-terminal "neck", L12, L8)

1) When KinI recognizes and binds a tubulin dimer at the end of a MT, L2 binds to α-tubulin, and another KinI element, such as L12 and/or the neck, binds to β-tubulin. The majority of the KinI core binds at the intradimer interface.

2) When ATP binds to KinI, it induces a conformational change in the catalytic core that pulls the tubulins at the L2 and "neck" attachments and pushes in at the intradimer interface, curving the dimer.

3) With KinI in this new tubulin-binding conformation, ATP hydrolysis is stimulated.

4) ATP hydrolysis weakens the tubulin dimer's connection to the MT, releasing the dimer-KinI complex. It also weakens KinI binding to tubulin, freeing KinI into solution for rebinding and continued depolymerization of MT.

Supp. Figure Alignment of pKinI motor domain with those of well-studied KinI's and two non-KinI kinesins
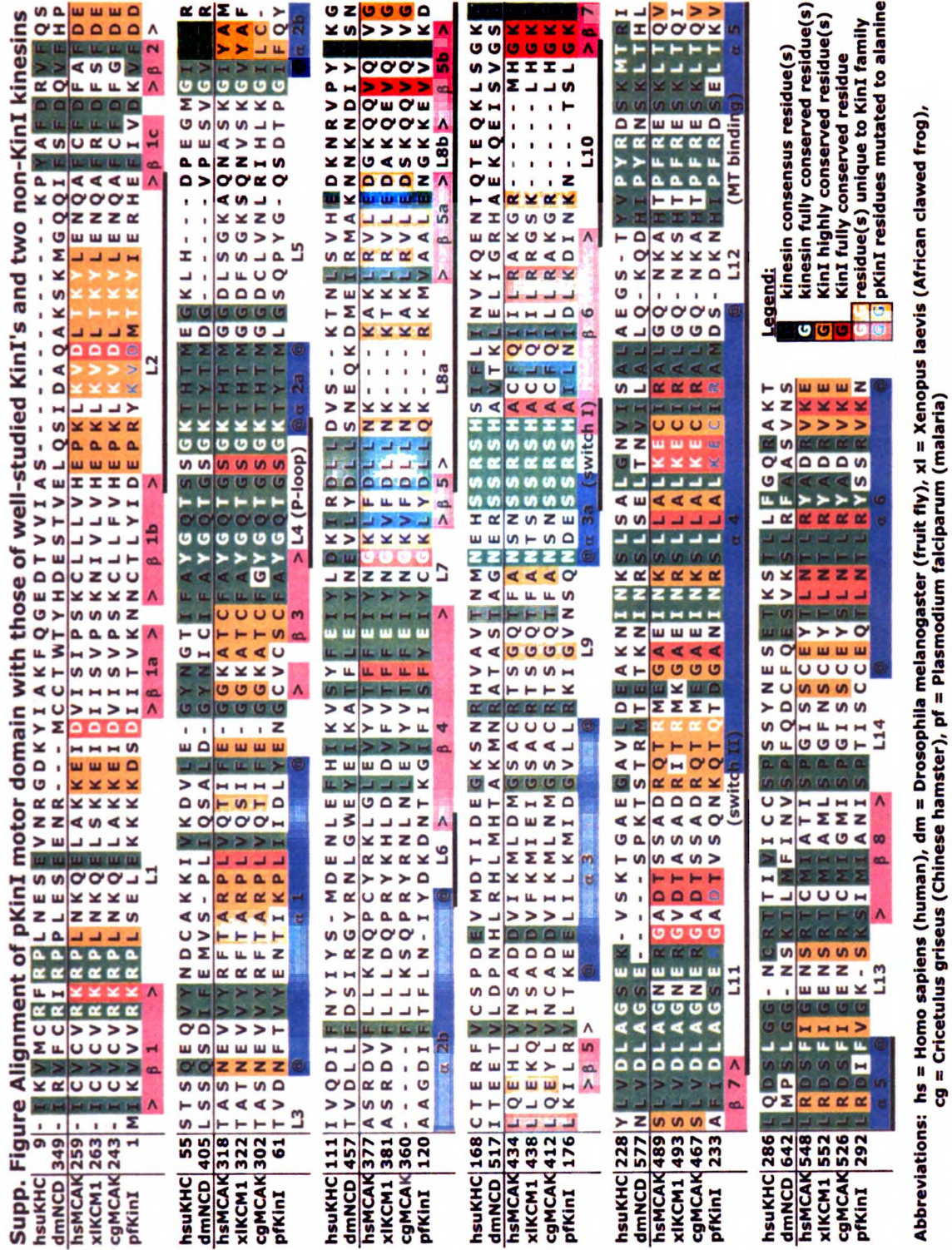
Supplementary Figure 1-10. Alignment of pKinI motor domain with those of well-studied mammalian KinI's and with the walking kinesins hsuKHC and dmNCD.

Abbreviations: hs = Homo sapiens (human), dm = Drosophila melanogaster (fruit fly), xl = Xenopus laevis (African clawed frog), cg = Cricetulus griseus (Chinese hamster), pf = Plasmodium falciparum (malaria)

Legend:
- kinesin consensus residue(s)
- kinesin fully conserved residue(s)
- kinesin highly conserved residue(s)
- KinI fully conserved residue
- KinI residue(s) unique to KinI family
- pKinI residues mutated to alanine

41

Chapter 2: Testing sufficiency of KinI Loop2 and neck for

microtubule end-targeting and depolymerization

Introduction

After publishing my journal article in EMBO Journal (reprinted as Chapter 1), I

needed to choose a good project involving Kinesin-13/KinI that could be done in two

years. The most interesting one for most in the field would be determining the X-ray

crystal structure of the complex of *Pf* KinI with tubulin heterodimer, possibly in the 13-

fold ring form (Moores et.al., 2002) and probably with both proteins bound to non-

hydrolyzable nucleotide analogues (AMPPNP and GMPCPP, respectively). While this

would have been valuable experience in crystallography, and an extremely strong

publication if it worked, it was overly optimistic to think it could be done in two years,

especially because the rings hadn't yet been purified by anyone to a degree close to that

required for crystallography. So as a simpler plan, I decided to look at the most

important KinI regions for depolymerization, and test their sufficiency by introducing

them into walking kinesins.

Importance of Loop2 for Depolymerization

KinI's (Kinesin-13's) all contain a large, unique and highly conserved insert in

the motor core's Loop 2 (Supplementary Figure 1-10), which forms a structured beta-

hairpin rather than the unstructured loop found in most kinesins (Figure 1-1; Ogawa et.al.

2004). In our previous study (covered in Chapter 1), mutation of the key *Pf* KinI Loop2 residues K40-V41-D42 to alanine led to protein that could still bind microtubules (Figure 1-7) and could hydrolyze ATP at levels near that of unmutated protein in the presence of free tubulin (Figure 1-6 yellow bars), but had greatly reduced depolymerization activity (Figure 1-6 blue bars). Because this could not be explained as weakening of the machinery for ATP hydrolysis or microtubule binding, the results strongly suggested that these residues, and probably other conserved residues in Loop2, are specifically required for depolymerization.

Another paper describing the structure of the mouse KinI Kif2C with class-specific neck (Ogawa et.al., 2004) found similar results to ours after mutating the KVD triplet to alanines. Their assays were slightly different from ours: they looked at microtubule-binding and depolymerization activity *in vivo*, and did not measure ATP hydrolysis activity. With neck in the construct (see next section for a focus on neck specifically), the KVD mutant showed only 30% of wild-type activity, and even mutation of just one of the three residues led to 50-70% wild-type activity. It did not decorate microtubules, but neckless KVD mutant did, the same as our KVD mutant (Figure 1-8), and this construct showed effectively no depolymerization activity *in vivo*. From these results, they also conclude that KVD is specifically important for depolymerization.

Importance of KinI neck for Microtubule-end Targeting

Another region specifically conserved in (vertebrate) KinI's is the ~50 amino acid N-terminal neck region, which contains many positively charged residues. Earlier studies

found that lack of neck led to very low depolymerization activity compared even to motor with the neck (Maney et.al., 2001). Addition of polylysine or the K-loop from Kif1a, which can walk/diffuse on microtubules as a monomer, to neckless KinI mostly rescues depolymerization activity, and suggests that the neck also improves activity by helping the motor stay attached to and diffuse along the microtubule lattice.

The Kif2C structure (Ogawa et.al., 2004) includes the neck, and shows an interesting difference from other kinesins: rather than acting as an unstructured and flexible linker between dimers that points toward the plus-end-oriented motor "tip", it forms a helix and points more toward the minus-end in much the same direction as Loop2 (Figure 2-1). This neck would be situated to recognize exposed lateral tubulin surface when the motor is bound at the microtubule plus end, and possibly exposed longitudinal surface at the microtubule minus end (though Loop2 is in a better position to do that). Their *in vivo* activity studies showed that neckless Kif2C has very low depolymerization activity and decorates microtubules, while Kif2C with neck does not bind everywhere along the microtubule lattice. These results suggest how the neck could improve depolymerization efficiency by targeting the motor to either of the microbutule ends, the only place where depolymerization can occur and where ATP hydrolysis would not be wasted.
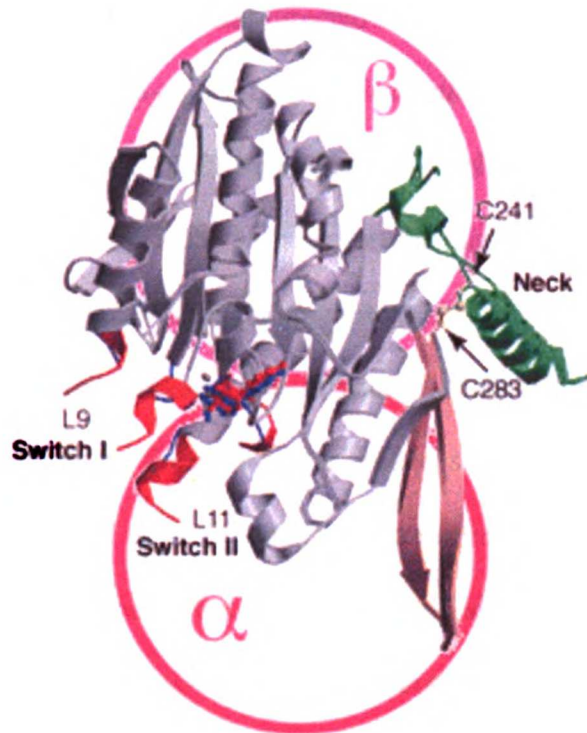
Figure 2-1: Structure of Kif2C with the N-terminal neck. The view looks down onto Kif2C as if it were sitting on top of the tubulin heterodimer. The neck is shown in green, Loop2 is the long pink beta-hairpin next to it. Structure reprinted from Ogawa et.al., 2002, with permission from Elsevier – the tubulin circles were added by me.

<u>Testing Requirement and Sufficiency of L2 and Neck for Depolymerization</u>

Both the KinI neck and Loop2 appeared to play important roles in microtubule depolymerization, where the neck targets the motor to the microtubule ends, and Loop2 helps induce curvature in the tubulin heterodimer, leading to further depolymerization. However, it wasn't yet certain whether they play the proposed roles, and whether these two functions are sufficient for depolymerization. To test this idea, I planned to add neck and Loop2 from human MCAK (hMCAK), which we have on hand, to motor cores from

well-studied walking kinesins: plus-end-directed human ubiquitous Kinesin Heavy Chain (huKHC or KHC), minus-end-directed *Drosophila melanogaster* NCD (dmNCD), and the Kif1a homologue *Caenorhabditis elegans* Unc104 (ceUnc104). They would be added where they are found in KinI's, with neck at the motor N-terminus and the KinI-specific insert added to Loop2 of the walking motors.

To study whether these regions are sufficient, I proposed to use two assays. First, I would add the neck and assay the neck-motor protein's ability to localize to the microtubule ends. This could be easily done using a fluorescence microscope and fluorescently labeled microtubules, but the motor would also need to be labeled – I chose to use Green Fluorescent Protein (GFP) in the gene constructs to visualize the motors' locations. Next, if the neck-motors were indeed able to localize preferentially to the microtubule ends, I would add the Loop2 insert, and use the cosedimentation assay from the previous paper (Chapter 1) to check for depolymerization activity. I would use the same cloning techniques with the hMCAK motor to make positive controls, and also make the neckless (and L2-less) versions of each for negative controls. GFP-less versions of each construct might also be preferable for the depolymerization assay, to reduce possible interference with activity.

Unfortunately, although the project was expected to be easy to do, the cloning ended up being much more difficult and time-consuming than expected, as detailed later. I ended up changing the experimental plans to doing the depolymerization assay first with neck-L2-motors, as it's the more interesting function to study, and success in that assay would imply ability to localize as well. The localization assay would be resorted to if no significant results were seen for the depolymerization assay. So far I have made all

46

three neck-motor-GFP constructs, and been able to express them in *E coli* and show that some soluble protein can be obtained. However, the expression and purification still needs to be optimized to make quantities sufficient for the assays, and the hMCAK Loop2 needs to be inserted and the expression/purification optimized for those constructs as well. In this chapter I detail the cloning, expression and purification of the neck-motor-GFP's, and give suggestions on how to perform the two assays and carry the project further.

Design of walking-kinesin motor cores with n-terminal KinI neck and GFP

Original construction plan: restriction-enzyme digests and ligation

For the localization assay, I wanted to make constructs of walking kinesins attached to GFP, so they would be visible on the microtubules. The Vale lab provided plasmids for human ubiquitous KHC, Drosophila melanogaster NCD and C. elegans Unc104 (a substitute for Kif1a, which is hard to get from the Hirokawa lab). The KHC plasmid included GFP, so I used this as my source for GFP DNA in cloning. We also had human MCAK (hMCAK) DNA that Jennifer Turner had acquired, so I used that for cloning out the KinI neck. I chose 3 different kinesins in order to improve the odds that at least one would work; KHC and NCD are very well studied, so if both constructs with hMCAK neck and L2 worked, it would be easier to do further studies (such as structural or ATPase activity) to compare with the current information. It would also suggest that

these two regions truly are sufficient to change function, if they work in two different motors.

Because I was using 3 different kinesins, I chose a cloning strategy that should work the same with all of them (Figure 2-2). All would have, from the N-terminus: 1) 6X-His tag for purification, 2) GFP, 3) a TEV cleavage site (QNLYFQG) to remove the GFP and His-tag for crystallography later, and 4) the 250-bp conserved hMCAK neck. Because I was using restriction enzyme digestion and ligation for cloning, I chose the conserved Arginine-Proline (RP) in beta-sheet-1a near the kinesin motors' N-terminus to use as an EagI (CGGCCG) restriction site linking the neck (with GFP and tag) to the 3 different motors. Two other restriction enzyme sites, KpnI at the GFP N-terminus and SalI at each motor's C-terminus, would also be added to insert the whole construct into a vector with a N-terminal His-tag already in place.
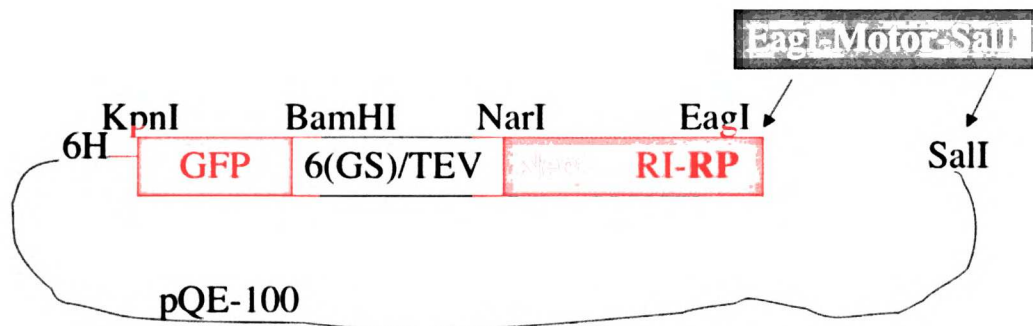
Figure 2-2: First Cloning Strategy. pQE-100 was the first vector I chose, and contains the N-terminal His-tag (6H) and the restriction sites for KpnI and SalI for inserting the entire construct. 6(GS) are a set of 6 glycine-serine pairs before the TEV protease site, which gives good extra space for the protease to bind and cleave the polypeptide. RI is the boundary between the neck and motor, and RP is the conserved site mentioned above.

To make the GFP-TEV-neck construct (Figure 2-3), I used PCR to clone GFP with n-terminal KpnI site (GGTACC) and c-terminal BamHI site (GGATCC), and hMCAK neck+motor (through conserved RP) with n-terminal NarI (GGCGCC) and c-terminal EagI (which codes for RP). I used two oligonucleotides to make a double-stranded construct of 5 Gly-Ser pairs and the TEV site (good to have extra loop space before the TEV site), with BamHI and NarI sticky ends. This was much easier than trying to add the entire 51 bp GS-TEV site to both of the clones by PCR. I then digested the GFP clone with BamHI and the neck clone with NarI, used T4 DNA ligase to link them together with the TEV oligos, and used PCR with primers for the GFP N-terminus and neck C-terminus to amplify the full GFP-TEV-neck construct successfully, which was seen as a 1 kb product and confirmed by sequencing (Elim Biosciences).
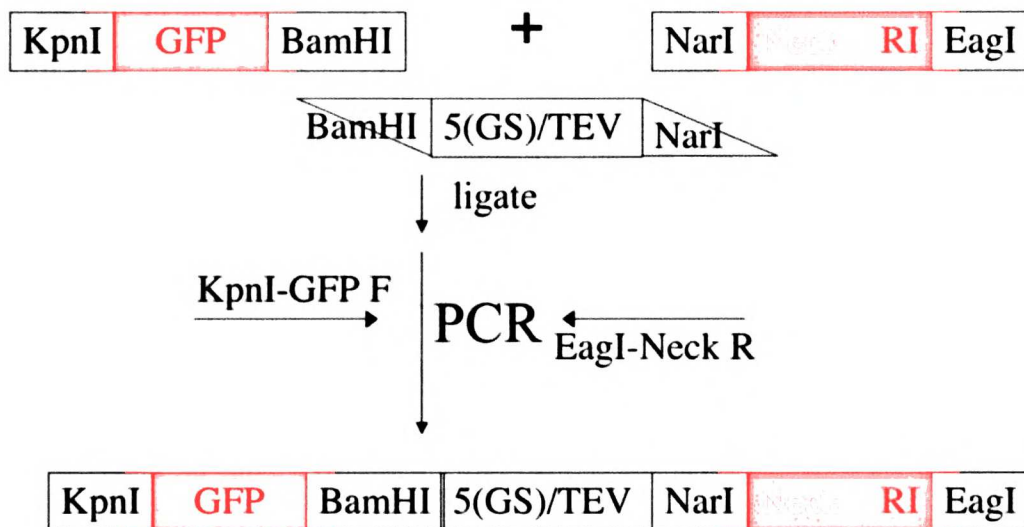
Figure 2-3: GFP-TEV-neck Construction. The parallelogram represents the two oligonucleotides, that pair up to form the double-stranded sequence for 5 Glycine-Serine pairs + TEV protease site, with sticky ends that match up with BamHI and NarI digests.

Next, I used a pQE-100 vector from Qiagen, which includes a T5 promoter, N-terminal His-tag, and KpnI and SalI sites in the multiple cloning region after it. I also used primers to clone out the 3 motors (KHC, NCD, Unc104) starting from an N-terminal EagI (conserved RP) and adding a SalI site at the C-terminus. The plan was to digest both the GFP-TEV-neck DNA and one of the motor constructs (I chose Unc104) with EagI, ligate together and PCR amplify the desired dimer using GFP-forward and motor-reverse primers, the same way I made the GFP-TEV-neck construct. This would then be digested at the ends with KpnI and SalI to insert into the plasmid and complete the desired construct (Figure 2-2); the KHC and NCD constructs could be made by redigesting the new plasmid with EagI and SalI and ligating in a different motor clone.

Unfortunately, because the motor clones and GFP-TEV-neck constructs are all about 1 kb in size, it was impossible to distinguish the desired GFP-Unc dimer from GFP-GFP or Unc-Unc homodimers, and little of the expected 2 kb product was available to purify in either case. I tried digesting the plasmid with KpnI and SalI, GTN with KpnI and EagI and Unc104 with EagI and SalI, then ligating all together overnight and using the mix to transform competent cells. However, I only got *one* colony after 2 ligation and 3 transformation attempts with various amounts plated; as usual, such a single colony result was a fluke that yielded no product.

To simplify the digestions and ligations and improve their chance of success, I chose to add another KpnI site to the GTN C-terminus after the EagI site, so I could insert the construct into the plasmid with just a KpnI digestion. Digesting the resulting primers with EagI and SalI would let me distinguish the correct product from the inverted insert, as such a digest would lead to GTN loss in the invert product. Unfortunately, I got very

low yield of GTN-KpnI PCR product, and couldn't reproduce it with later PCR attempts, getting a 200 bp product instead; none of the attempted ligations yielded colonies after transformation – which probably indicates the cells were not competent. I then used a new oligo to introduce SalI sites at both ends of the GFP-TEV-neck construct. SalI is a better-behaved enzyme, and after inserting into the plasmid with SalI digestion, a KpnI digestion (with reannealing) would leave GTN in only the desired orientation. However, I decided to switch to using Invitrogen's Gateway system for cloning, instead of the digestion and ligation method that had been giving me so much trouble.

Multisite Gateway construction

Invitrogen's Gateway cloning system uses lambda recombination sites, instead of restriction enzyme sites and ligation, to get quick directed insertion. There's a Multisite Gateway kit that allows you to put 3 DNA pieces together in one final recombination reaction; since I had neck, motor and GFP, I decided to use this (Figure 2-4). Unfortunately, the destination vector specific for Multisite does not include a promoter or His-tag, because they assume that's what people want to put in their special N-terminal addition. So, I used the T5 promoter and 6X-His tag from the pQE-100 vector I had on hand, by digesting the GFP-TEV-neck DNA I'd made previously with BamHI (between GFP and GS's), and cutting the vector with BamHI (right after the His-tag) and XhoI (before the T5 promoter). I ligated the two pieces together, and amplified using primers around the XhoI site and neck's *real* C-terminus, which also added the attB4 and attB1 Gateway recombination sites at the ends.
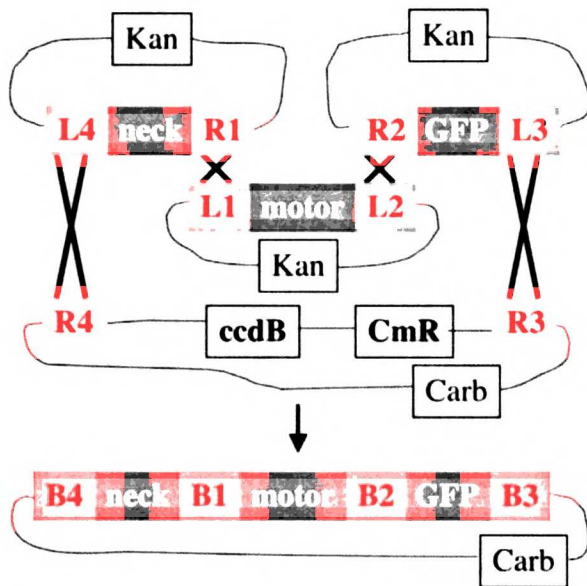
Figure 2-4: Multisite Gateway Strategy. To clarify: "neck" contains the T5 promoter, 6X His tag and TEV-site; "Kan", "Carb" and "CmR" signify genes for resistance to kanamycin, carbenicillin (same mechanism as ampicillin) and chloramphenicol.

In a similar (but much simpler) fashion I added attB1 and attB2 sites to the ends of the 3 (whole) motor cores, and attB2 and attB3 sites to the ends of GFP, which would be placed at the polypeptide C-terminus rather than the N-terminus. The first step in Gateway cloning is the BP reaction (Figure 2-5), which recombines the PCR products into individual donor vectors; the next reaction, LR, places the gene inside the destination vector, with small 24-bp attB recombination sites surrounding it. Multisite uses a special destination vector and enzyme (LR Clonase PLUS) to recombine the 3 DNA pieces together in order and insert into the destination vector. This leaves an attB1 site between the neck and motor, and an attB2 site between the GFP. Although a short loop between motor and GFP is probably good to have, I didn't want more sequence between the neck and motor than absolutely necessary. So, I included restriction enzyme sites in the PCR

52

primers, to use later for removing attB sites, and also to remove neck or GFP for controls (Figure 2-6).
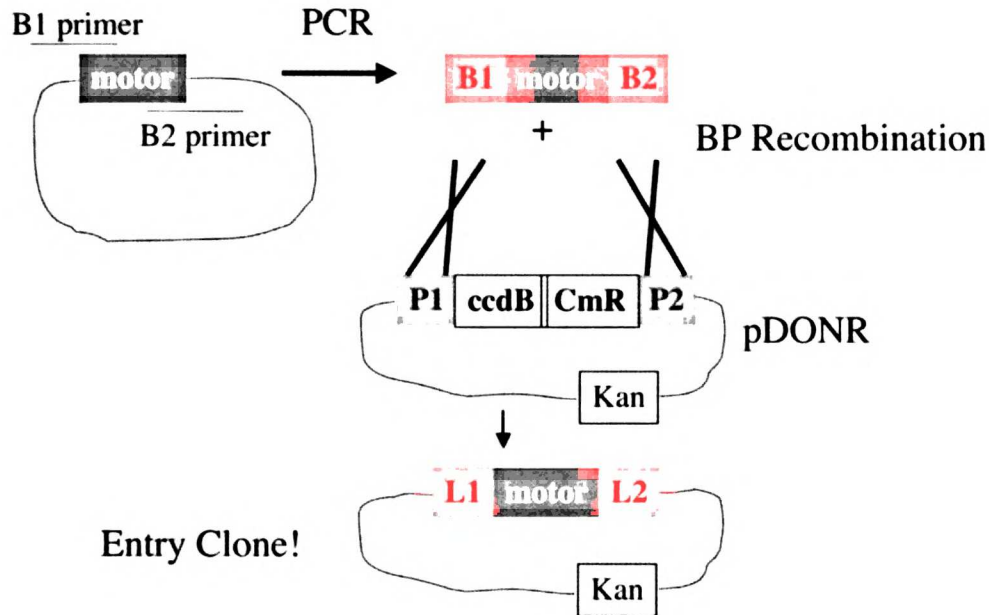
Figure 2-5: BP Recombination. Recombination occurs between matching attB and attP sites; the ccdB gene suppresses growth in bacteria transformed with the plasmid, and is used for negative selection. Recombining the desired gene in also recombines the ccdB gene out, so bacteria transformed with this plasmid can grow, while bacteria transformed with the original unrecombined plasmid do not grow.
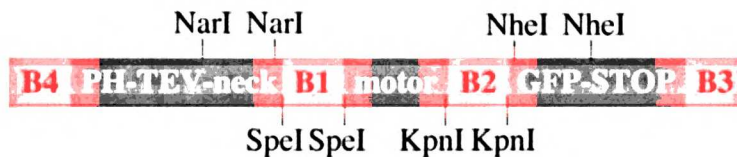
Figure 2-6: Restriction Enzyme sites for editing Multisite product. NarI for neckless controls, SpeI to have the neck and motor more directly joined, KpnI to remove the attB2 site (less urgent, probably good to have the spacer), and NheI to make GFP-less controls.

I used the BP reaction to make entry clones for all 3 motor cores and for GFP, and confirmed the results by sequencing (ElimBio, Inc.). However, I had very great difficulty getting the correct T5-TEV-neck entry clone; the reaction and transformation yielded only a small number of colonies, all of which had odd recombinations that spit out the ccdB gene (used to repress growth in cells with nonrecombined vector) while not including the gene I wanted. This was especially frustrating because I had to keep producing the T5-TEV-neck insert by PCR, which didn't always work very well. I was finally able to use blunt-end TOPO cloning to place it inside a vector for larger-scale production, but growing the DNA in overnight cultures of TOP10 cells gave much lower yield after miniprep than usual. This pointed me to the fact that the neck protein piece was probably expressing and poisoning the cells: T5 promoter is very strong, and pQE vectors require lac repressor to prevent expression, but the cells I was using did not make lac repressor. Therefore, any correct BP insertion of my T5-TEV-neck construct led to cells that were expressing the neck, plus extra sequence due to no STOP site in the construct, which kept the cells from growing and being seen on the plate as colonies. I solved this problem by reamplifying the construct with a STOP site before the attB1 site, and then transforming the BP DNA into TOP10F' cells which make lac repressor. TOP10F' cells are ccdB resistant however, so I also saw many small colonies from unrecombined vector, but by picking larger colonies I was able to get the desired T5-TEV-neck entry clone and confirm it by sequencing (Elim Biosciences).

Finally I performed the LR reaction to put the neck, motors and GFP together in pDEST R4-R3 – these worked for all motor constructs (Unc104, KHC, NCD and hMCAK) and were confirmed by sequencing. Unfortunately, I could not express these

proteins due to the STOP site inserted after the neck. I first tried removing the

STOP+attB1 site by digesting with SpeI at the sites I'd engineered in (Figure 2-7), but I

either got no colonies, or the vector religated without the piece gone. The main

problem, after many attempts, seems to have been that the gel purification residue

inhibited the ligation. Another big difficulty was recognizing double-cut vector on the

gel when there was only a 32-bp difference in size; I could barely do this when it was run

at 60V, but couldn't cut the bands separately.
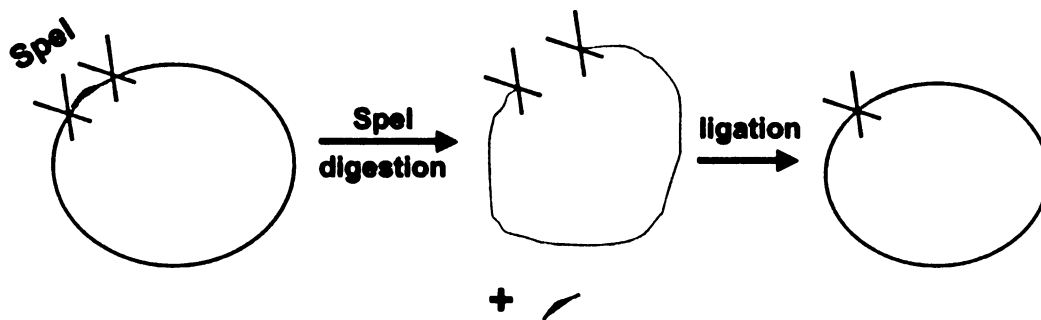
Figure 2-7: Deletion by Restriction Enzyme Digestion and Ligation. In this case the

plan was to use SpeI to cut the two sites (marked with blue X's) surrounding the attB1

site (red). Ligation of the double-cut vector would give the desired product, but ligation

of a single-cut vector would only give back the original vector.

I had another set of problems when using that same strategy to make neckless

controls, by cutting the T5-neck donor vector with NarI. It turns out that NarI is known

to have site preferences, which explains why I got very little double-cut vector, and

longer digests did not improve this. Gel purification residue might have prevented even

this small amount of purified product from being usable. Whatever the reason, I didn't find any colonies that had the neck deleted.

So, I tried using QuikChange to remove the two sites, by ordering oligo pairs that had the sequences flanking each region, but missing the part I wanted to delete. These are used for PCR (need Pfu for high fidelity on long runs) to make vector with the change, then DpnI is added afterward to destroy the methylated template (Figure 2-8). In this case I wanted to delete attB1 (NarI-SpeI-STOP-attB1-SpeI) and neck-attB1 (NarI-neck-NarI-SpeI-STOP-attB1-SpeI). However, I was only able to make the neck-attB1 deletion for NCD; the attB1-only NCD deletion didn't work, and neither deletion worked for any of the other motors. I ended up sending the four LR neck-motor-GFP construct vectors to BioMeans, Inc., to have the remaining 7 deletions made. Fortunately those were successful, according to their sequencing and my own independent check (through Elim Biosciences).
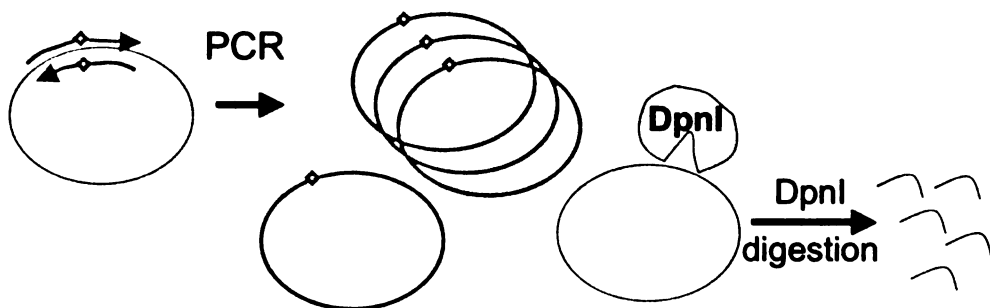
Figure 2-8: General QuikChange mutagenesis. A primer pair (green) is made that contains the desired mutation (red) and enough matching sequence on both sides. This is used to perform high-fidelity PCR, giving unmethylated product (green). The original methylated template (black) is then digested by DpnI, leaving only the mutated product.
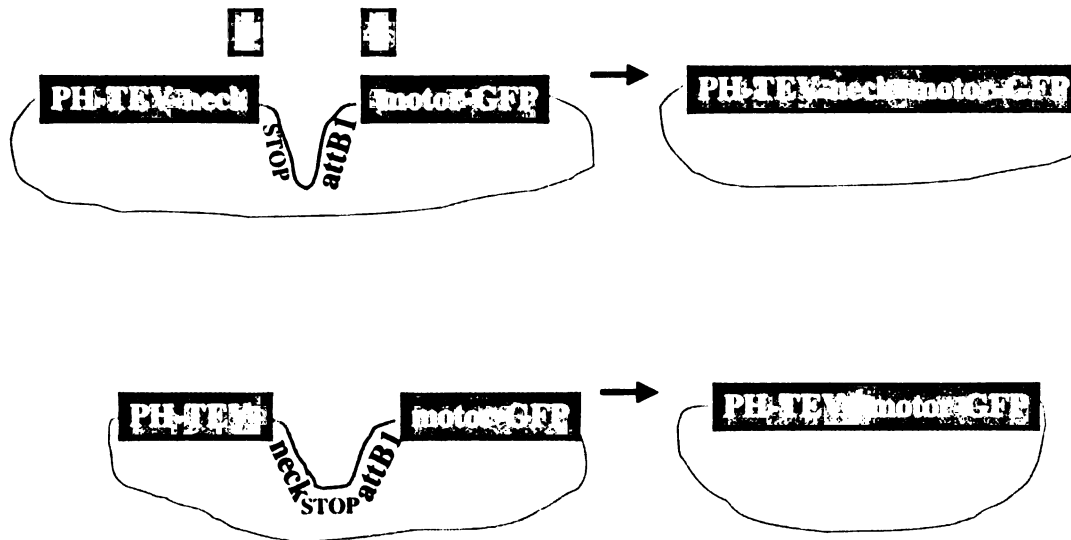
Figure 2-9: QuikChange deletion of STOP-attB1 and neck-attB1. The QuikChange primer pairs (green, yellow) contain only sequence flanking the desired deletion – assume the two pieces shown for each are directly connected, and missing the loop below. PH = T5 Promoter with 6X His tag.

<u>Promoter, vector and cell line considerations and changes</u>

I cover the details of the first expression and purification attempts later, but some difficulties came up that required further cloning to overcome. First, in order to control expression, I needed to use expression cells that make lac repressor, but the standard BL21(DE3) cells do not do this. XL1-Blue does make the repressor, and was readily available to buy, but the expression protocols for motor proteins, with or without GFP, all assume use of BL21(DE3) cells. I ultimately decided that the T5 promoter was something I could and should do without. T7 promoter is less strong, but it does not require repressor to keep it controlled, relying on IPTG to activate it instead. It's often

better to start with the more standard systems, such as T7-promoter with BL21(DE3) cells, so it's easier get more help when things are difficult; switch to a different system only if there are compelling reasons to do so.

To switch from T5 to T7 promoter, I simply found a destination vector that has T7 promoter and a His-tag at the N-terminus (pDEST17), then used PCR to clone out the full-length neck-motor-GFP constructs, replacing the end attB4 and attB3 sites with attB1 and attB2, respectively. I got about half of my BP product missing the GFP due to recombination with the other attB2 site, but otherwise this method worked well (Figure 2-10). With the new vector and BL21(DE3)-Star cells, I had no trouble with transforming cells and much less difficulty growing cultures for expression.
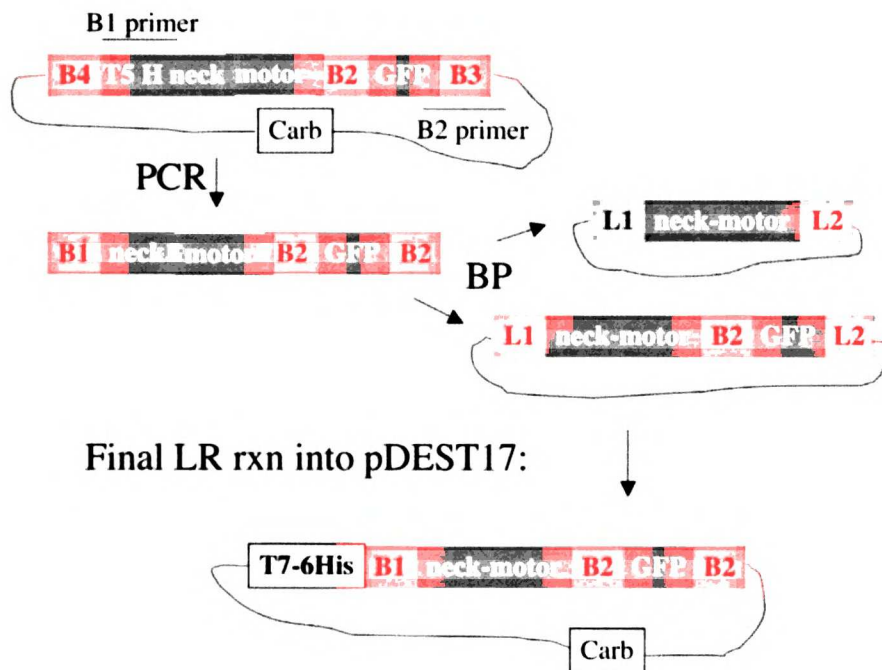
Figure 2-10: Move to pDEST17 vector for more reliable handling. The "neck" includes the 5 GS pairs and the TEV site, but not the promoter (T5) or His tag (H).

Overview of Gateway strengths and limits, with recommendations for future multi-piece gene construction

Gateway recombination worked much more dependably for my cloning than restriction digestion with ligation, and it is quicker too: the product is immediately used for transformation, so no gel purification is necessary as an intermediate, and the product is oriented properly. It does add ~24 bp to the sequence at each attB site, so artifactual 8 amino acids in the protein sequence need to be considered, and possibly removed from the sequence later.

The only reason I had any difficulty with Gateway was because I was trying to clone the n-terminal neck fragment linked with T5 promoter. First of all, the hMCAK neck appears to be not well tolerated by the cells, plus there was probably additional sequence expressed beyond that. Second, T5 promoter was not well suited to Gateway: repression of this promoter requires either special cells ordered from Qiagen, or cells that make lac repressor, and the Invitrogen One-Shot TOP10F' cells that make lac repressor are also ccdB resistant, making Gateway screening much more difficult. Because of this, it took months of effort to finally obtain the T5-neck N-terminal donor clone.

When using Multisite Gateway, my recommendation is to avoid expression in intermediate stages by leaving the promoter to the final destination vector. The special pDEST R4-R3 should just be used for subcloning to assemble the 3 pieces of the gene of interest, rather than as the end point. That full-length construct can then have attB1 and attB2 sites added at the ends by PCR, in order to insert the gene into a more optimal destination vector, with the promoter and the His-tag position best suited to the project, as

well as to the competent cell line that works best. If promoter must be included in the 3-piece construct itself, I suggest using T7 or another one that won't lead to high levels of un-induced expression. The one difficulty of this method is that it leaves two copies each of the attB1 and attB2 sites, both within the construct and at the ends, so several BP colonies need to be miniprepped and checked to be certain that the full sequence is obtained. In my case the internal attB1 site had been removed, so only half of the prepped colonies had truncated product lacking the C-terminal GFP.

The difficulty mentioned above can be put to use in creating control constructs that lack the N- and/or C-terminal additions. The extra 8 amino acids at either or both ends (from the attB sites) would have to be tolerable for protein function, but if the final destination vector has a STOP site immediately after the L2 site (as most do) the cloning artefact should be limited to that.

On that note, it may be feasible to include restriction sites to excise portions and eliminate the attB sites, but the enzyme chosen should not show site preferences (the way NarI does) and the piece being excised should be large enough to recognize the desired product on gel fairly easily. Of course, the restriction site must not be one already in the gene or pDEST R4-R3 (better to do cloning with the smaller, more bare-bones destination vector). Smaller deletions, such as attB sites, are probably better to do by QuikChange, which can even use two sets of mutagenic primers to remove both attB sites at once. This method can have its own difficulties, so alternative methods may be considered, such as commercial mutagenesis (BioMeans, Inc., etc.).

Expression and purification of kinesin motors with N-terminal KinI neck

Initial attempts, before moving to T7-promoter vector

For my first attempts at neck-motor-GFP expression, I used the constructs with T5 promoter that I'd had BioMeans make usable, and transformed them into XL1-Blue supercompetent cells so that lac repressor would be around. I first picked 5 colonies for each motor (Unc104, KHC, NCD) to grow overnight cultures, and then used 500 ul each to start 10 mL cultures in 50 mL tubes. I used 1.5 mL of each overnight culture to make glycerol stocks that were kept at -80°C, and used those to start expression cultures for later attempts. I grew the 10 mL cultures at 37°C until they reached an OD600 of 0.5 – the Unc104 cultures reached this quicker than the KHC & NCD ones, but for all of them I induced with 1 mM IPTG and expressed for 4 hours at 37°C, then spun down cells 15 minutes at 5000 x g before freezing in liquid nitrogen. To lyze the cells I suspended them in 1 mL BPER (Pierce), then spun down the insoluble fraction 5 minutes at 15000 x g before checking the presence of GFP in each supernatant (A488 nm).

The results weren't conclusive, so I repeated the expression starting from all 15 glycerol stocks, using 1.5 mL to inoculate 10 mL instead, but also used one overnight culture for each motor to start a non-induced control culture. KHC and NCD still grew slower. I induced all but the controls at OD600 of 0.5 with 1 mM IPTG, and let grow at 37°C for 5 hours before spinning down the cells more strongly for 10 minutes at 5000 x g and putting the pellets at -20°C. I lysed again with 1 mL BPER, spun down the insoluble fraction and checked A488 nm of the supernatants. The induced controls had higher

"green" levels than the controls, mostly, but they should be more clearly green if the expression is good. I mixed samples of each supernatant with SDS buffer and ran them on a gel, but there were no obvious strong bands around the expected 75 kDa size, so the expression could not be very high.

I then tried another expression at 25°C, since motors tend to express better at lower temperature. I repeated the expression and lysis the same as the previous attempt, but switched the tubes to 25°C after adding IPTG, and then used only 500 μL BPER for each pellet, to get them more concentrated. On a gel (Figure 2-12) I saw clear bands around 75 kDa, but the induced cultures weren't really different from the controls, and the bands weren't especially strong. It's possible that the IPTG was bad, or that 1 mM was too much – sometimes expression is better with 0.1 mM IPTG. Also, it's better to grow the cultures to a good density, and then split them up into a set of expression cultures to test different conditions, knowing that they started from the same OD600.
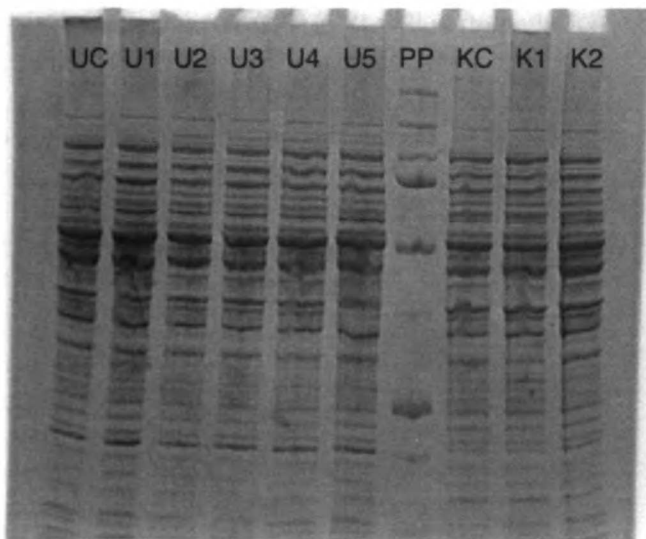
Figure 2-11: 37°C expression in XL1-Blue, different neck-motor-GFP preps.

(U = neck-Unc104-GFP, K=neck-KHC-GFP, C= control, PP= Precision Plus standard)

So, for my final attempt with expression in XL1-Blue cells, I grew two overnight cultures of the Unc104 construct (since the grow faster), used 500 µL to start 2 10 mL cultures, which I grew 2 hours at 37°C before splitting into 4 1.5mL cultures in 14mL tubes. These were the four conditions I sampled: 1) expression at 37°C with no IPTG, 2) 37°C with 0.1mM IPTG, 3) 37°C, 1mM IPTG, and 4) 25°C, 1mM IPTG. After 5 hours expression I spun the cells down and resuspended the pellets in 300 µL BPER, then spun 5 minutes at 15000 x g to separate out the insoluble fractions, which I then separately resuspended in 300 µL BPER (or tried to). Checking the samples on a gel (Figure 2-12), the "pellet" samples were all lines with no resolved bands, so they didn't get resolubilized well enough. The soluble samples had bands around 75 kDa, but they were basically the same for all conditions. At this point I stopped using these constructs and cells, and moved the genes to pDEST17 vector and BL21*(DE3) cells, as described in the cloning section.
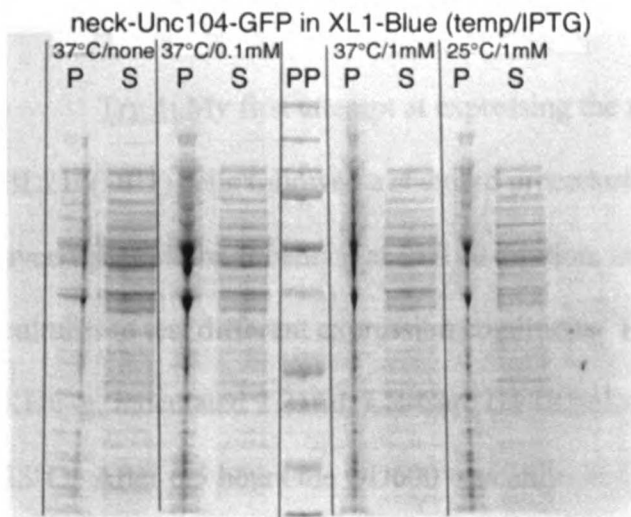
Figure 2-12: Expression of neck-Unc104-GFP in XL1-Blue, different expression temperatures and IPTG concentrations.

(P=pellet/insoluble fraction, S= supernatant/soluble fraction)

One problem, aside from the use of unfamiliar promoter and cells, was that I didn't really know the purification protocol for motor proteins (with or without GFP). It turns out that the cells need to grow to a higher density (OD600 between 0.6 and 1.0) and express longer, at least overnight. Kinesin bands often aren't clearly visible in the crude lysate, only after some purification, and I also really need to have protease inhibitors in the lysis and purification buffers and keep everything on ice all the time, since the motors are easily digested. Because I only expressed for 5 hours, used BPER at room temperature to lyse the cells, and did no additional purification, it's no wonder that I saw nothing significant on the gels. If optimized expression in BL21*(DE3) cells still doesn't yield enough protein for experiments, the T5-promoter constructs in XL1-Blue might be a viable alternative if the better motor-GFP expression and purification are used.

Expression and purification in BL21* (DE3) cells

Try 1: My first attempt at expressing the neck-motor-GFP constructs in BL21*(DE3) cells followed a standard procedure for optimizing motor expression: grow overnight culture, inoculate at ~1/100 dilution, and once at good OD600 split into smaller cultures to test different expression conditions. I grew 2 3mL overnight cultures of n-KHC-g, inoculated 2 25mL LB-Carb (in 125mL flasks) with 500 µL of each, grew at 25°C. After 6.5 hours the OD600 was only ~0.4, but went ahead and split each into 4 5mL cultures in 14mL tubes, expressed under 4 different conditions: 1) no IPTG, 3 hrs, 2) no IPTG, overnight, 3) 0.2mM IPTG, 3 hrs, 4) 0.2mM IPTG, overnight. From the rest of each 25mL culture, spun down cells from 1mL and kept the pellet as a preinduction

baseline. I put all the cell pellets (including from the expression cultures) at -20°C. At that point I had to wait to get the motor-GFP expression protocol from the Vale lab, for information on what buffers to use. I just redid the expression instead of purifying these, but this method of sampling conditions would probably be useful for optimizing expression later.

Try 2: My second attempt followed the Vale lab protocol for expression and purification of motor-GFP constructs. I freshly transformed neck-Unc104-GFP and neck-NCD-GFP into BL21* cells, used a restreak from the older neck-KHC-GFP plate. I also made new 1M IPTG and 50mg/mL (1000x) Carbenicillin, filtered into aliquots, and used both from this point. I inoculated 50mL cultures from picked colonies, grew about 8 hours (getting OD600's ranging from 0.5 to 1.8!), then induced with 0.3mM IPTG and expressed overnight at 22°C (~18 hours). I spun down the cells 15 minutes at 5000xg, and froze the pellets in liquid nitrogen. Meanwhile I made the purification buffers (phosphate/imidazole, see appendix) without beta-mercaptoethanol or ATP, since those should be added fresh before use, and also made 1mL of a 1000x cocktail (10 mg each) of the protease inhibitors leupeptin, pepstatin and aprotinin.

For my first protein purification (see appendix for general outline), I resuspended each pellet in 10mL Lysis Buffer, and then sonicated to lyse the cells – it foamed up pretty quickly with the first Unc104 pellets, so they probably didn't lyse well. The other prep pairs (KHC & NCD) were sonicated better, in 14mL tubes, but those were also probably not lysed properly because I only sonicated for a couple rounds, at room temperature (better to keep chilled with ice). I used 1mL Ni-NTA resin for each pellet, washed each column with 25mL Wash Buffer, then eluted in 6 1mL fractions with high-

imidazole Elution Buffer. I took samples of the post-lysis supernatant, post-resin-binding supernatant, wash and each of the 6 fractions (but not of the total lysate), and ran them on gels (Figure 2-14: Unc – 1&2, NCD – 3&4, KHC – 5&6). There were two faint bands around 75 kD, but the bands were all faint even before the Ni-NTA purification, likely due both to using buffer volumes that were too high for purifying 50mL culture pellets, and also to insufficient sonication. The KHC gel is warped due to reusing MOPS buffer – unlike with DNA gels, you cannot reuse buffer for protein gels, or it gets cooked at the high voltage. I couldn't draw any definite conclusions about expression from the gels, but there was certainly expression of a GFP construct in all the cultures, because the post-lysis pellets were all clearly green in color (Figure 2-13).
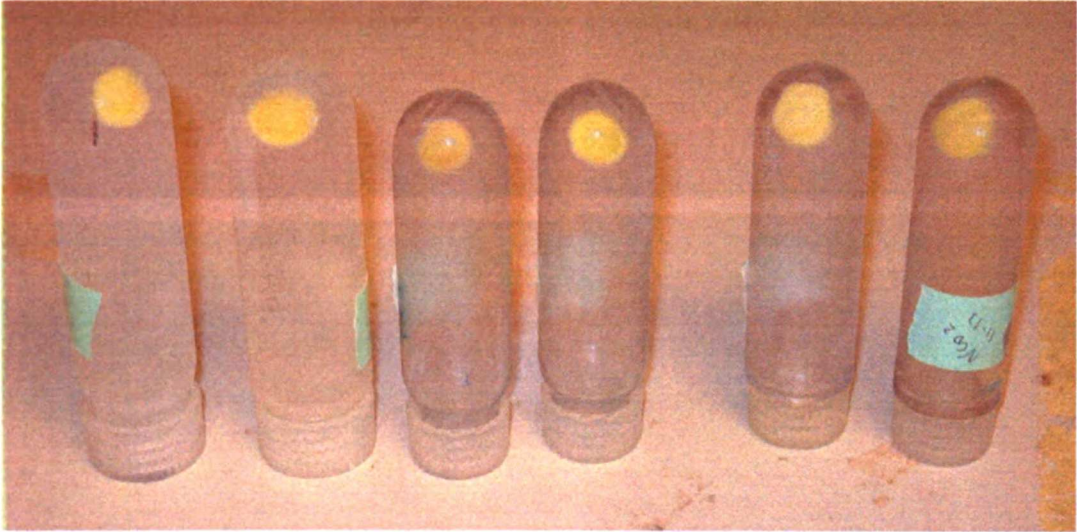
Figure 2-13: Post-lysis pellets, all green
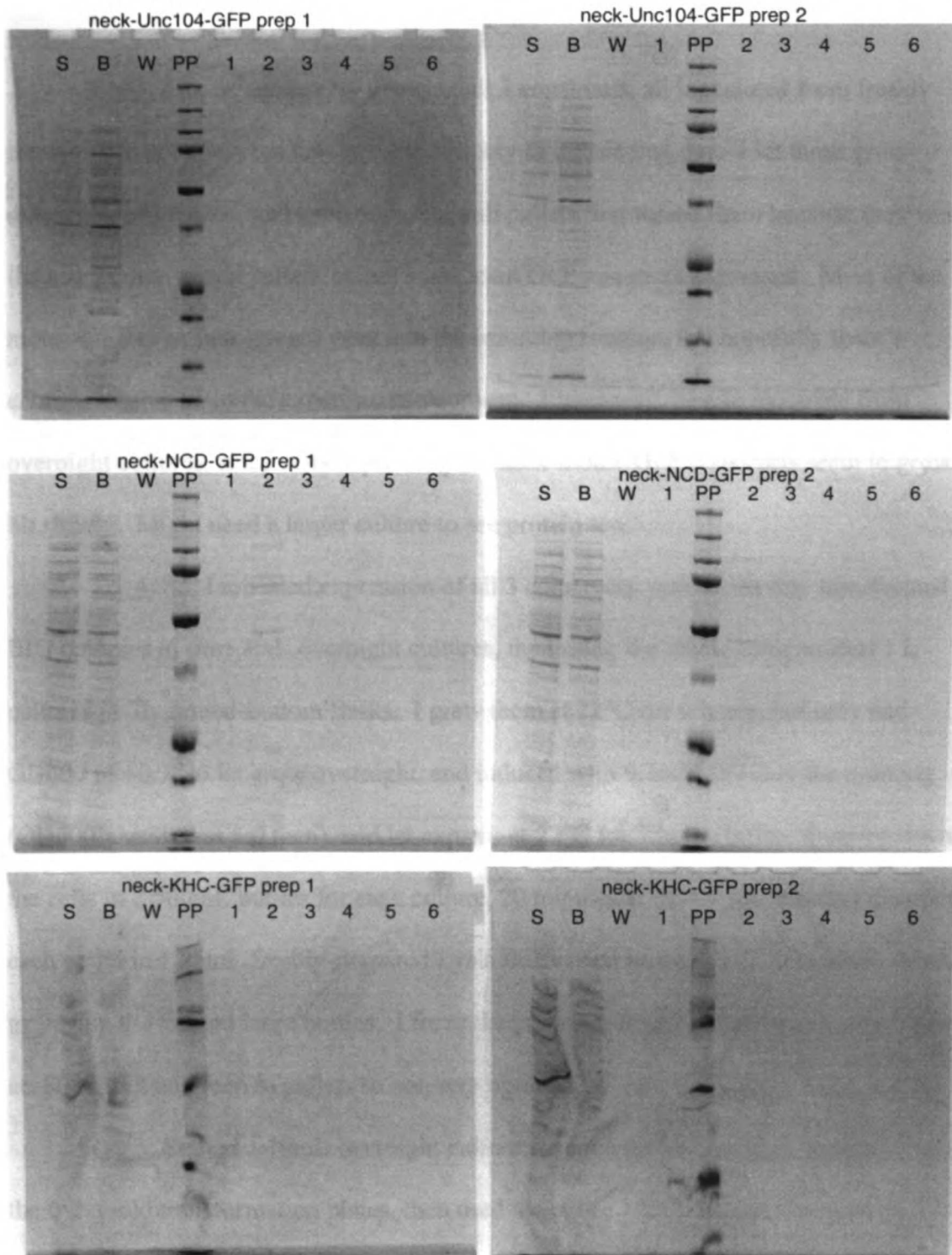
Figure 2-14: neck-motor-GFP expressions, two preps each, at 22°C, 0.3mM IPTG and excessively large purification buffer volumes. (S=soluble fraction, B=didn't bind to NiNTA resin, W=wash, and 1-6 are the eluted fractions)

Try 3: I made another try growing all 3 constructs, all inoculated from freshly transformed colonies, but they grew too slowly to induce that day. I let those grow overnight, uninduced, and spun down the cell pellets, but tossed them because they were the usual color of cell pellets, so not significant GFP-construct expressed. Most of the motor-GFP construct (green) goes into the insoluble fraction, but hopefully there's enough soluble to do the experiments you want. Either way, best to inoculate from overnight cultures, since cells expressing the neck-motor-GFP constructs seem to grow a bit slowly. Might need a larger culture to see protein too.

Try 4: So, I repeated expression of all 3 constructs, picking freshly transformed BIG colonies to start 3mL overnight cultures, then using the whole thing to start 1 L cultures in 3L dented-bottom flasks. I grew them at 22°C for 6 hours, but only had OD600 of ~0.3, so let grow overnight, and induced with 0.1mM IPTG in the morning (OD600's well over 1.0 then), and let express at 22°C for 7 hours before spinning down the cells in 2 500mL bottles for each culture, 20 minutes at 5000 rpm. I had to resuspend each pellet in 12.5mL freshly-prepared Lysis Buffer and respin the cells in 50mL tubes, to free up the limited large bottles. I froze the pellets in liquid nitrogen, and saved them at -80°C, but no green in pellets so not very optimistic.

Try 5: Started a 10mL overnight culture for each motor construct, picking from the 6-day-old transformation plates, then used the entire 10mL each to inoculate 1L LB-Carb in 2.8mL smooth-bottomed flasks (so less foamy). I grew them at 37°C, but they still grew slowly. When OD600 of each culture finally reached ~0.8-0.9 (Unc culture was only ~0.5 though), I let them cool to 22°C for about 30 minutes, then induced with

0.1mM IPTG and let express overnight (16 hours). I spun down two 50mL tubes of each culture and froze the pellets separately to use for test purifications, then spun down the rest of each big culture in 2 500mL bottles, resuspended the pellet in lysis buffer and spun down again in 50mL tubes as before, froze all in liquid nitrogen and left at -80°C. No green pellets this time either.

For a test purification of one of the small neck-NCD-GFP cell pellets, I used smaller buffer volumes proportional to the smaller pellet size. Resuspended the pellet in 3mL Lysis Buffer, transferred to a 14mL tube and kept the tube chilled in a beaker of ice during sonication. The sonication settings were: duty cycle 50%, output 3 or 4, 20 pulses each round, then let cool 4-5 minutes between rounds. Started at output 4 for 2 cycles, but the solution got too warm so went down to output 3. After a total of 6 rounds of sonication the solution still wasn't becoming clear from membrane breakdown, but that's probably as good as it was going to get, so I continued with purification from there. Used 200μL resin to bind the soluble fraction, washed column with 2mL *Lysis* buffer (similar enough to other buffers to use for all but elution), and then collected 3 x 200μL fractions after adding elution buffer. Took samples of total lysate, soluble fraction, post-bind supernatant, wash and each of the 3 fractions, and checked on gel (Figure 2-15). The bands were definitely stronger, but more of them than expected (2 or 3 ~75kD), and none of them quite the right size. Lots of smaller kD bands too, maybe due to degradation.
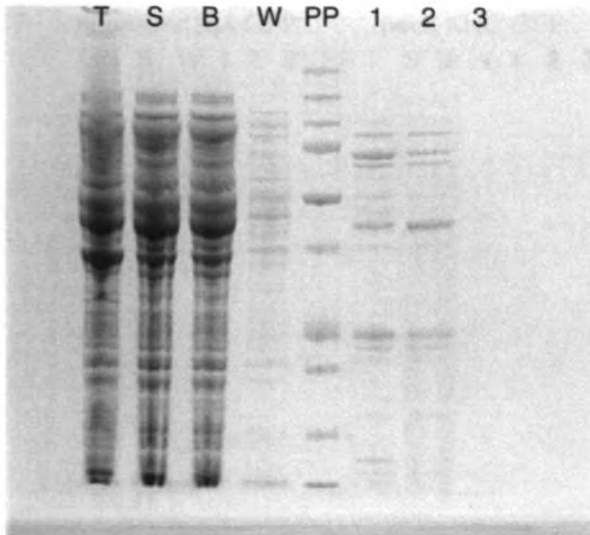
Figure 2-15: Expression of neck-NCD-GFP at 22°C, 0.1mM IPTG.

(T=total post-lysis, both insoluble and soluble, S=soluble fraction,

B=didn't bind the NiNTA resin, W=wash, PP=Precision Plus standard, 1-3= fractions)

To help combat degradation, I used protease inhibitors in ALL the solutions,

including the elution buffer, and repeated the purification with one each of the small

neck-KHC-GFP and neck-Unc104-GFP cell pellets. The gels for those (Figure 2-16)

looked much the same as for the neck-NCD-GFP prep. The ~75kD bands are probably

all background, because there are *E coli* proteins that stick to Ni-NTA resin and run at

that molecular weight on an SDS gel - this implies that I'm not getting any soluble neck-

motor-GFP protein. Because proteins don't always run at the expected molecular weight

on an SDS gel, it'd be helpful to run an anti-GFP Western Blot to determine if any of the

bands are my neck-motor-GFP construct.
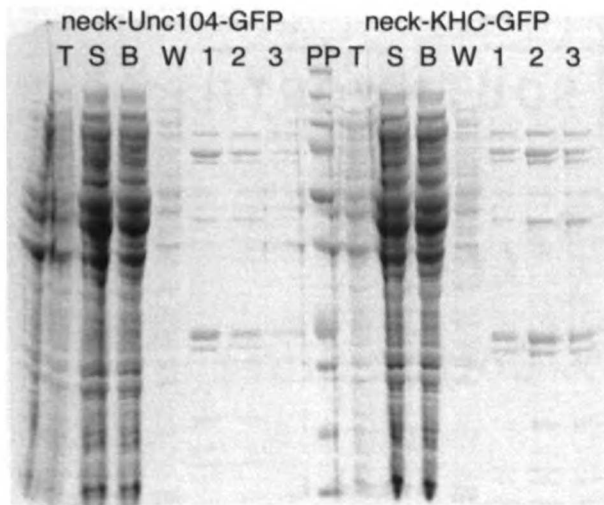
Figure 2-16: Expression of neck-Unc104-GFP and neck-KHC-GFP, same conditions as Figure 2-15.

Try 6: Looking back, I noticed that I'd used 0.3mM IPTG for the one prep (Try2) that gave green pellets, so I repeated using the same expression method, but with the better purification method. Fresh transformed, picked two colonies for each motor to start 50mL cultures, all but one at good density after 8 hours at 37°C. Induced with 0.3mM IPTG and expressed overnight (~18 hours) at 22°C, before spinning down and freezing the cell pellets. The pellets weren't very green, but were definitely bright yellow, different from the typical brown cell pellet (compared in Figure 2-17). Resuspended in 3mL lysis buffer for sonication, batch bound the soluble fraction with 100μL Ni-NTA resin (less is more), washed with 2mL lysis buffer and eluted 3 x 100μL fractions. Checked the usual samples on a gel (Figure 2-18), but the bands were still weak, and saw ~75kD band pattern similar to prior preps. With color evidence of expression but inclusive results for soluble protein, I definitely needed to do a Western Blot. However, for that I also needed a negative control.
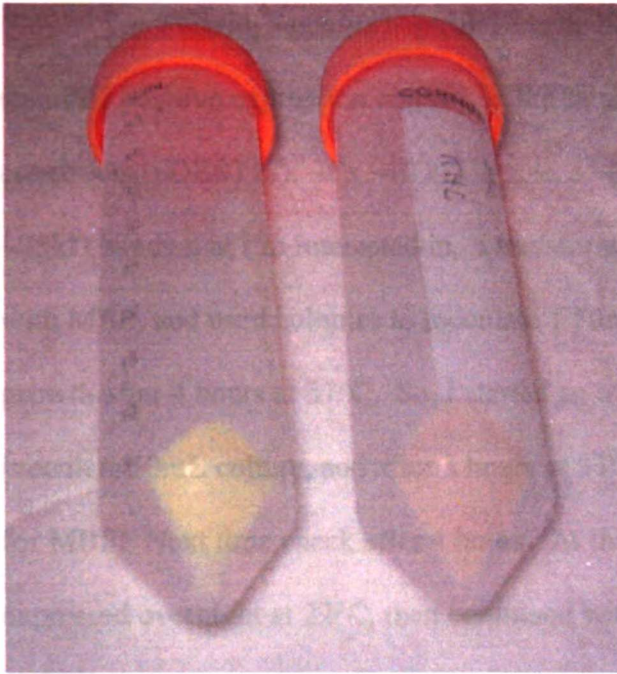
Figure 2-17: Comparison of neck-KHC-GFP pellets expressed with 0.3 mM IPTG (left) and 0.1mM IPTG (right), note the color difference.
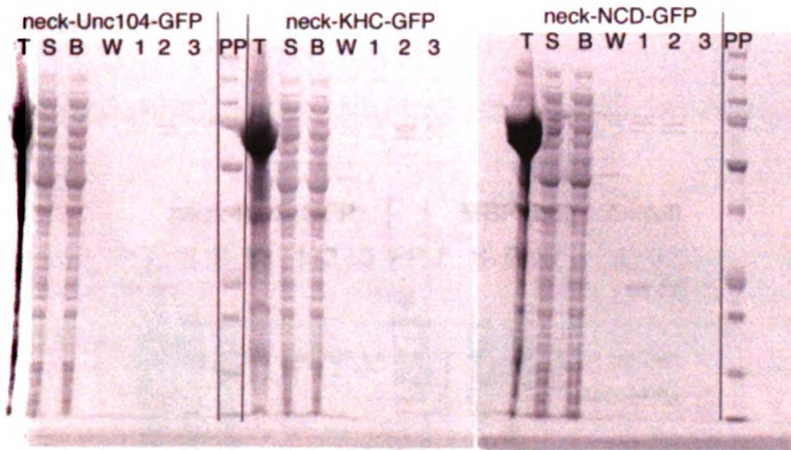
Figure 2-18: All neck-motor-GFP's expressed at 22°C and with 0.3mM IPTG.

Try 7 – with negative control: Eugene had maltose-binding protein (MBP), a standard positive expression control, in the same Gateway vector I was using for my constructs (pDEST17). It's ~40 kD in size, so the MBP band shouldn't interfere with the ~75kD bands that I'm interested in. I transformed cells fresh with neck-KHC-GFP and with MBP, and used colonies to inoculate 1 50mL culture each, but there was very little growth after 4 hours at 37°C. So, I started an overnight culture for each, used 0.5mL to inoculate 50mL culture, and after 5 hours at 37°C I had OD600 of 1.8 for KHC and 2.1 for MBP! Next time check after 4 hours. At this point I induced with 0.3mM IPTG and expressed overnight at 22°C, then continued with purification same as before. I accidentally ran the gel at half voltage, but it's readable, and shows a similar band pattern at ~75kD for the negative MBP control as well as for neck-KHC-GFP (Figure 2-19). Those bands are probably *E coli* proteins then, but I needed to check for certain using a Western blot or mass spectrometry.
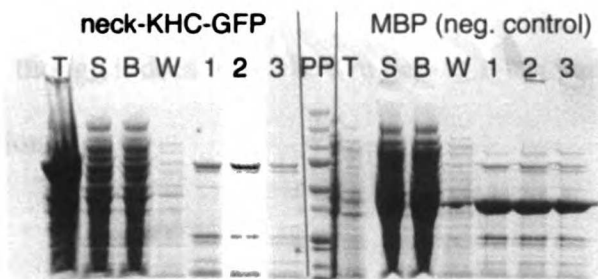
Figure 2-19: Expression of neck-KHC-GFP with Maltose-Binding-Protein in pDEST17 as negative control.

<u>Try 8 – 15°C:</u> I decided to try again using 15°C for expression, since that's even more likely to keep proteins stable and soluble than 22°C. I picked from the 6-day-old neck-KHC-GFP plate to start 2 overnight cultures, used 0.5mL each of culture 1 to start 2 50mL cultures, grew 24 hours at 15°C. It increased only 5-fold in 24 hours, nowhere near enough; the cells were probably too old. So retransformed neck-KHC-GFP, started two overnight cultures, used 0.5mL each of culture 1 to start 3 50mL cultures, grew 4 hours at 37°C, when OD600 ~0.6-0.7 for all. At that point I induced with 1) nothing, 2) 0.1mM IPTG, and 3) 0.3mM IPTG, dropped temperature to 15°C and let express overnight. Froze cell pellets (all bright yellow) and did purification as before, but messed up gel (Figure 2-20) the first two times – the decent one shown has smaller amounts of just the total, soluble and fractions 2 & 3 for each prep, all on one gel (post-binding looked much like soluble, and wash didn't show anything significant). Interestingly, the ~75kD bands are strongest in the no-IPTG fractions, but the one total fraction that loaded well (0.1mM IPTG) has a nice fat band at ~ 75kD, so there's certainly a lot of neck-KHC-GFP being made. This gel was inconclusive again for whether I'm getting soluble protein, though it does look like I'm getting more soluble something with 15°C expression.
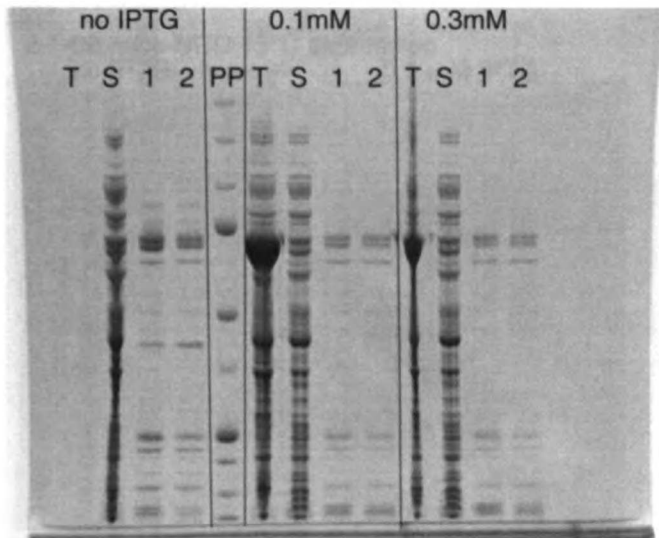
Figure 2-20: Expression of neck-KHC-GFP at 15°C, different IPTG concentrations.

Try 9 – GFP-less: In case the GFP is causing trouble with expression or purification (though I suspect the neck is the bigger irritant), I tried using the mis-recombined neck-NCD construct, which lost the GFP gene. Transformed fresh, didn't grow well when inoculated straight from colonies, so I grew an overnight culture and used it to start 2 50mL cultures as usual, grew about 4 hours at 37°C until OD600 ~0.7, induced with 0.1mM IPTG in one flask and left the other uninduced, expressed overnight at 15°C. Purified protein with the same procedure, and ran the usual gel samples (Figure 2-21). Expected ~53kD product for neck-NCD, but the gel shows a band at ~40kD and a strong one again at ~75kD! A little stronger with no IPTG, like Try 8. I couldn't be sure if I was getting expression, since the cells won't change color with no GFP, but it seems like it's expressing well and getting a decent amount soluble. Need to check by mass spectrometry to be more certain what the two bands are.
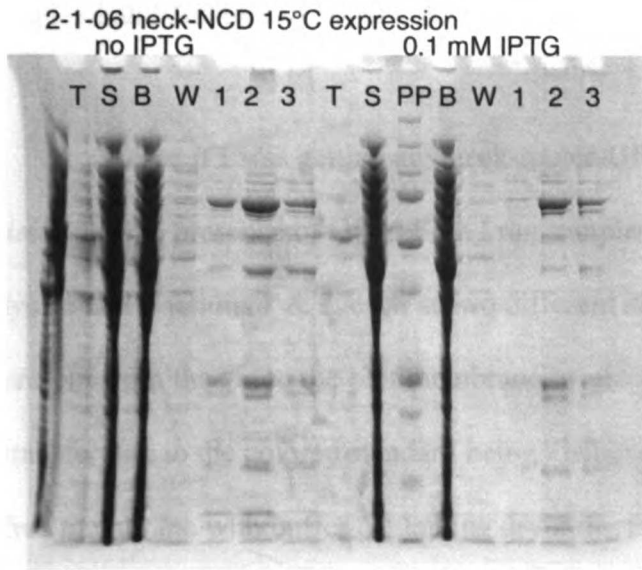
Figure 2-21: Expression of neck-NCD (GFP-less).

Table 2-1: Summary of Expression and Purification trials in BL21(DE)Star

Try #	Prot.	Inoc.	mL culture	temp (°C)	mM IPTG	hrs expr	pellet color	μL Ni	Figure #
1	nKHCg	culture	25/5	25/25	0	3,on	?	xx	xx
1	nKHCg	culture	25/5	25/25	0.2	3,on	?	xx	xx
2	nALLg	colony	50	37/22	0.3	18	green	1 mL	13
3	nALLg	colony	50	37/x	0	on	brown	xx	xx
4	nALLg	culture	1000	22/22	0.1	7	brown	xx	xx
5	nALLg	culture	1000/50	37/22	0.1	16	brown	200	15,16
6	nALLg	colony	50	37/22	0.3	18	yellow	100	18
7	nKHCg	culture	50	37/22	0.3	on	yellow	100	19
7	MBP	culture	50	37/22	0.3	on	brown	100	19
8	nKHCg	culture	50	37/15	0	on	yellow	100	20
8	nKHCg	culture	50	37/15	0.1	on	yellow	100	20
8	nKHCg	culture	50	37/15	0.3	on	yellow	100	20
9	nNCD	culture	50	37/15	0	on	brown	100	21
9	nNCD	culture	50	37/15	0.1	on	brown	100	21

Confirmation of soluble neck-KHC-GFP and neck-NCD

To see if I was getting any neck-motor-GFP expression, I ran a Western Blot to assay for the presence of GFP. First I ran samples of the neck-KHC-GFP and MBP total lysate and fractions 1 & 2, each at two different dilutions. Then we transferred the protein from the gel to the blot membrane by electrophoresis, confirming a successful transfer due to the colored standard being visible on the membrane. Then we blocked the free membrane with buffer containing dry milk, then incubated with 1/5000 diluted anti-GFP primary antibody, washed well, then incubated with the anti-rabbit secondary antibody and washed well again. Finally we added the horseradish peroxidase reagent, which makes a luminescent product, and exposed the gel to film to visualize where the antibody attached. It needed at least 1 minute for the bands to be visible, so I exposed for 10 minutes. The results were good: single bands in all neck-KHC-GFP lanes ~75 kD in size, nothing on the MBP (negative control) side, a very clean blot (Figure 2-22). It seems that the full-length product was being expressed, but not at a very high level, and there's an *E coli* protein sticking to the Ni-NTA resin and running at the same place on the gel, obscuring the bands and making the test culture and negative control look the same.
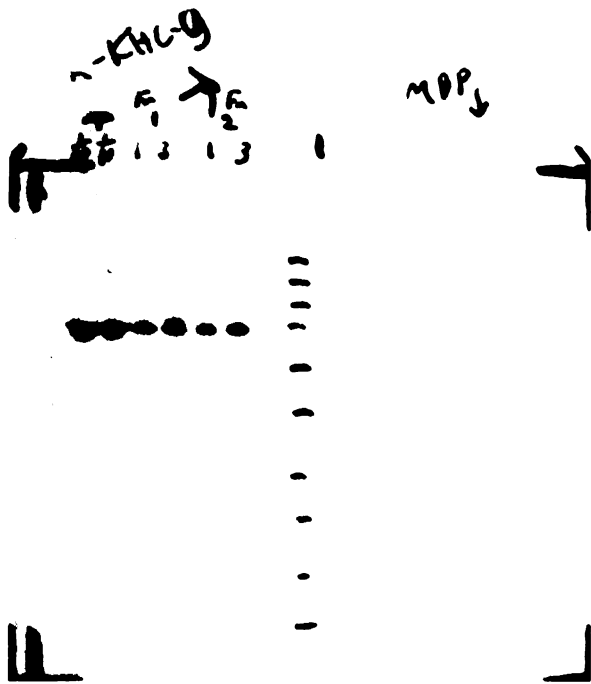
Figure 2-22: Western Blot of neck-KHC-GFP and negative control (MBP) with anti-GFP antibody.

I also checked two of the bands from the neck-NCD prep by mass spectrometry. I checked the strong ~75 kD band and the ~40 kD band, from the 0 mM IPTG culture's fraction 1, because the expected neck-NCD product size is ~52 kD so either could be the right one, depending on the protein's pI and other idiosyncracies. I digested both in the gel with trypsin (see in-gel digestion protocol), mixed with alpha matrix to make 2 1μL spots each, and checked them using the MALDI mass spectrometer on the first floor. Compared with the expected trypsin peptides, as predicted by Protein Prospector, the ~40 kD band seems to fit rather well. The ~75 kD band didn't spot well, so the results are inconclusive, but none of the acquired peaks matched the prediction. On the whole, this is a good sign that the correct neck-NCD product is being expressed, but it'd be good to use these samples for an anti-GFP Western Blot, to rule out the ~75 kD bands being

neck-NCD-GFP in spite of the plasmid sequence. Those strong bands are also evidence that the ~75 kD *E coli* protein is solubilizing better at 15°C as well.

<u>Suggestions for further expression and purification</u>

See Table 2-1 for a summary of the different expression and purification conditions I tried. I note in the appendix what seems to be the best procedure for expression and purification, for both large and small cultures. The main things to remember are: use either freshly transformed colonies or freezer stock; inoculate expression cultures from an overnight culture with ~1/100 dilution; grow at 37°C until the desired density (OD600 ~0.6-1.0), then drop to 15°C for induction and overnight expression. The pellets are more clearly colored after induction by 0.3mM IPTG, but the ~75 kD bands seemed stronger for the 0 IPTG culture than the 0.3mM IPTG culture in the last set of preps that I tried, so there might be a better soluble protein yield with lower IPTG. I suggest redoing cultures at different IPTG concentrations (0, 0.1, and 0.3 mM) and running another Western Blot to assay more clearly under which condition the soluble neck-motor-GFP concentrations are highest – it could be that the ~75 kD *E coli* proteins being copurified are also solubilizing better at lower temperature and IPTG. As for those proteins, it is clear that the Ni-NTA column purification needs to be followed by an ion-exchange-based MonoS purification, to separate out the expressed protein from *E coli* background. I did not try that myself yet, but have included the Vale lab protocol for it in the appendix. Note that NCD precipitates in PIPES buffer, so MOPS should be used instead, at the same concentration, for all buffers contacting the NCD constructs.

<u>Proposed continuation of the study: microtubule depolymerization assay and localization assay</u>

<u>Necessary gene constructs and mutagenesis</u>

<u>Making neckless, GFP-less and hMCAK controls from constructs on hand</u>

Currently I have 3 neck-motor-GFP constructs in pDEST17, ready for expression. The neck-hMCAK-GFP control still needs to be cloned out and moved to the pDEST17 vector, along with all 4 neckless controls made by BioMeans and myself. The primer for adding attB1 at the N-terminus only includes sequence from the BamHI site and two more of the GS's before the TEV site, and the attB2 site is added after the GFP+STOP. Since all my constructs have and will retain the TEV site, this same primer pair can be used to transfer all the motor-GFP constructs to the T7-based pDEST17 vector. Enough BP colonies should be prepped and sequenced to identify ones that recombined with and without GFP, to produce GFP-free controls as well as the desired constructs – but it'd be good to check that the extra protein sequence from the attB2 site and a bit after won't cause problems. Expression and purification will probably be similar to what I recommended from my results with the neck-motor-GFP constructs, except that the controls will be a different size on the gel, and of course the GFP-less constructs won't be as easily assessed by their color. The hMCAK constructs might also express or purify less well, depending on whether L2/depolymerase is toxic to the cells; neckless constructs might express or purify better for the opposite reason.

Loop2 sequence to insert/mutate, with locations for each motor core

The hMCAK L2 region lies between two hydrophobic "anchors" as shown: (V)HEPKLKVDLTKYLENQA(F). This would replace the KHC sequence (I)ASKP(Y), the NCD sequence (V)ELQSIDAQAKSKMGQQI(F), and the Unc104 sequence (H)SINKENFSFN(F), though since there's no Unc104 structure I'm less certain of the L2 boundaries for it.. The hMCAK L2 coding sequence for HEP...NQA is:

CATGAACCCAAGTTGAAAGTGGACTTAACAAAGTATCTGGAGAACCAAGCA. This rather long sequence could be inserted/mutated in using several rounds of QuikChange, but it would be much faster (and possibly cheaper in terms of materials) to have that done by BioMeans, Inc. They quoted me about $425 for that type of mutation.

It would be best to see which of the 3 motor constructs work best for the complete purification, and order L2 addition for that one first. However, a talk I heard by Lisa Sproul at the Biophysical Society Conference (February 2006) suggested that NCD is itself able to depolymerize microtubules – this supports the idea of a L2 insert being important for this function, but makes NCD less useful as an experimental subject for gain of function. I recommend keeping the current neck-NCD constructs as an interesting semi-positive control, and adding hMCAK L2 to KHC and possibly Unc104.

<u>Depolymerization assay</u>

Because the KHC MT-binding surface is probably not optimized for

depolymerization the way hMCAK is, I don't expect the neck-KHC or neck-Unc104

constructs with hMCAK L2 to show much depolymerization activity if there is any. So I

suggest starting with the spin-down depolymerization assay procedure used with the

neckless pKinI, as described in Chapter 1. This requires polymerizing microtubules and

stabilizing them with 20 μM taxol at 37°C, then incubating with the motor in roughly a

1:4 motor:tubulin ratio and 3 mM ATP. For controls use the same mixture without

motor, or the L2-less neck-motor construct. These mixtures are incubated for 15 minutes

at room temperature, then 150 μL samples of each are ultracentrifuged at 55000 rpm for

15 minutes at 25°C to separate the microtubule polymers (pellet) from free tubulin

(supernatant). Resuspend the pellets in 150 μL buffer, then run aliquots (10 μL as a start)

of the supernatant, pellet and total fractions on an SDS-PAGE gel, and stain with

Coomassie Blue dye. To quantify the amounts in each gel band, run a protein standard

with a known concentration on the same gel, and take and save a high-resolution picture

of the gel. I'm less certain what is the best software for more exact quantifying of bands,

but a start could be made with the software on the GelMac, which is able to make those

calculations.

Figure 2-23 shows an example of such a gel. The tubulin bands are the ones to be

quantified, to obtain the ratio of polymerized to free tubulin. It is also worth checking for

the motor band, noting in which fraction the motor is found, and calculating a ratio as

well if there's a significant amount both bound to microtubules (pellet) and in solution

(supernatant). Although the microbutules are stabilized by taxol, there is still some dynamic instability leading to some breakdown into free tubulin, so as in Chapter 1 the percentage of free tubulin obtained with no motor present should be calculated and subtracted from the results with motor construct, to obtain the percentage of tubulin that was depolymerized by the motor. At least three sets of assays should be performed for each condition, and the concentrations of motor and tubulin should be adjusted as needed. And of course, they should be done with motor controls as well, L2-less and possibly also neckless, as well as the hMCAK constructs as a positive control. I'm not sure how the conditions need to be changed to measure hMCAK's higher depolymerization activity, but it would probably require using lower concentrations of motor – as a starting point, see Howard et.al, 2003, for methods used with full-length MCAK.

+KinI   −KinI
super   pellet   super   pellet
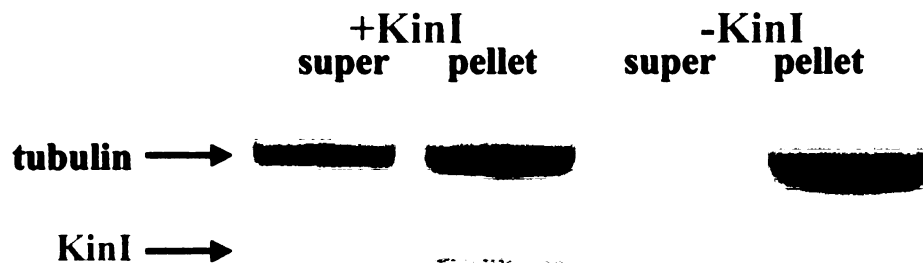
tubulin ⟶

KinI ⟶

Figure 2-23: Example of a gel from a MT-depolymerization spin-down assay. The relative locations of the tubulin and KinI bands will of course depend on the size of the KinI construct. Used with permission from Carolyn Moores.

If the depolymerization assays show no significant activity with neck-KHC (L2) compared with L2-less neck-KHC, first check the activity of the hMCAK constructs to rule out effects of cloning artifacts (His-tag and attB2-site residues at the C-terminus).

Delete the attB2 site from the constructs through QuikChange or other means, and remove the His-tag by digestion with TEV protease, to see if their removal has any significant effect on hMCAK activity.

If hMCAK works fine, and the effect of cloning artifacts can be ruled out, then it's possible that the lack of neck-KHC (L2) activity is due to inability to target to the microtubule ends, leading to less efficient depolymerization. Although neck is expected to be sufficient for targeting the microtubule ends, it's worth checking if this is true for the neck-KHC construct. If it *is* able to localize to the microtubule ends, then L2 is not sufficient for depolymerization. See the next section for the localization assay.

Localization assay

It's best to consult with Ron Vale's lab on how to do this assay, as they do this type of experiment often and have most of the necessary materials available. However, I can give a basic idea of what's involved in the procedure. First, the Vale lab has a Total Internal Fluorescence (TIRF) microscope, which gives the best signal-to-noise for visualizing molecules attached at the glass surface. It uses a prism and a shallow-angled laser to excite fluorescence in just the molecules at the surface, reducing blurred fluorescence (effectively noise) from other fluorescent molecules in solution (Figure 2-24). For this assay it's sufficient to see the overall localization of GFP-bound neck-motor constructs on the microtubule, so the more precise techniques for visualizing single molecules aren't necessary – it's best to consult with the Vale lab on what would be the

easiest method that would work. Either way, much less tubulin and kinesin is required

for this microscopic assay than for structural studies or other assays (such as ATPase).
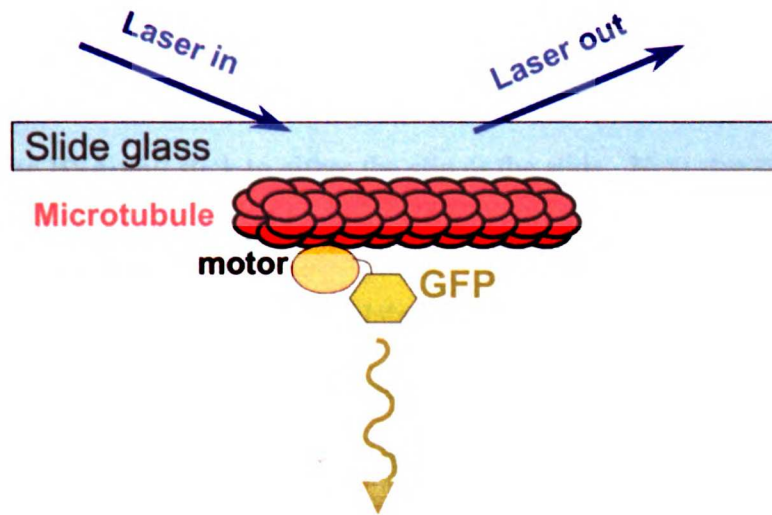
Figure 2-24: General setup of TIRF microscopy. Laser light is shined in at an angle

to excite fluorescent molecules on the glass surface, in this case the labeled microtubules

and the GFP attached to a kinesin motor.   The camera located below sees only the

fluorescence emitted by the molecules, and not the laser itself or molecules in solution.

Of course, in order to see the microtubules and neck-motor constructs, both the

tubulin and motors need to be fluorescently labeled, and the microtubules need to be

stuck to the glass surface (which isn't trivial). I already have the neck-motor-GFP gene

constructs and have partially purified some of each as soluble protein, as covered in the

previous section. Microtubules can be labeled with one of three different red dyes:

rhodamine, Cy3, and Cy5. The Vale lab has tubulin with any of these labels, and they are

often available commercially, for example from Cytoskeleton, Inc. Alternatively, they

have frozen axonemes (bundles of microtubules) from sea urchin sperm, which is easily labeled and then diluted for use on microscope slides, no polymerization required.

To stick microtubules to glass, they often use the extremely tight-binding properties of the protein streptavidin to the molecule biotin. First bovine serum albumin (BSA) attached to biotin is flowed into the space between a coverslip and a microscope slide; the BSA will stick to either the slip or the slide. Next streptavidin is flowed in, and sticks tightly to the biotin. Finally biotinylated microtubules (polymerized from a mixture of fluorescent and biotinylated tubulin) are flowed in, and these stick to the streptavidin and therefore to the surface. I'm less certain of whether axoneme microtubules can be biotinylated, but the Vale lab would know best how these are stuck to glass. Now the desired motor-GFP constructs can be flowed in, and the results visualized on the fluorescent light microscope. It'll probably be necessary to vary the concentrations of each component in order to see single microtubules, and it'll also be good to include different nucleotides, such as ATP, ADP, AMPPNP and ADP-AlF$_4$, to see if they affect behavior.

To quantify degree of microtubule-end localization, images should be taken of whole single microtubules with a reasonable density of neck-motor-GFP bound. If the entire microtubule lattice is covered (decorated) with the motors, the motor concentration should be reduced, probably to 1/10 of what was used. I suggest dividing each microtubule image into fourths, and quantifying the amount of green fluorescence in the two end fourths vs. the amount in the middle half (two fourths). If the end:middle fluorescence ratio is significantly greater than 1, then the neck-motor-GFP construct is targeting to the ends. The exact difference required for significance will depend on such

statistics as sample size and standard deviation of the values. It may be necessary to compare the outer sixths versus the middle two-thirds (need end:middle ratio greater than 1:2 in this case), or further refinement of the "end" definition, but fourth-half-fourth seems a good place to start.

These assays would be best performed with constructs lacking L2 from hMCAK, but because here we're assuming that the depolymerization activity is low, the presence of L2 shouldn't be a problem as long as the slides are used less than 15 minutes after preparation. It is more likely to be a problem when testing the positive control neck-hMCAK-GFP; in that case it'd be good to take images at 1, 5, 10 and 15 minutes for a time-course of depolymerization, and to make sure that the concentrations are low and that ATP or AMPPNP is not used if depolymerization activity is significant. As a negative control, neckless motor-GFP constructs should also be visualized, to obtain a baseline for the end:middle ratio.

Another Project Idea – Loop2 Deletion from hMCAK

Looking at the recent reviews of Kinesin-13/KinI work (Moore & Wordeman 2004, Wordeman 2005), it seems that the point made in my paper (Chapter 1) and the Kif2C paper (Ogawa et.al., 2004) about KVD/Loop2 might have been ignored. It's likely that the neckless *Pf* motor, which hasn't yet been shown to play a role in mitosis, is considered different enough from more conventional KinI's such as MCAK that general conclusions can't be drawn from our results. However, Kif2C is a vertebrate KinI, and they saw behavior with their KVD triple-alanine mutant that matches what we saw

(Ogawa et.al. 2004). Another possible interpretation of our results is that the set of three alanines are forming a sticky spot (hydrophobic) that is making the motor stick to the microtubule lattice more than it normally would, and be unable to diffuse to the ends. Although this could also explain the disparity between microtubule-stimulated and tubulin-stimulated ATPase activities, it seems to be ruled out by the fact that the KVD mutant of Kif2C+neck did NOT decorate microtubules, while the neckless KVD mutant behaves the same as neckless *Pf* KinI KVD mutant: it decorates microtubules but can no longer depolymerize them. Even so, the role of Loop2 has still been somewhat overlooked, and could stand to be better specified.

To establish Loop2's importance more concretely, I propose deleting the entire Loop2 insert from hMCAK {(V)HEPKLKVDLTKYLENQA(F)} and replacing it with the short one found in KHC {(I)ASKP(Y)}, removing the long and structured "loop" from the construct. This could probably be done fairly easily by QuikChange mutation, because the section of added nucleotides would be fairly short. Of course BioMeans, Inc. is another option if QuikChange decides not to work. This L2-less mutant of hMCAK (both full-length and neck-motor versions would be useful to make) could then be assayed for its depolymerization and ATPase abilities, similar to how *Pf* KinI was assayed in Chapter 1. This construct would have the neck, and Okada et.al. saw that neckless motors decorated the microtubules while motors with neck did not, both with and without KVD mutated to alanine, so I'd expect the L2-less hMCAK to also not decorate microtubules.

Lack of both microtubule decoration and depolymerization ability, along with tubulin ATPase but low microtubule ATPase, would support the assertion that Loop2

plays an active and specific role in depolymerization. If the construct still decorates the microtubule lattice, then perhaps L2 is also helping to target the microtubule ends. It could be that stabilizing curved tubulin at the ends is enough to induce depolymerization, even in stabilized microtubules (which might have transient end curving that is too brief to see by EM). In that case the entire microtubule-binding surface, which is more convex than in conventional kinesin (Ogawa et.al. 2004), would be necessary for the change in function. This project should be relatively easy to do, and would be good to try as a complement to the "walking-kinesins + hMCAK neck & L2" project, especially if no depolymerization activity is obtained for neck-KHC but the construct is able to target the microtubule ends (as seen in the localization assay).

Appendix A: Oligonucleotides used in Cloning

Bold letters = extra sequence, normal type = bases that match template, **Underline = restriction enzyme site**

T_M, when included, is melting temperature in °C as calculated by Invitrogen's OligoPerfect Designer. Before parentheses is the melting temperature for just the matching base pairs, inside parentheses is the melting temp for the whole oligo.

Initial Restriction-Enzyme+Ligation Cloning

The "GTCAGT" at the start of each PCR primer acts as a spacer before the RE site, since Restriction Enzymes prefer to cut within the DNA sequence rather than at the ends. They weren't included when using the OligoPerfect Designer, so the full-length T_M's aren't accurate.

OLIGOS FOR GFP-TEV-NECK CONSTRUCTION

These cloned out GFP, adding a KpnI site before it and a BamHI site after it.

GFP F T_M = 59.79(~68)   38bp
5'- **GTCAGT** <u>**GGTACC**</u> AGTAAAGGAGAAGAACTTTTCACTGG -3'

GFP R T_M = 60.95(~69)   36bp
5'- **GTCAGT** <u>**GGATCC**</u> TTTGTATAGTTCATCCATGCCATG -3'

These cloned out the hMCAK neck, giving it a NarI site at the start and ending with the conserved Arg-Pro (EagI site), and also mutating the residue before the Arg-Pro from Lys to Ile.

hMCAK neck F T_M = 58.64(~75)   32bp
5'- **GTCAGT** <u>**GGCGCC**</u> TCAGTTCGGAGGAAATCATG -3'

hMCAK neck R T_M = 58.26(~73)   39bp
5'- **GTCAGT** <u>**CGGCCG**</u> **TA** TCCTAACACAGACACATATTCTGTG -3'

These paired up to form double-stranded DNA containing a series of 5 Gly-Ser pairs (the first being a BamHI site) and the TEV-protease cleavage site, with BamHI and NarI sticky ends to link the digested GFP and neck sequences. This strategy actually worked!

TEV Insert F   52bp
5'-**GATCC** GGTTCCGGTTCCGGTTCCGGTTCC GAAAACCTGTATTTTCAGGGA GG-3'
TEV Insert R   50bp
5'-**CGCC** TCCCTGAAAATACAGGTTTTC GGAACCGGAACCGGAACCGGAACC G-3'

These were meant to pair up to form double-stranded DNA with EagI and SalI sticky ends, to bridge the gap between the neck EagI site and the SalI site in the vector. They didn't actually work though – ligation is tricky.

EagI-SalI Spacer F   16bp
5'- GGCCG TT ACGCGT AA G -3'
EagI-SalI Spacer R   16bp
5'- TCGAC TT ACGCGT AA C -3'

MOTOR PRIMERS
These cloned out the three motor cores, starting at the conserved Arg-Pro (EagI site) and ending with STOP-SalI.

dmNCD F T_M = 63.65(~82)   29bp
5'- GTCAGT <u>CGGCCG</u> CCGCTGGAGTCCGAGGA -3'

dmNCD R T_M = 63.01(~74)   33bp
5'- GTCAGT <u>GTCGAC</u> TTA GGAGTTTACGGAGGCCGC -3'

hsuKHC F T_M = 58.99(~77)   34bp
5'- GTCAGT <u>CGGCCG</u> CTCAACGAGTCTGAAGTGAACC -5'

hsuKHC R T_M = 59.03(~67)   37bp
5'- GTCAGT <u>GTCGAC</u> TTA TGTGTTCTTAATTGTTTTGGCC -3'

ceUnc104 F T_M = 59.91(~76)   32bp
5'- GTCAGT <u>CGGCCG</u> TTCAACCAACGGGAAATCTC -3'

ceUnc104 R T_M = 60.49(~69)   34bp
5'- GTCAGT <u>GTCGAC</u> TTA TTGTTTCGCTCTATCGGCA -3'

This, with the original **GFP F**, added a KpnI site at the 3' end of the GFP-TEV-neck construct cloned previously, to improve chances of ligating into vector.

GTN-R T_M = 61.04(~70)   26bp
5'- GTCAGT <u>GGTACC</u> CGGCCG TA TCCTAACACAGA -3'

These were for adding SalI sites at both ends of the GFP-TEV-neck construct, for the same strategy as above, since SalI more reliable than KpnI. Abandoned this strategy for Gateway Cloning soon after ordering.

SalI-GTN-F T_M = 60.30(~70)   39bp
5'- GTC AGT <u>GTC GAC</u> <u>GGT ACC</u> AGT AAA GGA GAA GAA CTT TTC -3'

SalI-GTN-R T_M = 59.16(~70)   31bp
5'- GTA CGT <u>GTC GAC</u> <u>CGG CCG</u> TAT CCT AAC ACA G -3'

Multisite Gateway Cloning

To clone out the T5 promoter, TEV protease site, and hMCAK neck (ligated together previously) with attB4 and NarI/SpeI/attB1 at the ends.

GW5' T5-TEV-neck (B4)   T_M = 58.06(77.53)   55 bp
5'- GGG GAC AAC TTT GTA TAG AAA AGT TGC CCT CGA GAA ATC ATA AAA AAT TTA TTT G -3'

GW3' T5-TEV-neck + Nar/Spe (B1) T_M = 57.09(84.53)   60 bp
5'- GGG GAC TGC TTT TTT GTA CAA ACT TGT ACT AGT GGC GCC TCT GTG CTC TTC GAT AGG ATC -3'

To clone out the dmNCD motor with attB1/SpeI and KpnI/attB2 at the ends.

GW5' NCD + SpeI (B1)   55 bp
5'- GGG GAC AAG TTT GTA CAA AAA AGC AGG CTC CAC TAG TAT CCG GGT CTT CTG TCG A -3'

GW3' NCD + KpnI (B2)   53 bp
5'- GGG GAC CAC TTT GTA CAA GAA AGC TGG GTT GGT ACC GGA GTT TAC GGA GGC CG -3'

To clone out GFP with attB2/KpnI/NheI and NheI/STOP/attB3 on the ends

GW5' GFP + Kpn/Nhe   T_M = 59.79(85.62)   66 bp
5'- GGG GAC AGC TTT CTT GTA CAA AGT GGC TGG TAC C GC TAG CAG TAA AGG AGA AGA ACT TTT CAC TGG -3'

GW3' GFP + Nhe/STOP   T_M = 60.95(78.47)   60 bp
5'- GGG GAC AAC TTT GTA TAA TAA AGT TGT TTA GCT AGC TTT GTA TAG TTC ATC CAT GCC ATG -3'

To clone out the human MCAK motor with attB1/SpeI and KpnI/attB2 sites on the ends. Two forward primers, to clone motor with and without neck.

hMCAK neck F (B1/SpeI)   T_M = 59.54(84.11)   58 bp
5'- GGG GAC AAG TTT GTA CAA AAA AGC AGG CTC CAC TAG TTC AGT TCG GAG GAA ATC ATG T -3'

hMCAK motor F (B1/SpeI)   T_M = 59.50(82.61)   61 bp
5'- GGG GAC AAG TTT GTA CAA AAA AGC AGG CTC CAC TAG TAT ATG TGT CTG TGT TAG GAA ACG C -3'

hMCAK motor R (B2/KpnI)   T_M = 60.26(87.20)   56 bp
5'- GGG GAC CAC TTT GTA CAA GAA AGC TGG GTT GGT ACC CTC CTT GAC CCT GTC TGC AT -3'

92

To clone out the huKHC motor with attB1/SpeI and KpnI/attB2 at the ends.

GW5' hsuKHC + SpeI   59 bp
5'- GGG GAC AAG TTT GTA CAA AAA AGC AGG CTC C<u>AC TAG T</u>AT CAA AGT GAT GTG TCG CTT CA -3'

GW3' hsuKHC + KpnI   58 bp
5'- GGG GAC CAC TTT GTA CAA GAA AGC TGG GTT <u>GGT ACC</u> TGT GTT CTT AAT TGT TTT GGC C -3'

To clone out ceUnc104 motor with attB1/SpeI and KpnI/attB2 at the ends.

GW5' ceUnc104 + SpeI   61 bp
5'- GGG GAC AAG TTT GTA CAA AAA AGC AGG CTC C<u>AC TAG T</u> GT TAA AGT AGC TGT ACG TGT TCG C -3'

GW3' ceUnc104 + KpnI   55 bp
5'- GGG GAC CAC TTT GTA CAA GAA AGC TGG GTT <u>GGT ACC</u> TTG TTT CGC TCT ATC GGC A -3'

Use with **GW5' T5-TEV-neck (B4)** to clone out T5-TEV-neck with a STOP site before the attB1 site, so no long unwanted proteins are expressed during subcloning. Still got neck expression, which was a problem. Better not to include promoter in Multisite Gateway subcloning, as I noted in Chapter 2.

gw3' T5N + Stop   48bp
5'- GGG GAC TGC TTT TTT GTA CAA ACT TGT TTA ACT AGT GGC GCC TCT GTG -3'

QuikChange Deletions

To remove the STOP-attB1 sites (also called B1 D) or neck-STOP-attB1 (NB1 D), so that the full-length neck-motor-GFP constructs can be expressed, and the neckless controls made. Only worked for neck-B1 deletion from NCD. A dash "-" indicates the break between the two template-matching sites; the sequence between them in the template is deleted.

attB1 deletion F – NCD   **27bp**
5'- CGA AGA GCA CAG A-AT CCG GGT CTT CTG -3'

attB1 deletion R – NCD   **27bp**
5'- CAG AAG ACC CGG AT-T CTG TGC TCT TCG -3'

neck/attB1 del F – NCD   **33bp**
5'- CCT GTA TTT TCA GGG A-AT CCG GGT CTT CTG TCG -3'

neck/attB1 del R – NCD   **33bp**
5'- CGA CAG AAG ACC CGG AT-T CCC TGA AAA TAC AGG -3'

KHC NB1 D   **34bp**
5'- CCT GTA TTT TCA GGG A-AT CAA AGT GAT GTG TCG C -3'

GC - KHC NB1 D   **34bp**
5'- GCG ACA CAT CAC TTT GAT -TCC CTG AAA ATA CAG G -3'

KHC B1 D   **35bp**
5'- CCT ATC GAA GAG CAC AGA -ATC AAA GTG ATG TGT CG -3'

GC - KHC B1 D   **35bp**
5'- CGA CAC ATC ACT TTG AT-T CTG TGC TCT TCG ATA GG -3'

Unc NB1 D   **35bp**
5'- CCT GTA TTT TCA GGG A-GT TAA AGT AGC TGT ACG TG -3'

GC - Unc NB1 D   **35bp**
5'- CAC GTA CAG CTA CTT TAA C-TC CCT GAA AAT ACA GG -3'

Unc B1 D   **35bp**
5'- CCT ATC GAA GAG CAC AGA -GTT AAA GTA GCT GTA CG -3'

GC - Unc B1 D   **35bp**
5'- CGT ACA GCT ACT TTA AC-T CTG TGC TCT TCG ATA GG -3'

hMCAK NB1 D   **38bp**
5'- CCT GTA TTT TCA GGG A-AT ATG TGT CTG TGT TAG GAA AC -3'

GC - hMCAK NB1 D   **38bp**
5'- GTT TCC TAA CAC AGA CAC ATA T-TC CCT GAA AAT ACA GG -3'

hMCAK B1 D   **36bp**
5'- CCT ATC GAA GAG CAC AGA -ATA TGT GTC TGT GTT AGG -3'

GC - hMCAK B1 D   **36bp**
5'- CCT AAC ACA GAC ACA TAT- TCT GTG CTC TTC GAT AGG -3'

These two were to help screen colonies after QuikChange deletion in the NCD constructs, using colony PCR. The amplified portion contains the attB1 site, and the size is small enough that deletion of the site should be visible on a gel. Didn't work so well in practice, though.

neck attB1 detect F   **20bp**
5'- TTT CGG GCT ACT TTG GAA TG -3'

NCD attB1 detect R   **20bp**
5'- GTC CAG GTG CAA CAC ATA CG -3'

*Final Gateway Cloning

For cloning out the neck-motor-GFP constructs with attB1 and attB2 on the ends, to transfer to the final pDEST17 expression vector.

GWattB1 - GS-TEV   **T$_M$ = 61.26(85.26)**   **48 bp**
5'- GGG GAC AAG TTT GTA CAA AAA AGC AGG CTC A<u>GG ATC C</u>GG TTC CGG TTC **-3'**

GWattB2 - GFP-C   **T$_M$=60.41(81.83)**   **58 bp**
5'- GGG GAC CAC TTT GTA CAA GAA AGC TGG GTG <u>TTA</u> <u>GCT AGC</u> TTT GTA TAG TTC ATC CAT G **-3'**

Appendix B: DNA and protein sequences

C elegans Unc104 motor core

```
1/1                             31/11
atg tca tcg gtt aaa gta gct gta cgt gtt cgc cca ttc aac caa cgg gaa atc tcg aac
 M   S   S   V   K   V   A   V   R   V   R   P   F   N   Q   R   E   I   S   N

61/21                           91/31
act tca aaa tgt gtc ctt caa gta aat gga aat acg aca ata aat ggt cat tca att
 T   S   K   C   V   L   Q   V   N   G   N   T   T   I   N   G   H   S   I

121/41                          151/51
aac aag gag aac ttc agt ttc aat ttt gat cat tca tat tgg tcg ttt gcg agg aat gac
 N   K   E   N   F   S   F   N   F   D   H   S   Y   W   S   F   A   R   N   D

181/61                          211/71
cca cat ttt atc acc caa aaa caa gta tat gaa gag ctc gga gtt gaa atg ttg gaa cac
 P   H   F   I   T   Q   K   Q   V   Y   E   E   L   G   V   E   M   L   E   H

241/81                          271/91
gca ttt gaa ggg tat aat gtc tgc att ttt gca tac ggt caa aca gga tca gga aaa tca
 A   F   E   G   Y   N   V   C   I   F   A   Y   G   Q   T   G   S   G   K   S

301/101                         331/111
tat aca atg atg gga aaa gcc aat gat gaa atg gga ata att cca cgt ttg tgc
 Y   T   M   M   G   K   A   N   D   P   D   E   M   G   I   I   P   R   L   C

361/121                         391/131
aat gat tta ttt gca cga att gat aat aat aaa gat gtt caa tat tct gta gag
 N   D   L   F   A   R   I   D   N   N   N   D   K   D   V   Q   Y   S   V   E
```

```
421/141
gta tcg tat atg gaa att tat tgt gaa cga  gta aaa gat ctt ctg aat cct gga aac tct
 V   S   Y   M   E   I   Y   C   E   R   451/151
                                          V   K   D   L   L   N   P   G   N   S

481/161
ggt aac cta agg gtt cgt gaa cat cct tta  ctt gga cct tac gtc gat gac ctt acc aaa
 G   N   L   R   V   R   E   H   P   L   511/171
                                          L   G   P   Y   V   D   D   L   T   K

541/181
atg gca gtt tgt tct tac cac gac att tgc  aat ctg atg gac gaa gga aat aaa gcg aga
 M   A   V   C   S   Y   H   D   I   C   571/191
                                          N   L   M   D   E   G   N   K   A   R

601/201
act gtt gct gca aca aat atg aat tcg aca  tca aga tcc cat gcg gta ttc aca ata
 T   V   A   A   T   N   M   N   S   T   631/211
                                          S   R   S   H   A   V   F   T   I

661/221
gta ctc act caa aaa aga cat tgt gct gat  tct aat ttg gat act gag aag cat tca aaa
 V   L   T   Q   K   R   H   C   A   D   691/231
                                          S   N   L   D   T   E   K   H   S   K

721/241
att tct ttg gtt gat ttg gca gga tca gaa  aga gcc aat tct aca gga gcg gaa ggt caa
 I   S   L   V   D   L   A   G   S   E   751/251
                                          R   A   N   S   T   G   A   E   G   Q

781/261
cga cta aaa gaa gga gca aat atc aac aag  agc ttg aca acg ttg ggt ctt gta atc agt
 R   L   K   E   G   A   N   I   N   K   811/271
                                          S   L   T   T   L   G   L   V   I   S

841/281
aaa ctt gca gaa gaa tca aca aag aag aaa  aag tcc aac aaa ggt gtg att cct tat cgt
 K   L   A   E   E   S   T   K   K   K   871/291
                                          K   S   N   K   G   V   I   P   Y   R
```

97

```
901/301
gat tct gtg ctg acg tgg ctt ctg aga gaa aat ctg gga gga aat tcg aaa act gcg atg
 D   S   V   L   T   W   L   L   R   E   N   L   G   G   N   S   K   T   A   M

931/311

961/321
ctc gcg gca tta tct cca gct gat att aac ttt gat gaa aca ctg agt act ttg aga tat
 L   A   A   L   S   P   A   D   I   N   F   D   E   T   L   S   T   L   R   Y

991/331

1021/341
gcc gat aga gcg aaa caa
 A   D   R   A   K   Q
```

Drosophila melanogaster NCD motor core

```
                                1051/351
gac ctg cgc ggc aac atc cgg gtc ttc tgt cga ata cga ccg ccg ctg gag
 D   L   R   G   N   I   R   V   F   C   R   I   R   P   P   L   E

1081/361                    1111/371
tcc gag gag aac cgt atg tgt tgc acc tgg acc tat cac gac gag tcc acc gtg gag ctg
 S   E   E   N   R   M   C   C   T   W   T   Y   H   D   E   S   T   V   E   L

1141/381                1171/391
cag agc att gac gca cag gcc aaa agc atc ttc gac cag
 Q   S   I   D   A   Q   A   K   S   I   F   D   Q

                    1201/401                        1231/411
gtc ttc cac ccg ctc tcc tcg cag tcg gac atc ttc gag atg gtc tcg ccg ctc atc cag
 V   F   H   P   L   S   S   Q   S   D   I   F   E   M   V   S   P   L   I   Q

                1261/421                        1291/431
tcg gcc ctg gat ggc tac aat atc tgc atc ttt gcc tac gga cag acg ggc agt ggc aag
 S   A   L   D   G   Y   N   I   C   I   F   A   Y   G   Q   T   G   S   G   K

            1321/441                        1351/451
acc tac aca atg gac gga gtg ccg gag agt gtc ggc gtc ata ccg cgc acg gtg gat ctg
 T   Y   T   M   D   G   V   P   E   S   V   G   V   I   P   R   T   V   D   L

        1381/461                        1411/471
ctc ttc gac tcc atc cgg gga tat cgc aac ttg ggc tgg gag tac gag atc aag gcc acc
 L   F   D   S   I   R   G   Y   R   N   L   G   W   E   Y   E   I   K   A   T

    1441/481                        1471/491
ttt ctg gag atc tac aac gag gtg ctc tac gat ctg ctg agc aac gag cag aag gac atg
 F   L   E   I   Y   N   E   V   L   Y   D   L   L   S   N   E   Q   K   D   M
```

1501/501
```
gag att cga atg gcc aag aac aag aac gac atc tac gtg tcc aac ata acg gag gag
 E   I   R   M   A   K   N   K   N   D   I   Y   V   S   N   I   T   E   E
```
1531/511

1561/521
```
acg gtt ctg gat cca aat cac ctg cgc cac acg gcc aag atg aac cgt gcc
 T   V   L   D   P   N   H   L   R   H   T   A   K   M   N   R   A
```
1591/531

1621/541
```
acc gcc tcg aca gct ggc aac gag cgc tcc cgt tcc cac gcg gtt acc aag ctt gag
 T   A   S   T   A   G   N   E   R   S   R   S   H   A   V   T   K   L   E
```
1651/551

1681/561
```
ctc atc gga cgc cat gcc gaa aag caa gag atc tcc gtg ggt tcc ata aac ctg gtg gat
 L   I   G   R   H   A   E   K   Q   E   I   S   V   G   S   I   N   L   V   D
```
1711/571

1741/581
```
ttg gcc ggc tct gag tct ccc aag acg agc atg acc cgg acc gag aca aag aac atc aat
 L   A   G   S   E   S   P   K   T   S   T   R   M   T   E   T   K   N   I   N
```
1771/591

1801/601
```
cgc tcg cta tcg gag ctc acc aac gta atc ctg gcg ctg ctg cag aag cag gac cac atc
 R   S   L   S   E   L   T   N   V   I   L   A   L   L   Q   K   Q   D   H   I
```
1831/611

1861/621
```
ccg tac agg aac tcc aag ctg acg cac ctg atg ccc tcg ctg ggc ggc aac tcg aaa
 P   Y   R   N   S   K   L   T   H   L   M   P   S   L   G   G   N   S   K
```
1891/631

1921/641
```
acg ctt atg ttc atc aac gtc tcg ccg ttc caa gac tgt ttc caa gag tcc gtc aag tcg
 T   L   M   F   I   N   V   S   P   F   Q   D   C   F   Q   E   S   V   K   S
```
1951/651

100

1981/661   2011/671
ctg cgc ttc gcg gcc tcc gta aac tcc tgc aaa atg acc aag gcc aag cgg aat cgc tac
L   R   F   A   A   S   V   N   S   C   K   M   T   K   A   K   R   N   R   Y

2041/681   2071/691   2101/701
ctg aac aac tcg gtg gcc aac agc agc aca cag agc aac aac agc ggc agt ttc gat aaa taa
L   N   N   S   V   A   N   S   S   T   Q   S   N   N   S   G   S   F   D   K   *

Human ubiquitous Kinesin Heavy Chain (KHC) motor core

```
1/1                                                 31/11
atg gcg gac ctg gcc gag tgc aac atc aaa gtg atg tgt cgc ttc aga cct ctc aac gag
 M   A   D   L   A   E   C   N   I   K   V   M   C   R   F   R   P   L   N   E

61/21                                               91/31
tct gaa gtg aac cgc ggc gac aag tac atc gcc aag ttt cag gga gaa gac acg gtc gtg
 S   E   V   N   R   G   D   K   Y   I   A   K   F   Q   G   E   D   T   V   V

121/41                                              151/51
atc gcg tcc aag cct tat gca ttt gat cgg gtg ttc cag tca agc aca tct caa gag caa
 I   A   S   K   P   Y   A   F   D   R   V   F   Q   S   S   T   S   Q   E   Q

181/61                                              211/71
gtg tat aat gac tgt gca aag aag att gtt aaa gat gta ctt gaa gga tat aat gga aca
 V   Y   N   D   C   A   K   K   I   V   K   D   V   L   E   G   Y   N   G   T

241/81                                              271/91
ata ttt gca tat gga caa aca tcc tct ggg aag aca cac aca atg gag ggt aaa ctt cat
 I   F   A   Y   G   Q   T   S   S   G   K   T   H   T   M   E   G   K   L   H

301/101                                             331/111
gat cca gaa ggc atg gga att att cca aga ata gtg caa gat att ttt aat tat att tac
 D   P   E   G   M   G   I   I   P   R   I   V   Q   D   I   F   N   Y   I   Y

361/121                                             391/131
tcc atg gat gaa aat ttg gaa ttt cat att aag gtt tca tat ttt gaa ata tat ttg gat
 S   M   D   E   N   L   E   F   H   I   K   V   S   Y   F   E   I   Y   L   D

421/141                                             451/151
aag ata agg gac ctg tta gat gtt tca aag acc aac ctt tca gtt cat gaa gac aaa aac
 K   I   R   D   L   L   D   V   S   K   T   N   L   S   V   H   E   D   K   N
```

481/161
cga gtt ccc tat gta aag ggg tgc aca gag 511/171 ttt gta tgt agt cca gat gaa gtt atg
R   V   P   Y   V   K   G   C   T   E   F   V   C   S   P   D   E   V   M

541/181
gat acc ata gat gaa gga aaa tcc aac aga 571/191 gca gtt aca aat atg aat gaa cat
D   T   I   D   E   G   K   S   N   R   A   V   T   N   M   N   E   H

601/201
agc tct agg agt cac agt ata ttt ctt att 631/211 aat gtc aaa caa gag aac aca caa acg gaa
S   S   R   S   H   S   I   F   L   I   N   V   K   Q   E   N   T   Q   T   E

661/221
caa aag ctg agt gga aaa ctt tat ctg gtt 691/231 gat tta gct gaa aag gtt agt aaa
Q   K   L   S   G   K   L   Y   L   V   D   L   A   G   S   E   K   V   S   K

721/241
act gga gct gaa ggt gct gtg ctg gat gaa 751/251 aac atc aac aag tca ctt tct gct
T   G   A   E   G   A   V   L   D   E   K   N   I   N   K   S   L   S   A

781/261
ctt gga aat gtt att tct gct ttg gct gag 811/271 agt gga aca tat gtt cca tat cga gat agt
L   G   N   V   I   S   A   L   A   E   G   S   T   Y   V   P   Y   R   D   S

841/281
aaa atg aca aga atc ctt caa gat tca tta 871/291 ggt ggc aac tgt aga acc att gta att
K   M   T   R   I   L   Q   D   S   L   G   G   N   C   R   T   I   V   I

901/301
tgc tgc tct cca tca tca tac aat gag tct 931/311 gaa aca aaa tct aca ctc tta ttt ggc caa
C   C   S   P   S   S   Y   N   E   S   E   T   K   S   T   L   L   F   G   Q

103

961/321
agg gcc aaa aca att aag aac aca
R   A   K   T   I   K   N   T

Human MCAK (hMCAK) neck & motor core (green = neck, red = L2 insert)

```
          571/191
          tca gtt cgg agg aaa tca tgt ctt gtg aag gaa gtg gaa aaa
           S   V   R   R   K   S   C   L   V   K   E   V   E   K

601/201
atg aag aac cga gaa gag aag gcc cag aac tct gaa atg aga gct
 M   K   N   R   E   E   K   A   Q   N   S   E   M   R   A

          631/211
          cag gag tat gac agt ttt cca aac tgg gaa ttt gcc cga atg att aaa gaa ttt cgg
           Q   E   Y   D   S   F   P   N   W   E   F   A   R   M   I   K   E   F   R

661/221
cag gag tat gac agt ttt cca aac tgg gaa
 Q   E   Y   D   S   F   P   N   W   E

          691/231
          ttt gcc cga atg att aaa gaa ttt cgg
           F   A   R   M   I   K   E   F   R

721/241
gct act ttg gaa tgt cat cca ctt act atg gat cct atc gaa gag cac aga ata tgt
 A   T   L   E   C   H   P   L   T   M   D   P   I   E   E   H   R   I   C

          751/251
          gct act ttg gaa tgt cat cca ctt act atg gat cct atc gaa gag cac aga ata tgt
           A   T   L   E   C   H   P   L   T   M   D   P   I   E   E   H   R   I   C

781/261
gtc tgt gtt agg aaa cgc cga cca ctg aat aag caa gaa ttg gcc aag aaa gaa att gat gtg
 V   C   V   R   K   R   R   P   L   N   K   Q   E   L   A   K   K   E   I   D   V

          811/271
          gtc tgt gtt agg aaa cgc cga cca ctg aat aag caa gaa ttg gcc aag aaa gaa att gat gtg
           V   C   V   R   K   R   R   P   L   N   K   Q   E   L   A   K   K   E   I   D   V

841/281
att tcc att cct agc aag tgt ctc ctc ttg gta cat gaa ccc aag ttg aaa gtg gac tta
 I   S   I   P   S   K   C   L   L   L   V   H   E   P   K   L   K   V   D   L

          871/291
          att tcc att cct agc aag tgt ctc ctc ttg gta cat gaa ccc aag ttg aaa gtg gac tta
           I   S   I   P   S   K   C   L   L   L   V   H   E   P   K   L   K   V   D   L

901/301
aca aag tat ctg gag aac caa gca ttc tgc ttt gac ttt gca ttt gat gaa aca gct tcg
 T   K   Y   L   E   N   Q   A   F   C   F   D   F   A   F   D   E   T   A   S

          931/311
          aca aag tat ctg gag aac caa gca ttc tgc ttt gac ttt gca ttt gat gaa aca gct tcg
           T   K   Y   L   E   N   Q   A   F   C   F   D   F   A   F   D   E   T   A   S

961/321
aat gaa gtt gtc tac agg ttc aca gca agg cca ctg gta cag aca atc ttt gaa ggt gga
 N   E   V   V   Y   R   F   T   A   R   P   L   V   Q   T   I   F   E   G   G

          991/331
          aat gaa gtt gtc tac agg ttc aca gca agg cca ctg gta cag aca atc ttt gaa ggt gga
           N   E   V   V   Y   R   F   T   A   R   P   L   V   Q   T   I   F   E   G   G
```

1021/341
aaa gca act tgt ttt gca tat ggc cag aca gga agt ggc aag aca cat act atg ggc gga
K   A   T   C   F   A   Y   G   Q   T   G   S   G   K   T   H   T   M   G   G

1051/351

1081/361
gac ctc tct ggg aaa gcc cag aat gca tcc atg gcc tcc cgg gac
D   L   S   G   K   A   Q   N   A   S   M   A   S   R   D

1111/371

1141/381
gtc ttc ctc ctg aag aat caa ccc tgc aag ttg ggc ctg gaa gtc tat gtg aca
V   F   L   L   K   N   Q   P   C   Y   R   K   L   G   L   E   V   Y   V   T

1171/391

1201/401
ttc ttc gag atc tac aat ggg aag ctg ttt gac ctc ctc aac aag aag gcc aag ctg cgc
F   F   E   I   Y   N   G   K   L   F   D   L   L   N   K   K   A   K   L   R

1231/411

1261/421
gtg ctg gag gac ggc aag caa cag gtg caa gtg ggg ctg cag gag cat ctg gtt aac
V   L   E   D   G   K   Q   Q   V   Q   V   G   V   L   Q   E   H   L   V   N

1291/431

1321/441
tct gct gat gat gtc atc aag atg ctc gac atg ggc agc gcc tgc aga acc tct ggg cag
S   A   D   D   V   I   K   M   L   D   M   G   S   A   C   R   T   S   G   Q

1351/451

1381/461
aca ttt gcc aac tcc aat tcc tcc cgc tcc cac gcg tgc ttc caa att att ctt cga gct
T   F   A   N   S   N   S   S   R   S   H   A   C   F   Q   I   I   L   R   A

1411/471

1441/481
aaa ggg aga atg cat ggc aag ttc tct ttg gta gat ctg gca ggg aat gag cga ggc gca
K   G   R   M   H   G   K   F   S   L   V   D   L   A   G   N   E   R   G   A

1471/491

```
1501/501
gac act tcc agt gct gac cgg cag acc cgc atg gag ggc gca gaa atc aac aag agt ctc
 D   T   S   S   A   D   R   Q   T   R   M   E   G   A   E   I   N   K   S   L

1531/511

1561/521
tta gcc ctg aag gag tgc atc agg gcc ctg gga cag aac aag gct cac acc ccg ttc cgt
 L   A   L   K   E   C   I   R   A   L   G   Q   N   K   A   H   T   P   F   R

1591/531

1621/541
gag agc aag ctg aca cag gtg ctg agg gac tcc ttc att ggg gag aac tct agg act tgc
 E   S   K   L   T   Q   V   L   R   D   S   F   I   G   E   N   S   R   T   C

1651/551

1681/561
atg att gcc acg atc tca cca ggc ata agc tcc tgt gaa tat act tta aac acc ctg aga
 M   I   A   T   I   S   P   G   I   S   C   E   Y   T   L   N   T   L   R

1711/571

1741/581
tat gca gac agg gtc aag gag
 Y   A   D   R   V   K   E
```

Green Fluorescent Protein (GFP)

```
1/1                                          31/11
agt aaa gga gaa gaa ctt ttc act ggg att gtc cca gtt ctc att gag tta gac ggt gat
 S   K   G   E   E   L   F   T   G   I   V   P   V   L   I   E   L   D   G   D

61/21                                        91/31
gtc cat gga cat aaa ttc tct gtc aga gga gaa ggg gaa ggc gat gca gat tat gga aaa
 V   H   G   H   K   F   S   V   R   G   E   G   E   G   D   A   D   Y   G   K

121/41                                       151/51
ctt gaa atc aaa ttt att tgc act act gga aag cta cca gtt cca aca ctt gtt
 L   E   I   K   F   I   C   T   T   G   K   L   P   V   P   T   L   V

181/61                                       211/71
act aca ctc tct tat ggc atc cta tgt ttc gca aga tac cca gaa cac atg aaa atg aat
 T   T   L   S   Y   G   I   L   C   F   A   R   Y   P   E   H   M   K   M   N

241/81                                       271/91
gac ttc ttc aag agt gcc atg cct gag ggt tac att caa gaa aga acc atc ttt ttc caa
 D   F   F   K   S   A   M   P   E   G   Y   I   Q   E   R   T   I   F   F   Q

301/101                                      331/111
gat gat gga aaa tac aag aca cgt ggt gaa gtc aag gtt gaa ggt gat act ctt gtt aac
 D   D   G   K   Y   K   T   R   G   E   V   K   F   E   G   D   T   L   V   N

361/121                                      391/131
aga att gag ctc aaa ggt atg gac ttt aaa gaa gat ggc aat atc ctt gga cac aag ttg
 R   I   E   L   K   G   M   D   F   K   E   D   G   N   I   L   G   H   K   L

421/141                                      451/151
gag tac aat ttt aac tca cat aat gta tac att atg ccg gac aaa gcc aat aat gga ctc
 E   Y   N   F   N   S   H   N   V   Y   I   M   P   D   K   A   N   N   G   L
```

```
481/161
aaa gtc aat ttc aaa att aga cac aat atc aga ggt ggt gtc caa ctt gct gat cat
  K   V   N   F   K   I   R   H   N   I   R   G   G   V   Q   L   A   D   H

511/171

541/181
tac caa aca aat gtt ccc ctt gga gac ggt cct gtc ctt ata cca atc aat cac tac cta
  Y   Q   T   N   V   P   L   G   D   G   P   V   L   I   P   I   N   H   Y   L

571/191

601/201
tcc acg caa acg gcc att tca aaa gat cga aat gag acg aga gat cat atg gtg ttt ctg
  S   T   Q   T   A   I   S   K   D   R   N   E   T   R   D   H   M   V   F   L

631/211

661/221
gaa ttt ttc tca gct tgt gga cat aca cat ggc atg gat gaa cta tac aaa
  E   F   F   S   A   C   G   H   T   H   G   M   D   E   L   Y   K

691/231

TEV protease cleavage site (with 5 GS spacer in front)
1/1
gga tcc ggt tcc ggt tcc ggt tcc ggt tcc ggt tcc gga agc ctg tat ttt cag gga ggc gcc
  G   S   G   S   G   S   G   S   G   S   G   S   E   N   L   Y   F   Q   G   G   A

31/11
```

109

Plasmodium falciparum KinI neck & motor core (green = neck, red = L2 insert)

```
1/1                               31/11
atg ttt aag aaa acg atg cag cag aaa aga caa tct ttt ata aag gta atg gat
 M   F   K   K   T   M   Q   Q   K   R   Q   S   F   I   K   V   M   D

61/21                             91/31
gaa aga aaa aaa aaa aaa aat aat agt atg tgt ata aat ctg att ggt agc aac
 E   R   K   K   K   K   N   N   S   M   C   I   N   L   I   G   S   N

121/41                            151/51
atg tgt agt gaa gtc tat cct caa aaa agc gta aat ctt ggt aat aaa gtg agg
 M   C   S   E   V   Y   P   Q   K   S   V   N   L   G   N   K   V   R

181/61                            211/71
agt aaa act atg aac agt aaa ata aaa gtt gtg agg aag aga cca ctg agc gaa tta
 S   K   T   M   N   S   K   I   K   V   V   R   K   R   P   L   S   E   L

241/81                            271/91
gaa aag aag aaa aaa gat agt gat ata att aca gta aaa aac aat tgt acg ctt tat ata
 E   K   K   K   K   D   S   D   I   I   T   V   K   N   N   C   T   L   Y   I

301/101                           331/111
gat gaa cca aga tat aaa gtg gat atg aca aaa tat ata gaa agg cat gaa ttt att gta
 D   E   P   R   Y   K   V   D   M   T   K   Y   I   E   R   H   E   F   I   V

361/121                           391/131
gat aaa gtt ttt gat gat acg gtt gat aat gtt tat aca gta tat gag aat acc ata aaa cca
 D   K   V   F   D   D   T   V   D   N   F   T   V   Y   E   N   T   I   K   P

421/141                           451/151
tta ata ata gat tta tat gag aat ggt tgt gta tgt tct tgt ttt gct tat ggg caa aca
 L   I   I   D   L   Y   E   N   G   C   V   C   S   C   F   A   Y   G   Q   T
```

110

```
481/161
ggt agc ggg aag act tat acg atg tta ggt tca caa ccg tat gga cag agt gat acc cct
 G   S   G   K   T   Y   T   M   L   G   S   Q   P   Y   G   Q   S   D   T   P

                                        511/171

541/181
ggt ata ttt caa tac gca gca ggg gat ata ttt acc ttt tta aat att tat gat aaa gat
 G   I   F   Q   Y   A   A   G   D   I   F   T   F   L   N   I   Y   D   K   D

                                        571/191

601/201
aat acg aaa ggg ata ttt ata tca ttt tat gaa att tat tgt ggt aaa tta tat gat tta
 N   T   K   G   I   F   I   S   F   Y   E   I   Y   C   G   K   L   Y   D   L

                                        631/211

661/221
tta caa aaa cgt aag atg gta gca gca tta gaa aat ggg aaa aaa gaa gtt gta aaa
 L   Q   K   R   K   M   V   A   A   L   E   N   G   K   K   E   V   V   K

                                        691/231

721/241
gat tta aaa ata tta aga gta tta aca aaa gaa gaa tta ata tta aaa atg ata gat ggt
 D   L   K   I   L   R   V   L   T   K   E   E   L   I   L   K   M   I   D   G

                                        751/251

781/261
gtt tta aga aaa att ggt gtt aat tca caa aac gat gaa tca tct aga tca cat gct
 V   L   R   K   I   G   V   N   S   Q   N   D   E   S   S   R   S   H   A

                                        811/271

841/281
ata tta aat att gat tta aaa gat ata aat aca aat aca tct ctt gga aaa att gct ttc
 I   L   N   I   D   L   K   D   I   N   K   N   T   S   L   G   K   I   A   F

                                        871/291

901/301
att gat tta gca gga agt gaa aga gga gct gat acc gtt tca caa aat aaa caa aca caa
 I   D   L   A   G   S   E   R   G   A   D   T   V   S   Q   N   K   Q   T   Q

                                        931/311
```

961/321
acc gat gga gct aat att aat aga tct tta cta gcc tta aag gaa tgt att cga gct atg
T   D   G   A   N   I   N   R   S   L   L   A   L   K   E   C   I   R   A   M

991/331

1021/341
gat tca gat aaa aat cat ata cct ttc aga gat gaa tta act aaa gtt tta aga gat
D   S   D   K   N   H   I   P   F   R   D   S   E   L   T   K   V   L   R   D

1051/351

1081/361
ata ttt gta ggg aaa tct aaa agt att atg ata gct aat att tct cct aca att agt tgt
I   F   V   G   K   S   K   S   I   M   I   A   N   I   S   P   T   I   S   C

1111/371

1141/381
tgt gag caa aca ttg aat aca tta aga tat tct tca aga gtt aag aac ttt aaa aat
C   E   Q   T   L   N   T   L   R   Y   S   S   R   V   K   N   F   K   N

1171/391

112

Appendix C: Vale lab motor-GFP expression/purification protocol

– with my notes and suggestions

Growth Conditions

1) Inoculate culture in the morning with a single, fresh colony.

    - I found that the results are more dependable by growing an overnight

    culture at 37°C and diluting at least 1/100 into the expression culture.

2) Grow at 37°C with shaking (I used 250 rpm) until OD600 = ~1.0 (~5-6 hours).

3) Drop temperature to 4°C for 45-60 minutes.

    - This is to cool down the culture quickly before induction, and can be skipped.

4) Change temperature to 22°C and induce with 0.1mM final IPTG. Continue to grow

with shaking overnight.

    - Might get better soluble yield with 15°C expression, try various IPTG conc.

5) Harvest cells the following morning. Spin in RC3B (appropriate size rotor), 5000 rpm,

20 minutes, 4°C.

    - Can do a 15 minute spin if a small culture volume, such as 50mL. I spun 15

    minutes at 5000 x g, not rpm.

6) Resuspend pellet in 25mL (for 1L culture) or 40ml (for 2L) of lysis buffer + protease

inhibitors, respin to obtain pellet in a smaller volume tube.

    - This is only for large cultures, to get the pellets into smaller disposable tubes

    and free up the 500mL or 1L bottles (which we don't have many of). Spin down

    50mL cultures in the smaller tubes from the start.

7) Freeze pellet in liquid nitrogen and store in -80°C freezer, or proceed directly to prep.

Cell disruption

1) Prepare buffers as noted later. When thawing cells, add ATP & βME fresh.

2) - Add lysis buffer to pellet (25mL for originally 1L cultures, 40mL for 2L, 2-3mL for 50mL test cultures) and homogenize with glass rod.

3) Lyse cells with the Microfluidizer

   – But need minimum 40mL liquid for Microfluidizer. For smaller volumes use the sonicator; put in 14mL orange-cap tube, and use the long-needle.

   – Sonicator settings: 50% duty cycle, output 4 or 5, keep tube chilled in beaker of ice, run for 20 pulses then let cool 4-5 minutes. If warming up in spite of the ice, reduce output to 4. Six such cycles should be enough.

4) Spin lysate in SS-34, 18500rpm, 45 minutes, 4°C

   - I spun 45 minutes at 14000 rpm, the maximum speed for the lab centrifuges. This pellets the insoluble fraction. Use the supernatant (soluble fraction) for further purification.

NiNTA column (see Qiagen Handbook)

1) Equilibrate 2mL (for 1L culture) or 3mL (for 2L) of packed NiNTA resin.

2) 2 washes with 15mL lysis buffer (without ATP & Imidazole), rock for 10 minutes each at 4°C.

3) Spin in clinical centrifuge setting #5 for 1-2 minutes

4) Resuspend in equal volume lysis buffer (without ATP & Imidazole)

   - I used 100 or 200μL resin for 50mL cultures. Measure out twice that volume of 50:50 NiNTA:ethanol slurry, spin down gently (2 minutes at 2000 rpm), carefully

remove liquid, add lysis buffer + additives (same volume as slurry), resuspend and spin again – this is "washing" once. Wash twice, then add supernatant or one more volume of lysis buffer.

5) Batch bind protein to resin by rocking for 45-60 minutes at 4°C. Spin down gently and carefully remove supernatant.

6) Load resin onto QIAGEN disposable column

- Use 1mL column for 100-200µL resin, 5 or 10mL column for 2mL resin.

7) Wash with 50mL Ni Wash Buffer

- For the small preps, I washed with 2mL <u>Lysis</u> buffer (similar enough to Wash).

8) Elute with 6 x 1mL fractions Ni Elution Buffer.

- I eluted from small columns with 500µL Elution Buffer, collected 3 fractions of the same volume as the resin.

9) Pool peak fractions (usually 2-4) – need to check on SDS-PAGE gel first.

10) Dilute with MonoQ Buffer A up to 30mL total (or a 1:10 dilution)

- Can leave protein in high imidazole until the next step (MonoQ or not?) is chosen, but the imidazole does need to be diluted for MonoQ.

<u>MonoQ (Ion Exchange Column)</u>

- I haven't done this yet myself, but I hear that conditions can vary from construct to construct. It's mainly for separating out His-tagged GFP degraded from full-length motor-GFP. Although my constructs won't have His-tagged GFP (they're located at opposite ends), it's necessary to separate neck-motor-GFP from the *E coli* proteins that migrate at ~75 kD, not to mention proteolyzed peptides.

1) Load sample at 10% Buffer B

2) Wash with 10mL 20% B (These are probably for larger 1L or 2L culture preps)

3) Elute with a 16mL 20-100% B gradient

4) Collect 1mL fractions

5) Protein elutes in ~1-2 fractions at ~350mM salt in the gradient

Preserve protein fractions by adding sucrose up to 20%, flash freeze in liquid nitrogen and keep at -80°C for posterity.

It might also be good to include **5% sucrose** in all the buffers (NiNTA and MonoQ) – could improve soluble yield.

NiNTA Purification Buffers

Additives (add fresh to NiNTA buffers before using in prep)

10mM βmercaptoethanol – add liquid from bottle

1mM ATP – add powder

Protease inhibitors: 1) 10μg/mL each leupeptin, pepstatin, and aprotinin (make 1000x

   cocktail and keep frozen, melt and resuspend powder then add fresh to buffer)

   2) 1mM PMSF (make 100mM in ethanol and add immediately)

   or 240μg/mL Pefablock (I used PMSF)

Lysis Buffer

50mM NaPO4, pH 8.0

250mM NaCl

2mM MgCl2

20mM Imidazole

(mix and pH the above in advance)

10mM βME, 1mM ATP

Ni Wash Buffer (but I used Lysis Buffer for washing as well as lysis)

50mM NaPO4, pH 6.0

250mM NaCl

1mM MgCl2

(mix and pH the above in advance)

10mM βME, 0.1 mM ATP

<u>Ni Elution Buffer</u> (I added protease inhibitors to this too, to be safe)

50mM NaPO4, pH 7.2

250mM NaCl

1mM MgCl2

<u>500mM</u> Imidazole

(mix and pH in advance)

10mM βME, 0.1mM ATP

<u>MonoQ (Ion Exchange) Purification Buffers</u>

Note: PIPES makes NCD precipitate, so for NCD preps replace PIPES with an equal

concentration of MOPS. The conditions might need to be optimized further.

<u>MonoQ Buffer A</u>

25mM PIPES (or MOPS), pH 6.8

2mM MgCl2

1mM EGTA

1mM DTT

0.1mM ATP

<u>MonoQ Buffer B</u>

MonoQ Buffer A + 1M NaCl

References

Aizawa H, Sekine Y, Yakemura R, Zhang Z, Nangaku M, Hirokawa N (1992) Kinesin family in murine central nervous system. *J Cell Biol* **119**: 1287-1296

Alonso MC, van Damme J, Vandekerckhove J, Cross RA (1998) Proteolytic mapping of kinesin/ncd-microtubule interface: nucleotide-dependent conformational changes in the loops L8 and L12. *EMBO J* **17**: 945-951

Brünger AT, Adams PD, Clore GM, DeLano WL, Gros P, Grosse-Kunstleve RW, Jiang J-S, Kuszewski J, Milges M, Pannu NS, Read RJ, Rice LM, Simonson T, Warren GL (1998) *Crystallography & NMR System*: A New Software Suite for Macromolecular Structure Determination. *Acta Cryst* **D54**: 905-921

Collaborative Computational Project No. 4 (1994) The CCP4 suite: programs for protein crystallography. *Acta Cryst* **D50**: 760-763

Coureux P-D, Wells AL, Menetrey J, Yengo CM, Morris CA, Sweeney HL, Houdusse A (2003) A structural state of the myosin V motor without bound nucleotide. *Nature* **425**: 419-423

Desai AS, Mitchison TJ (1997) Microtubule polymerization dynamics. *Annu Rev Cell Dev Biol* **13**: 83-117

Desai AS, Verma S, Mitchison TJ, Walczak CE (1999) Kin I kinesins are microtubule-destabilizing enzymes. *Cell* **96**: 69-78

Esnouf RM (1997) An extensively modified version of MolScript that includes greatly enhanced coloring capabilities. *J Mol Graphics* **15**: 132-134

Gerlt JA, Babbitt PC (2001) Divergent evolution of enzymatic function: mechanistically diverse superfamilies and functionally distinct suprafamilies. *Annu Rev Biochem* **70**: 209-246

Homma N, Takei Y, Tanaka Y, Nakata T, Terada S, Kikkawa M, Noda Y, Hirokawa N (2003) Kinesin Superfamily Protein 2A (KIF2A) Functions in Suppression of Collateral Branch Extension. *Cell* **114**: 229-239

Houdusse A, Szent-Györgyi AG, Cohen C (2000) Three conformational states of scallop myosin S1. *Proc Natl Acad Sci USA* **97**: 11238-11243

Huang TG, Hackney DD (1994) *Drosophila* kinesin minimal motor domain expressed in *Escherichia coli*. *J Biol Chem* **269**: 16493-16501

Hunter AW, Wordeman L (2000) How motor proteins influence microtubule polymerization dynamics. *J Cell Sci* **113**: 4379-4389

Hunter AW, Caplow M, Coy DL, Hancock WO, Diez S, Wordeman L, Howard J (2003) The kinesin-related protein MCAK is a microtubule depolymerase that forms an ATP-hydrolyzing complex at microtubule ends. *Mol Cell* **11**: 445-457

Inoué S, Salmon ED (1995) Force generation by microtubule assembly/disassembly in mitosis and related movements. *Mol Biol Cell* **6**: 1619-1640

Kapoor TM, Mitchison TJ (2001) Eg5 is static in bipolar spindles relative to tubulin: evidence for a static spindle matrix. *J Cell Biol* **154**: 1125-1133

Kikkawa M, Sablin EP, Okada Y, Yajima H, Fletterick RJ, Hirokawa N (2001) Switch-based mechanism of kinesin motors. *Nature* **411**: 439-445

Kline-Smith SL, Walczak CE (2002) The microtubule-destabilizing kinesin XKCM1 regulates microtubule dynamic instability in cells. *Mol Biol Cell* **13**: 2718-2731

Kull FJ, Endow SA (2002) Kinesin: switch I & II and the motor mechanism. *J Cell Sci* **115**: 15-23

Laskowski RA, MacArthur MW, Moss DS, Thornton JM (1993) PROCHECK: a program to check the stereochemistry of protein structures. *J Appl Cryst* **26**: 283-291

Löwe J, Li H, Downing KH, Nogales E (2001) Refined structure of αβ-tubulin at 3.5Å resolution. *J Mol Biol* **313**: 1045-1057

Mandelkow E, Hoenger A (1999) Structures of kinesin and kinesin-microtubule interactions. *Curr Opin Cell Biol* **11**: 34-44

Maney T, Wagenbach M, Wordeman L (2001) Molecular dissection of the microtubule depolymerizing ability of mitotic centromere-associated kinesin. *J Biol Chem* **276**: 34753-34758

McDonald HB, Stewart RJ, Goldstein LS (1990) The kinesin-like ncd protein of Drosophila is a minus end-directed microtubule motor. *Cell* **63**: 1159-65

Moore A, Wordeman L (2004) The mechanism, function and regulation of depolymerizing kinesins during mitosis. *Trends Cell Biol* **14**: 537-546

Moore AT, Rankin KE, von Dassow G, Peris L, Wagenback M, Ovechkina Y, Andrieux A, Job D, Wordeman L (2005) *J Cell Biol* **169**: 391-397

Moores CA, Yu M, Guo J, Beraud C, Sakowicz R, Milligan RA (2002) A mechanism for microtubule depolymerization by KinI kinesins. *Mol Cell* **9**: 903-909

Moores C, Hekmat-Nejad M, Sakowicz R, Milligan RA (2003) Regulation of KinI kinesin ATPase activity by binding to the microtubule lattice. *J Cell Biol* **163**: 963-971

Muller J, Marx A, Sack S, Song YH, Mandelkow E (1999) The structure of the nucleotide-binding site of kinesin. *Biol Chem* **380**: 981-992

Niederstrasser H, Salehi-Had H, Gan EC, Walczak C, Nogales E (2002) XKCM1 acts on a single protofilament and requires the C terminus of tubulin. *J Mol Biol* **316**: 817-828

Ogawa T, Nitta R, Okada Y, Hirokawa N (2004) A Common Mechanism for Microtubule Destabilizers – M Type Kinesins Stabilize Curling of the Protofilament Using the Class-Specific Neck and Loops. *Cell* **116**: 591-602

Okada Y, Hirokawa N (2000) Mechanism of the single-headed processivity: diffusional anchoring between the K-loop of kinesin and the C terminus of tubulin. *Proc Natl Acad Sci USA* **97**: 640-645

Otwinowski Z and Minor W (1997) Processing of X-ray Diffraction Data Collected in Oscillation Mode. *Methods in Enzymology* **276**: 307-326

Ovechkina Y, Wagenbach M, Wordeman L (2002) K-loop insertion restores microtubule depolymerizing activity of a "neckless" MCAK mutant. *J Cell Biol* **159**: 557-562

Rayment I, Rypniewski WR, Schmidt-Bäse K, Smith R, Tomchick DR, Benning MM, Winklemann DA, Wesenberg G, Holden HM (1993) Three-dimensional structure of myosin subfragment-1: a molecular motor. *Science* **261**: 50-58

Rice S, Lin AW, Safer D, Hart CL, Naber N, Carragher BO, Cain SM, Pechatnikova E, Wilson-Kubalek EM, Whittaker M, Pate E, Cooke R, Taylor EW, Milligan RA, Vale RD (1999) A structural change in the kinesin motor protein that drives motility. *Nature* **402**: 778-784

Rogers GC, Rogers SL, Schwimmer TA, Ems-McClung SC, Walczak CE, Vale RD, Scholey JM, Sharp DJ (2004) Two mitotic kinesins cooperate to drive sister chromatid separation during anaphase. *Nature* **427**: 364-370

Sablin EP, Case RB, Dai SC, Hart CL, Ruby A, Vale RD, Fletterick RJ (1998) Direction determination in the minus-end-directed kinesin motor ncd. *Nature* **395**: 813-816

Segerman B, Larsson N, Holmfeldt P, Gullberg M (2000) Mutational Analysis of Op18/Stathmin-Tubulin-interacting Surfaces. *J Biol Chem* **275**: 35759-35766

Shipley K, Hekmat-Nejad M, Turner J, Moores C, Anderson R, Milligan R, Sakowicz R, Fletterick R (2004) Structure of a kinesin microtubule depolymerization machine. *EMBO J* **23**: 1422-1432

Sindelar CV, Budny MJ, Rice S, Naber N, Fletterick R, Cooke R (2002) Two conformations in the human kinesin power stroke defined by X-ray crystallography and EPR spectroscopy. *Nat Struct Biol* **9**: 844-848

Sosa H, Dias DP, Hoenger A, Whittaker M, Wilson-Kubalek E, Sablin E, Fletterick RJ, Vale RD, Milligan RA (1997) A Model for the Microtubule-Ncd Motor Protein Complex Obtained by Cryo-Electron Microscopy and Image Analysis. *Cell* **90**: 217-224

Song H, Endow SA (1998) Decoupling of nucleotide- and microtubule-binding sites in a kinesin mutant. *Nature* **396**: 587-590

Thorn KS, Ubersax JA, Vale RD (2000) Engineering the processive run length of the kinesin motor. *J Cell Biol* **151**: 1093-1100

Turner J, Anderson R, Guo J, Beraud C, Fletterick R, Sakowicz R (2001) Crystal Structure of the Mitotic Spindle Kinesin Eg5 Reveals a Novel Conformation of the Neck-linker. *J Biol Chem* **276**: 25496-25502

Vale RD, Fletterick RJ (1997) The Design Plan of Kinesin Motors. *Annu Rev Cell Dev Biol* **13**: 745-777

Vale RD, Reese RS, Sheetz MP (1985) Identification of a novel force-generating protein, kinesin, involved in microtubule-based motility. *Cell* **42**: 39-50

Walczak CE (2000) Microtubule dynamics and tubulin interacting proteins. *Curr Opin Cell Biol* **12**: 52-56

Wang Z, Sheetz MP (2000) The C-terminus of tubulin increases cytoplasmic dynein and kinesin processivity. *Biophys J* **78**: 1955-1964

Woehlke T, Ruby AK, Hart CL, Ly B, Hom-Booher N, Vale RD (1997) Microtubule interaction site of the kinesin motor. *Cell* **90**: 207-216

Wordeman L (2005) Microtubule-depolymerizing kinesins. *Curr Opin Cell Bio* **17**:82-88
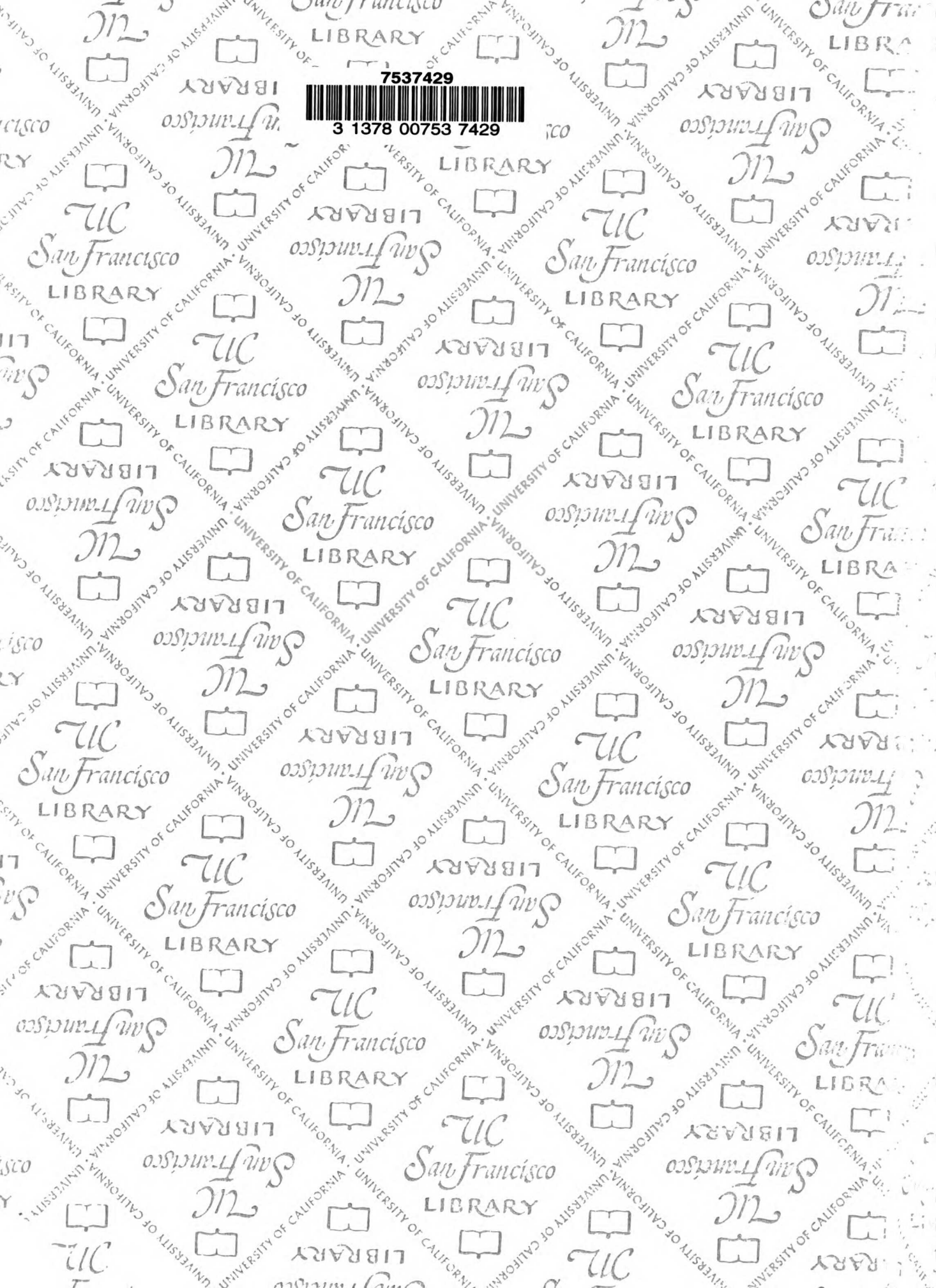
Wordeman L, Mitchison TJ (1995) Identification and partial characterization of mitotic centromere-associated kinesin, a kinesin-related protein that associates with centromeres during mitosis. *J Cell Biol* **128**: 95-104

Yun M, Zhang X, Park C-G, Park H-W, Endow SA (2001) A structural pathway for activation of the kinesin motor ATPase. *EMBO J* **20**: 2611-2618